Computerized Numerical Solutions to Combined Pure and Warping Torsion in Open Sections

by
Santanu Kumar Das

B.S., Civil and Environmental Engineering (1995)
University of Southern California

Submitted to the Department of Civil and Environmental Engineering
in partial fulfillment of the requirements for the degree of

Master of Science in Civil and Environmental Engineering

at the

MASSACHUSETTS INSTITUE OF TECHNOLOGY

February 1997

Author.....
Department of Civil and Environmental Engineering
January 10, 1997

Certified by.....
Jerome J. Connor
Professor of Civil and Environmental Engineering
Thesis Supervisor

Accepted by.....
Joseph M. Sussman
Chairman, Departmental Committee on Graduate Students

Computerized Numerical Solutions to Combined Pure and Warping Torsion in Open Sections

by

Santanu Kumar Das

Submitted to the Department of Civil and Environmental Engineering on January 10, 1997, in partial fulfillment of the requirements for the degree of Master of Science in Civil and Environmental Engineering

Abstract

In this thesis the topic of linear pure and warping torsion is investigated. The effects of these phenomena on an arbitrary cross section is presented. Due to the complexity of some sections, the problem of numerically identifying the shear center is resolved which is a key component in quantifying the shear and normal stresses caused by pure and warping torsion. For pure or St. Venant's torsion a governing differential equation will be developed and related to Laplace's equation for an expanding membrane so as to better understand the relationship between the torsional rotation on a beam and the shear stress it creates.

Closed thin-walled sections such as continuous and multicontinuous cells are examined under the influence of pure torsion and resolved in a manner comparable to that of planar bending. A connection between torsion and planar bending in such sections is also investigated. Built-up sections are also discussed along with a numerical approach to determining the torsional stiffness of a given cross section.

The normal and shear stresses caused by the out of plane torsion known as warping is also studied. Torsional properties such as the normalized unit warping function, statical warping moment, and the warping constant are numerically evaluated using Simpson's integration rules and plotted using MATLAB® sc the maximum values of these functions can be observed. The maximum combination of stresses created by pure and warping torsion together on any given beam with arbitrary supports and loading is also discussed. The finite difference method is used to solve the differential equations which govern the behavior of pure and warping torsion in combination.

An object-oriented computer program is also written to abet in pulling together the entire torsional analysis procedure. The implementation of classes and linked lists to store and create new information is discussed in the last part of this thesis.

Thesis Supervisor: Jerome J. Connor
Title: Professor of Civil and Environmental Engineering

Acknowledgments

In writing a thesis or any paper of such magnitude and intensity, there always lies a stigma of inspiration from a motley group of sources. I would sincerely like to express my gratitude to Professor Jerome Connor whose lectures and ideas have driven me to pursue a topic that no other professor would acknowledge. His goals and ambitions for the future of structural engineering are quintessential for our profession. It is not everyday a graduate student, after so many years of lectures and recitations, can go home inspired.

I would like to thank the great friends I have made here during the past year and a half. All of my buddies who went drinking, played football, and harassed me (Pete!), I thank you for your time and experiences. Jeff, Brian, Dave, Nick, Pete, and Mav I thank sincerely. I would especially like to thank my friend Jim Kennedy whose wise, and sometimes lifesaving, advice kept me going when times were rough. It is rare when I can confide and share my emotions about school, girls, and life in general with one person. My family has been a great source of inspiration for me during my stay here. Through their illnesses they always found time to support me and my goals. Without them this education and benefits from it would seem trivial. Last but not least, I would like to show my utmost love and gratitude to Donnajo Popielarski. There are people who believe life is like a race: get an education, get money, get married, etc. Happiness, of course, is first prize. If life is a race, I think I found my shortcut.

Santanu Das

Table of Contents

1 Introduction 10

1.1 Significance of torsion 12

1.2 Determination of shear center of variable cross sections 14

1.2.1 Physicality of shear center 14

1.2.2 Numerical procedures using Simpson's $1/3^{rd}$ integration scheme 21

1.2.3 Force Method 26

2 Pure Linear Torsion in Open and Closed Prismatic Sections 30

2.1 Differential representation of St. Venant's torsion 31

2.1.1 Airy's stress function 34

2.2 Laplace's equation for bidirectional flow 36

2.3 Prandtl's membrane analogy 37

2.3.1 Analogy of Prandtl's membrane and the pure torsion problem 37

2.3.2 Membrane analogy relationships 38

2.4 Solution of Laplace's equation using Prandtl's membrane 40

2.5 Differential equation describing shear stress caused by pure torsion 45

2.6 Approximation for torsional stiffness constant K_T 46

2.6.1 K_T for built-up solid cross sections 48

2.7 Pure torsion on closed thin-walled cell sections 50

2.7.1 Pure torsion on multicontinuous cells 54

2.7.2 Advantages of membrane analogy in analysis of multicell sections under torsion 59

3 Warping Torsion in Open and Closed Prismatic Sections 62

3.1 Significance of warping torsion; Assumptions made in theory 63

3.2 Warping moment in a general open cross section 64

3.2.1 Relationship of unit warping to tangential displacement.....67
3.2.2 Normal warping and shear stress; open form differential equation.....69
3.2.3 Normalized unit warping function of the cross section.....70
3.2.4 Warping statical moment and warping constant.....74
3.2.5 Normal warping stress as a function of the bimoment.....76
3.3 Numerical solution of warping torsional properties.....77
3.3.1 Assumptions and techniques used to numerically evaluate the normalize unit warping.....80
3.3.2 TORAB's capabilities in evaluating the normalized unit warping.....81
3.3.3 Numerical determination of the warping constant and the warping statical moment.....83

4 Combination of Pure and Warping Torsion 85

4.1 Governing differential equation for combined torsional resistance.....85
4.1.1 Solution of combined torsional resistance equation.....86
4.1.2 Support types and corresponding boundary conditions.....88
4.2 Closed form solution of governing torsional differential equation.....91
4.3 Torsional charts dimensionalizing force-rotation relationships.....93
4.4 Approximate solution to governing torsional differential equations using finite difference.....94
4.4.1 Solution for torsional rotation using central difference method.....97
4.4.2 Establishment of mesh patterns in tridiagonal form for finite difference equations (concentrated torque).....99
4.4.3 Establishment of mesh patterns in tridiagonal form for finite difference equations (distributed torque).....103
4.5 Comparison of finite difference solution to exact closed form solution.....106

5 Implementation of numerical algorithm to solve for the torsional response of a beam (TORAB) 110

5.1 User interface for defining a cross section in TORAB.....110

5.1.1 Joint and element orientation for cross sections 111
5.1.2 Local vs. global; element offsets and local centroids 113
5.1.3 Elemental properties 114
5.1.4 Distinction between closed cells and ordinary cross sections 115
5.2 User interface for defining a beam for analysis in TORAB 116
5.3 Evaluation of torsional properties using TORAB 117
5.3.1 Evaluation of torsional stiffness of a cross section in TORAB 117
5.3.2 Evaluation of normalized warping function of a cross section in TORAB 119
5.3.3 Evaluation of statical warping moment and warping constant of a cross section in TORAB 120
5.4 Graphical interface of torsional properties using MATLAB® and TORAB 121
5.5 Location of maximum stress combination using TORAB 122
5.6 Solution of torsional rotation and successive derivatives in TORAB 124

6 Conclusion **126**

Appendix A **129**

List of Figures

1-1 Area for deriving the section modulus.....12

1-2 Eccentrically loaded thin-walled section.....15

1-3 Resolution of forcing system.....15

1-4 Stresses on element of general open section.....17

1-5a Elements of Cross Section with a Positive ρ_{ij} for Element *ij*.....23

1-5b Liner variation of *w*.....23

1-6 Dimensions of skewed channel section. The centroid is calculated by TORAB as well.....28

1-7 TORAB input file for Figure 1-6.....29

2-1a Shear stress distribution on *x-y* plane of discrete element due to external torque at shear center of cross section.....33

2-1b 3-D shear stress distribution from element in Figure 2-1a.....33

2-2a Inflated membrane over a solid cross section.....39

2-2b Free body diagram of discrete membrane.....39

2-2c Free body diagram of axial forces on membrane.....39

2-3 Rectangular plate element subjected to external torque.....42

2-4a Inflated membrane over the *x-y* plane of plate in Figure 2-3.....43

2-4b Free body diagram of inflated membrane.....43

2-5 Built-up open cross section with assumed equal rotations.....49

2-6 Membrane of a thin-walled closed cross section.....52

2-7 Shear stress distribution in a 3-span multicell section. CCW is taken as the positive sense for stress and rotation.....57

3-1 Deformations and displacements of a discrete thin-walled element. The first two pictures show the *v* displacement along the *x* and *y* surfaces, respectively The last picture illustrates the relationship between the displacement *v* and the rotation ϕ.....65

3-2 Fictitious current flow though meshed wide-flanged section.....82

4-1a AISC Type 2 simple framing connection; $M_z=M_{pure}+M_{warp}$ and $M_{flexure}=0$...90

4-1b AISC Type 1 rigid framing connection with boxing; $M_z=M_{warp}$ and $M_{pure}=0$.....90

4-2 Force-rotation torsional chart for cantilever beam with concentrated torque.....95

4-3 Force-rotation torsional chart for cantilever beam with distributed torque.....96

4-4 Mesh points for finite difference equations.....98

4-5 General central difference mesh notation.....101

4-6 Comparison of exact solution of rotation and successive derivatives to that of finite central difference method for a pin-pin beam with distributed torque (m_z = -3 k•in/in, L=240", h=30", G=11.2 X 10^3 Ksi, E=30.0 X 10^3 Ksi, K_T=1.82 in^4, I_w=1881.0 in^6).....107

4-7 Comparison of exact solution of rotation and successive derivatives to that of finite central difference method for a cantilevered beam with a concentrated torque at free end (M_z = -2.5 k•in, L=240", h=30", G=11.2 X 10^3 Ksi, E=30.0 X 10^3 Ksi, K_T=1.82 in^4, I_w=1881.0 in^6).....108

5-1 Doubly linked list used to store element structures as they are read from the input file.....113

5-2 Example of element offset.....114

5-3 Sample continuous beam with TORAB input file.....116

5-4 Flow chart of TORAB's torsional properties calculations.....118

5-5 Normalized unit warping and statical warping moment plots of skewed channel section.....123

List of Tables

1-1 Shear center calculation using Force Method and TORAB. All values are referenced from origin of section.....28

2-1 Membrane and pure torsion relationship.....40

3-1 Relationship of a member under pure flexure and warping torsion.....78

3-2 Numerical evaluation of normalized unit warping.....81

4-1 Torsional boundary conditions for simple and rigid connections.....89

Chapter 1

Introduction

In the discipline of structural engineering, there are two quintessential facets of study which, when combined, help the engineer to more appropriately understand the behavior of a particular structure: analysis and design. Through the use of computers, the engineer is abetted in procuring accurate and reliable results in a fraction of the time it took by hand. In the area of analysis, however, the subject of linear torsion is widely avoided in most analyses due to the shear complication of solving a plethora of differential equations and then correctly combining them with any additional planar shear and bending forces on the structure.

The most common occurrence of torsion is in straight or curved girders where the loading is eccentric with respect to the axis of the girder or its shear center. Since this particular phenomena can not be neglected in most of these situations, engineers introduce only pure (St. Venant's) torsion in the analysis. St. Venant's torsion is a function of the rotation of the beam and its inherent torsional stiffness. When open and built-up sections are introduced, the computation of the aforementioned parameters become extremely complicated. Another significant aspect of torsion is warping which results when out of plane displacements caused by an external torque are restrained and thus, engender extra shear and bending forces throughout the beam. Warping is a function of three critical, innate parameters of a beam: the warping constant, the normalized unit warping function, and the warping statical moment. When arbitrary open cross sections are used, these constants have to be evaluated numerically.

This study is concerned with the computational aspects of torsional analysis in structural systems. These systems entail beams which possess arbitrary cross sections including open and closed multicontinuous cells. Several numerical solutions to the warping and pure torsion problems such as closed-form evaluation of differential equations and finite difference methods will be introduced and developed. Finally, an interactive computer program will be developed that will attempt to evaluate the behavior of torsion on a beam with a random cross section, various boundary constraints, and an arbitrary external torque (concentrated or distributed). The program will have an interface with Matlab® which will allow the user to graphically view the geometrically varying warping functions across the cross section of the member. This process is extremely imperative in the understanding of the superposition process which determines the location of the combined maximum planar and torsional forces along the longitudinal axis of the beam.

1.1 Significance of torsion

Frequently torsion is a secondary, though not necessarily, a minor effect that must be considered in combination with other types of behavior. The most efficient cross section for carrying an external torque is a hollow circular shaft. The mathematical reason for this deduction will be described in latter sections. Although circular shafts such as tubes or pipes are ideal in torsional loading situations, these shapes do not carry and/or transfer other types of loading in an efficient manner. The shapes that comprise "good" columns and beams are those that have their material distributed as far from their centroids as practicable. Thus, their resistance to bending at the extreme fibers is increased since most of the material is positioned as far from the neutral axis as possible. Efficient sections such as channels and wide-flanges minimize the following ratio

$$\text{MIN}\left(\frac{\int_A y_c^2 dA}{d_z}\right) \qquad 1.1$$

where the variables y_c and d_z are depicted in Figure 1-1. This ratio is defined as the section modulus.

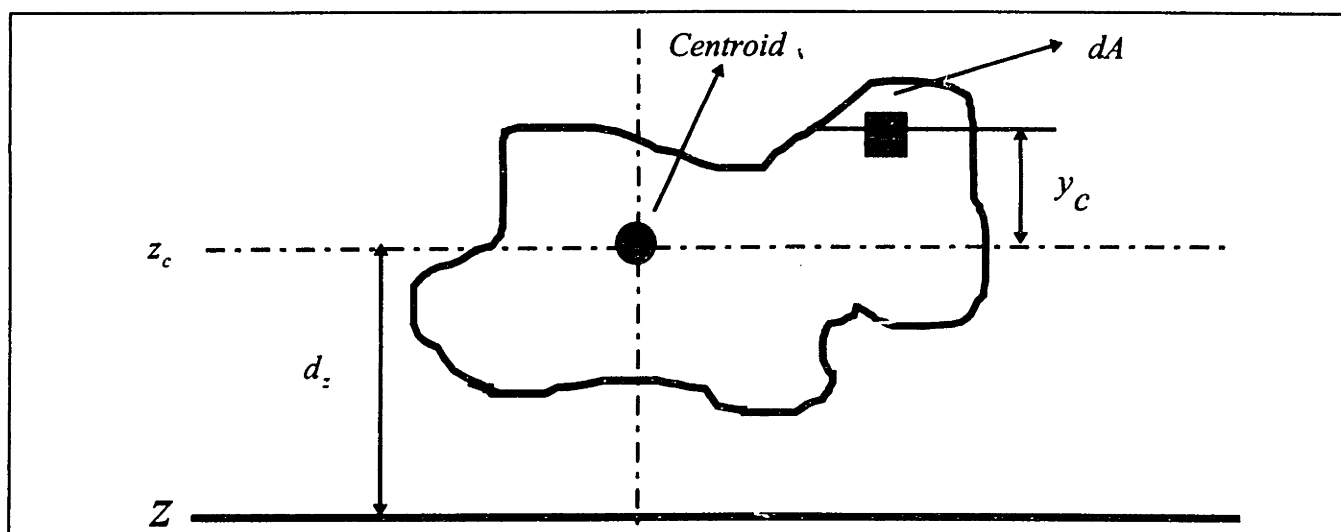

Figure 1-1 Area for deriving the section modulus

Box sections and thin walled circular shafts can not provide the same resistance in bending as a wide-flange or channel with the same cross sectional area. Common open sections (most of which are listed in the ASD Manual for Steel Construction) must be analyzed for torsion in case of any eccentric loadings.

There are relatively few occasions in actual practice where the torsional load can cause significant twisting. One instance is during the erection or construction of the actual structure. In most building constructions the members are laterally restrained by attachments along the length of the member and thus, are restricted to twist. Shear stiffeners or braces along the web of the beam are sometimes used as intermediate restraints for this purpose. Even without lateral restraints, the twisting bestowed on a member from an external torque may be limited by the rotation or slope of any existing transversely attached member. Suppose a column framed to a beam through a rigid connection imposes an eccentric load onto the beam. The rotation the beam undergoes from the eccentric loading is limited by the rotational bending stiffness of the column at its point of connection to the beam. Any torsional moment the beam is faced to resist will be reduced by the column which will have to pick up an additional end moment.

Other places where torsion may enter are in the analysis of spandrel beams where the torsional loading may be uniformly distributed. It also exists in situations where a beam frames into a girder on one side only, or where unequal reactions come to opposite sides of a girder. The design of crane runway girders involves the combination of biaxial bending and torsion which will be discussed in latter sections. When a high torsional stiffness is required for items like aircraft structural components and curved girders, closed sections become ideal and in some cases, a necessity. Single and multicontinuous thin-walled cells are utilized in these situations. Using the Prandtl membrane analogy, the torsional response of these cells can be analyzed numerically.

1.2 Determination of shear center of variable cross sections

In the development of the general stress equations for bending, it is assumed that the external force system is applied such that the resultant of these forces passes through a point called the shear center or center of twist. This implies that there is no twisting of the cross section and only plane bending will be induced. To correctly apply the general equations of bending, the location of the shear center must be known. Then, the loading pattern has to be modified so that the bending and torsional effects can be calculated independently. The location of this shear center can be found through two techniques. One is designated as the Force Method while the other is a numerical interpretation of the surface integrals used in the Force Method.

1.2.1 Physicality of shear center

In Figure 1-2 an arbitrary thin walled, open cross section is subjected to a vertical load P. The centroid and the shear center of the section are designated as c and $S.C.$, respectively. Since the load has an eccentricity with respect to the centroid of the section, it can be vectorally resolved into a force which acts through the center and a corresponding twisting moment T as shown in Figure 1-3. By resolving the force in this manner, the stresses on the body can be differentiated into two categories: stresses due to the vertical load P in plane bending conditions and stresses induced by a twisting moment $T = (e_x + x_o)P$. In order to obtain the torsional induced stresses, the location of the shear center is imperative. It is at this point where the externally applied forces balance any internal couple so as to prevent twisting. Thus, the assumptions of planar bending conditions can be applied without the introduction of extraneous axial or torsional loads.

An open prismatic section subject only to bending type stresses (i.e. planar normal and shear stresses) will be considered. This section has a cross sectional

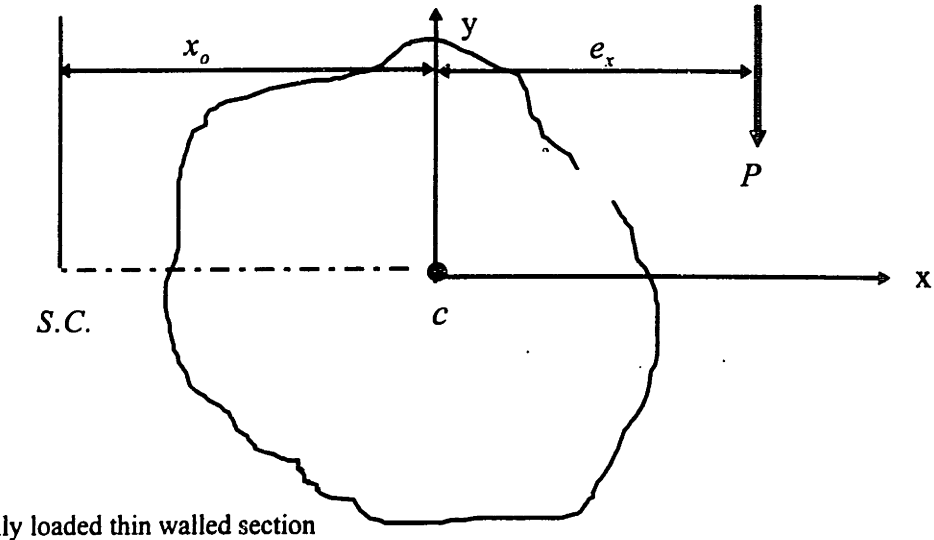

Figure 1-2 Eccentrically loaded thin walled section

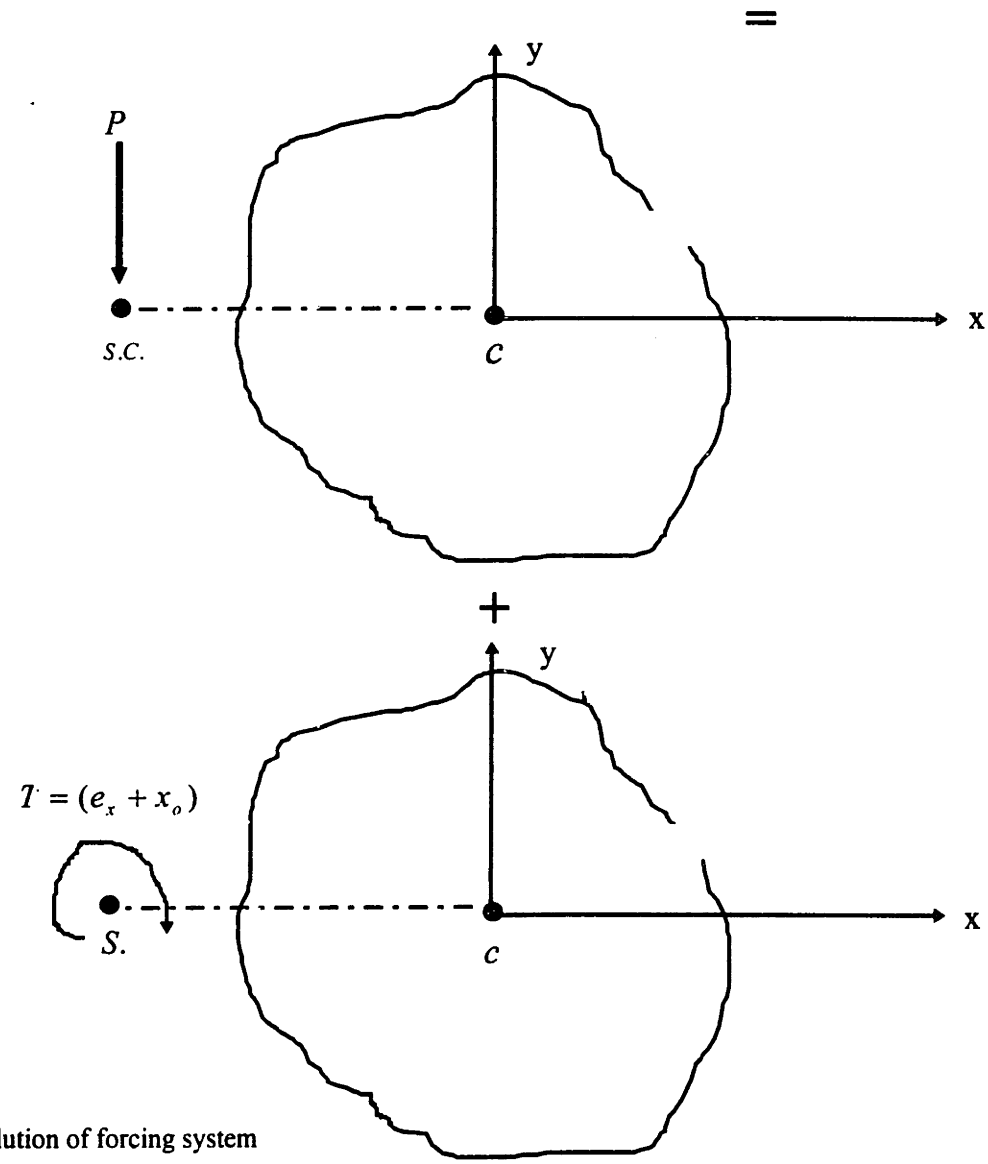

Figure 1-3 Resolution of forcing system

thickness t which is a function of the length s and does not vary along the longitudinal axis of the beam z. The walls of the section are assumed to be sufficiently thin so that the computations may be based on center line dimensions. Also, with thin wall theory, the shear stresses that develop across the beam are assumed to remain constant across the thickness of the walls. The cross section will also adhere to Navier's hypothesis which states that plane sections will remain plane during the loading of the section. The coordinate axes are referenced to the centroid of the cross section, but are not necessarily principal axes. This statement will become more lucid as the relation of the shear center to other known properties of the cross section are developed. An illustration of the depicted cross section along with the stress state of a small element located along the open cross section can be found in Figure 1-4. The normal bending stress and horizontal shearing stress are designated as σ_z and τ, respectively.

Since the discrete element must lie in a state of equilibrium, summation of forces along the longitudinal z axis must equate to zero or

$$\sigma_z t\,ds + \tau t\,dz - (\tau t\,dz + d(\tau t)dz) - (\sigma_z t\,ds + d\sigma_z t\,ds) = 0 \qquad 1.2$$

Since a force system is required, the stresses are multiplied by the surface area which they act upon. As the stresses move across the plane of the element, the stress increments by a finite differential (i.e. $d(\tau t)$ or $d\sigma_z$). Using the well known chain rule in calculus, these differentials in stress can alternatively be written as

$$d\sigma_z = \frac{\partial \sigma_z}{\partial z} dz, \quad d(\tau t) = \frac{\sigma(\tau t)}{\partial s} ds \qquad 1.3$$

Substituting 1.3 into 1.2 and simplifying, the equilibrium equation in the z direction becomes

$$t\frac{\partial \sigma_z}{\partial z} dz + \frac{\partial(\tau t)}{\partial s} ds = 0 \qquad 1.4$$

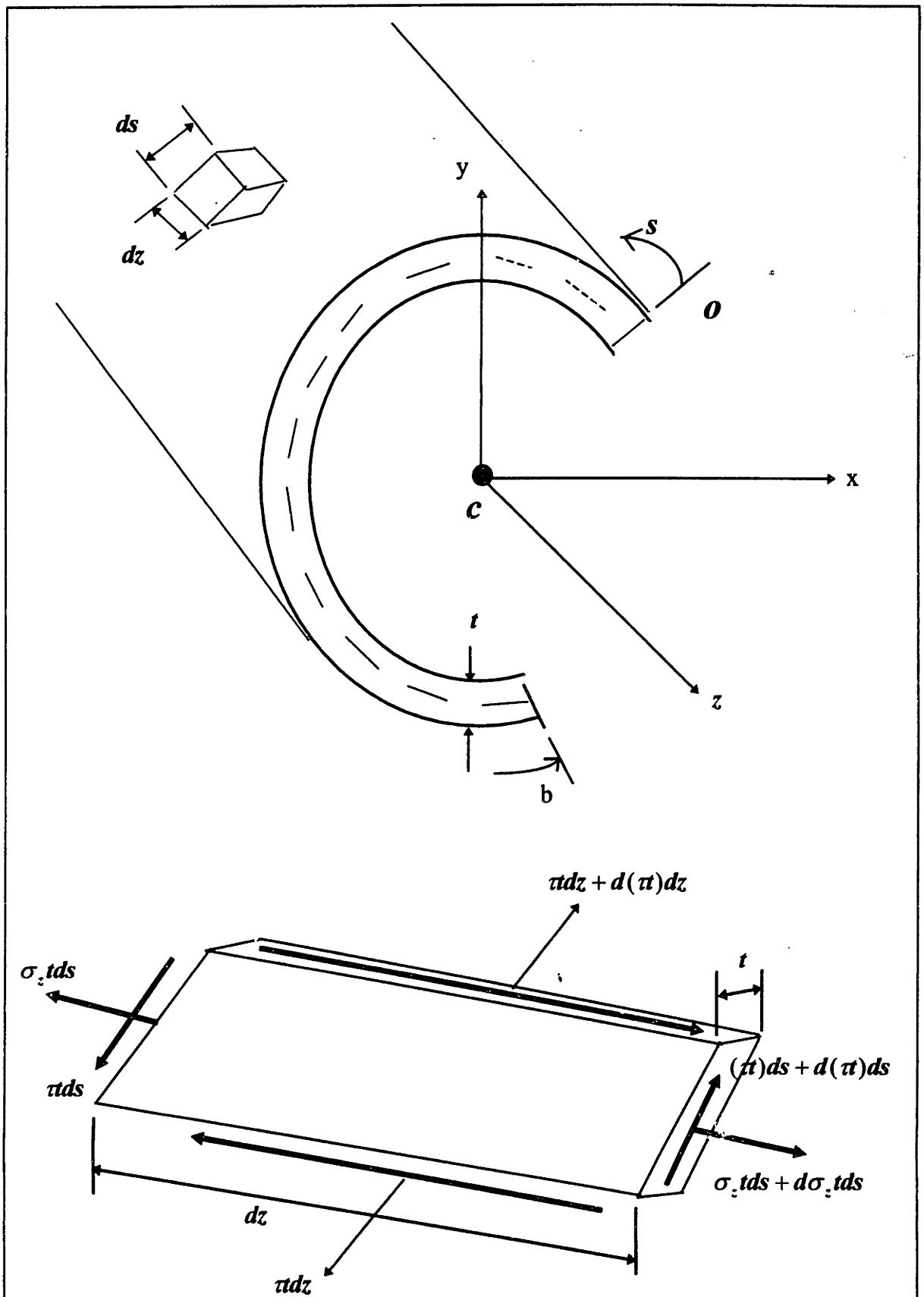

Figure 1-4 Stresses on element of general open section

From planar bending theory, the state of stress of a general cross section subjected to bending about two mutually perpendicular axes and an axial force is given by

$$\sigma_z = \frac{P}{A} + \frac{I_{xy}x - I_y y}{I_{xy}^2 - I_x I_y} M_x + \frac{I_{xy}y - I_x x}{I_{xy}^2 - I_x I_y} M_y \qquad \textbf{1.5}$$

The assumption that was made in developing this equilibrium equation was that the section was only subject to bending type forces so the axial term $\frac{P}{A}$ is zero. Taking the partial derivative of the normal bending stress σ_z with respect to z

$$\frac{\partial \sigma_z}{\partial z} = \frac{\partial M_x}{\partial z}\kappa + \frac{\partial M_y}{\partial z}\psi \qquad \textbf{1.6}$$

where κ and ψ are constants equal to $\frac{I_{xy}x - I_y y}{I_{xy}^2 - I_x I_y}$ and $\frac{I_{xy}y - I_x x}{I_{xy}^2 - I_x I_y}$, respectively. Since the goal is to derive a physical interpretation of the geometric location of the shear center of an arbitrary cross section, the moments about the perpendicular axes must be decomposed into shear forces. From mechanics, the first-order change of the moment along any axis is the resultant shear force. Thus, the resultant shear forces on the cross section are $V_x = \partial M_x / \partial z$ and $V_y = \partial M_y / \partial z$ which is convenient since equation 1.6 is already in this form. Substituting V_x and V_y into equation 1.6 and then, equation 1.6 into 1.4, the equilibrium equation becomes

$$\frac{\partial(\pi t)}{\partial s} = -V_x t\kappa - V_y t\psi \qquad \textbf{1.7}$$

Integrating across the surface of the section from o to s (some arbitrary point along the cross section) and substituting values in for κ and ψ, the shear flow πt along the cross section can be expressed as

$$\tau t = \frac{1}{[I^2{}_{xy} - I_x I_y]}\left[V_x\left(I_y\int_0^s ytds - I_{xy}\int_0^s xtds\right) + V_y\left(I_x\int_0^s xtds - I_{xy}\int_0^s ytds\right)\right] \qquad \textbf{1.8}$$

If the coordinate axes that are chosen are the principal axes of the section, the product of inertia I_{xy} is equal to zero. Equation 1.8 then reduces to

$$\tau t = -\frac{V_x}{I_x}\int_0^s ytds - \frac{V_y}{I_y}\int_0^s xtds \qquad \textbf{1.9}$$

The integrals in equation 1.8 are known as the statical moment or first moment of area. Letting $Q_y = \int_0^s ytds$ and $Q_x = \int_0^s xtds$ the shear flow for the cross section can simply be written as

$$\tau t = -\frac{V_x}{I_x}Q_y - \frac{V_y}{I_y}Q_x \qquad \textbf{1.10}$$

which is the familiar shear flow equation described in basic strength of materials. Similar to the discrete element, the cross section must also be in a state of equilibrium which means that the resultant torque caused by the shear stresses must be equal and opposite to the external torque produced by the forces V_x and V_y. The location of these forces are known as the shear center. Determination of either component of the shear center requires that the shear force in that direction have some magnitude while the other force be zero. Summation of moments about the centroid c, assuming V_x and V_y act singly or $V_y = 0$, gives

$$\sum M_c = 0 = V_x X_o - \int_0^b \rho(\pi) ds \qquad \text{or} \qquad X_o = \frac{1}{V_x}\int_0^b \rho(\pi) ds \tag{1.11}$$

where X_o is the horizontal component of the shear center. The integral $\int_0^b \rho(\pi) ds$ is the summation of all the shear forces acting along the surface of the cross section. While the force per unit length is the shear flow π, the corresponding moment arm is the variable ρ which is graphically represented in Figure 1-5a. The distance ρ is the perpendicular distance from the centroid of the section to a tangent line drawn through a segment ds. Substituting equation 1.8 for π, the horizontal component of the shear center is defined as

$$X_o = \frac{1}{[I_{xy}^{\ 2} - I_x I_y]}\left[I_x \int_0^b \left(\rho ds \int_0^s y t ds \right) - I_{xy} \int_0^b \left(\rho ds \int_0^s x t ds \right) \right] \tag{1.12}$$

where the integral $o - b$ is along the entire length of the cross section and $o - s$ is a particular discrete length. A similar equation will result in a formal expression for Y_o, the vertical component of the shear center, by assuming $V_x = 0$.

$$Y_o = \frac{1}{[I_{xy}^{\ 2} - I_x I_y]}\left[-I_x \int_0^b \left(\rho ds \int_0^s x t ds \right) + I_{xy} \int_0^b \left(\rho ds \int_0^s y t ds \right) \right] \tag{1.13}$$

The closed form solutions of these expression are quite complex, especially if the surface is arbitrary. Determining the moment arm can be difficult since the tangent line of each element must be calculated. In the next section, a numerical solution to the shear center problem will be examined along with an adaptive computer algorithm that will be able to solve the shear center of any geometry.

1.2.2 Numerical Procedure using Simpson's 1/3rd Integration Scheme

Let the variable w equal the following expression

$$w = \int_0^s \rho \, ds \quad \text{or} \quad dw = \rho \, ds \tag{1.14}$$

Substituting this expression into equation 1.13, the second integral expression reduces to

$$\int_0^b \left(\rho \, ds \int_0^s yt \, ds \right) = \int_0^b \left(dw \int_0^s yt \, ds \right) \tag{1.15}$$

Integrating this expression by parts gives

$$\int_0^b \left(\rho \, ds \int_0^s yt ds \right) = -\int_0^b wy \, tds \tag{1.16}$$

Similarly, for the first integral expression

$$\int_0^b \left(\rho \, ds \int_0^s xt \, ds \right) = -\int_0^b wxt \, ds \tag{1.17}$$

The expressions in equation 1.15 and 1.16 will be defined as

$$I_{wx} = \int_0^b wxt \, ds \tag{1.18}$$

$$I_{wy} = \int_0^b wyt\, ds \qquad 1.19$$

Substituting equations 1.17 and 1.18 into the expressions for the components of the shear center in equations 1.12 and 1.13, closed form expressions of the shear center are obtained which are solely dependent on geometric properties that can be solved numerically.

$$X_o = \frac{I_{xy} I_{wx} - I_y I_{wy}}{I_{xy}^{\ 2} - I_x I_y} \quad \textbf{and} \quad Y_o = \frac{I_x I_{wx} - I_y I_{wy}}{I_{xy}^{\ 2} - I_x I_y} \qquad 1.20$$

The introduction of equation 1.19 requires only the determination of two new geometric properties defined as I_{wx} and I_{wy} .

The following method, which employs Simpson's 1/3rd integration scheme, assumes that the members comprising the cross section are thin flat elements. Most structural members adhere to this assumption. If members contain curved surfaces, approximations can be made to utilize the following methods or direct use of the integrals can be applied. Calculation of I_{wx} and I_{wy} directly depends on the computation of the variable w which is equal to $\int_0^s \rho\, ds$. This integral can be expressed in index notation as

$$w_j = w_i + \rho_{ij} L_{ij} \qquad 1.21$$

where the points i and j are the starting and ending points of a particular element in the cross section (see Figure 1-5b). Since the integral can be decomposed into a summation over the entire cross section, the value of w at any point k in the cross section can be represented as

$$w_k = \sum_{i=1}^{j=k} \rho_{ij} L_{ij} \qquad 1.22$$

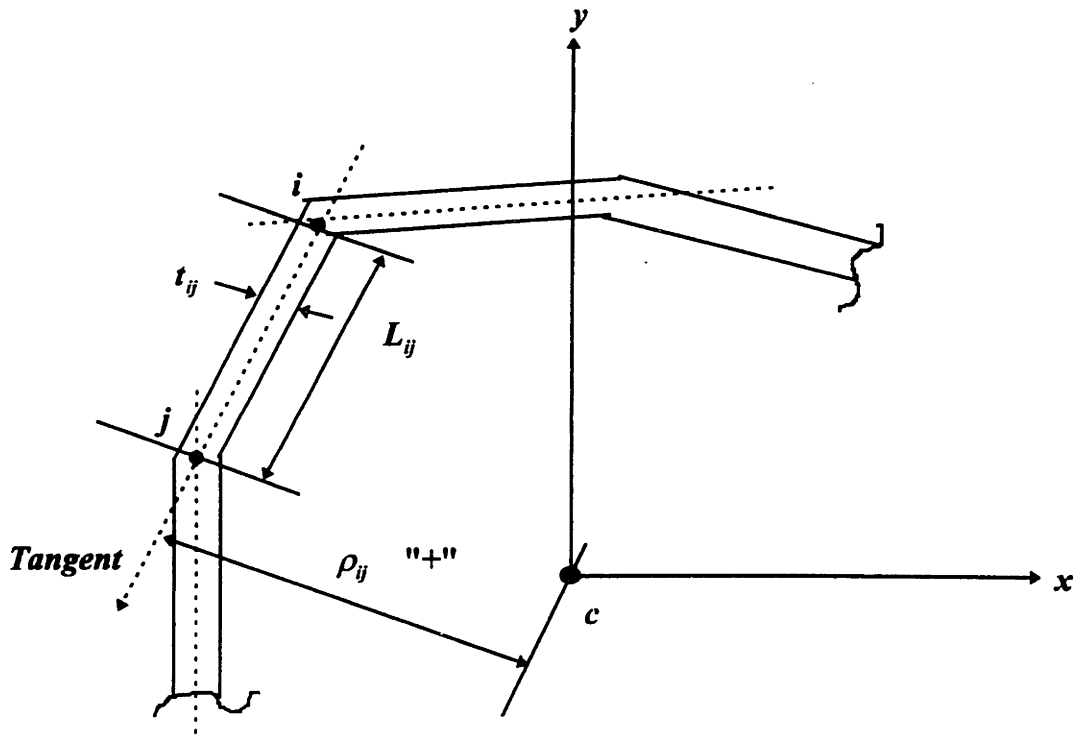

Figure 1-5a Elements of cross section with a positive ρ_{ij} for element ij

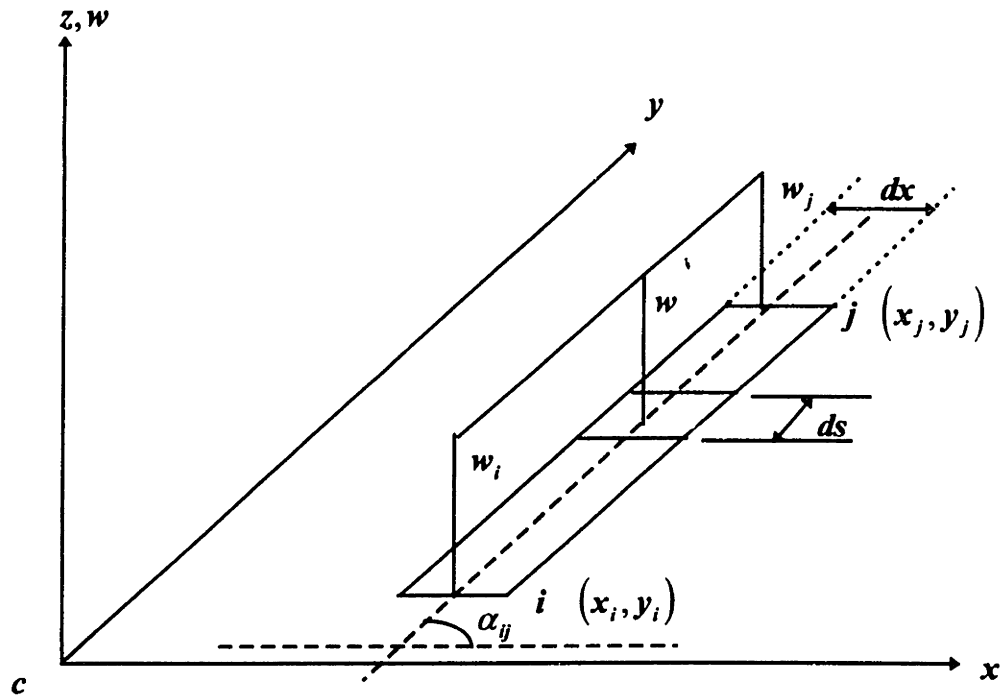

Figure 1-5b Linear variation of w

The moment arm ρ_{ij} will be defined as positive if the centroid is *to the left* when viewing the element from i to j along the tangent line. From equation 1.20, it is readily seen that the variable w varies, at most, linearly across any element. Thus, the value of an intermediate point of w, relative to w_i and w_j, can be linearly interpolated as

$$w = w_i + \frac{(w_j - w_i)(x - x_i)}{(x_j - x_i)} \qquad \textbf{1.23}$$

From Figure 1-5 a discrete elemental surface ds can be expressed as $dx / \cos\alpha_{ij}$. Substituting equation 1.22 and the value for ds into equation 1.17, the geometric property I_{wx} can now be represented as

$$I_{wx} = \sum_{0}^{b} \frac{t_{ij}}{\cos\alpha_{ij}} \int_{x_i}^{x_j} x\left(w_i + \frac{(w_j - w_i)(x - x_i)}{(x_j - x_i)} \right) dx \qquad \textbf{1.24}$$

Simpson's 1/3rd rule can now be used to interpolate the integrand with a second-order Lagrange polynomial. Thus, 1.23 can be numerically represented as

$$I_{wx} = \frac{1}{3}\sum_{0}^{b}\left(w_i x_i + w_j x_j\right)t_{ij}L_{ij} + \frac{1}{6}\sum_{0}^{b}\left(w_i x_j + w_j x_i\right)t_{ij}L_{ij} \qquad \textbf{1.25}$$

where the summation $\sum_{0}^{b}$ indicates the sum of each element in the cross section (b = number of elements the cross section is subdivided into). Following a similar procedure, the geometric property I_{wy} can be evaluated as

$$I_{wy} = \frac{1}{3}\sum_{0}^{b}\left(w_i y_i + w_j y_j\right)t_{ij}L_{ij} + \frac{1}{6}\sum_{0}^{b}\left(w_i y_j + w_j y_i\right)t_{ij}L_{ij} \qquad \textbf{1.26}$$

The moments of inertia and the product of inertia can also be derived in a similar fashion.

$$I_x = \frac{1}{3}\sum_0^b \left(y_i^2 + y_i y_j + y_j^2\right) t_{ij} L_{ij}$$

$$I_y = \frac{1}{3}\sum_0^b \left(x_i^2 + x_i x_j + x_j^2\right) t_{ij} L_{ij} \qquad \textbf{1.27}$$

$$I_{xy} = \frac{1}{3}\sum_0^b \left(x_i y_i + x_j y_j\right) t_{ij} L_{ij} + \frac{1}{6}\sum_0^b \left(x_i y_j + x_j y_i\right) t_{ij} L_{ij}$$

The convenience of equations 1.25 and 1.26 lies in the ability for these equations to decompose a particular cross section into a series of elements.

Incorporation of a computer algorithm to solve these geometric properties can easily be created by simply defining a loop which goes over all the elements and calculates I_x, I_y, I_{xy}, I_{wx}, and I_{wy} for each element. By implementing the algorithm in the C architecture, a *C structure* for the cross section with an associated *pointer* can be developed. This pointer could in turn point to a linked list of elements which comprise the cross section. This eclectic method of programming allows for each element to have its own identity and thus, be able to tell the cross section what its geometric properties are. The burden of a reference axis, especially when calculating the sign of the moment arm ρ_{ij}, can be eliminated since the orientation of each element will be known by the element itself. Also, since each element is internally linked to all the other elements, its orientation with respect to any adjacent element can be readily obtained.

The details of the structure of the code will be discussed in later chapters. It is imperative, however, to understand the significance of isolating each element and having it develop its own properties. Other torsional functions such as the unit warping constant or the normalized warping function across an element will directly depend on the values of the warping functions along adjacent elements. These functions are fully compatible at the boundaries of the elements which means that continuity must be preserved across the

entire cross section. If common arrays are utilized to check the compatibility, more storage would be required to preserve the relationships among the elements.

1.2.3 Force Method

The force method considers the resultant shear flow πt, as expressed in equation 1.10, and applies simple equilibrium to obtain the shear center. Magnitudes of the first moment of area around both axes are determined for a specified number of points along the cross section. The cross section is usually broken down into finite elements, each having its own Q_x and Q_y. After the first moments of area are determined, the summation of moments about the centroid of the cross section are taken. Since the body is in equilibrium, the shear flow caused by torsion must balance the external shear force being applied. The point of application of this force is the corresponding moment arm from the centroid (i.e. the shear center).

From equilibrium,

$$\sum M_c = 0 = -\int_0^b (\pi t)\rho ds + V_x X_o \qquad 1.28$$

where positive directions are those which cause a counterclockwise rotation about the centroid. Although equation 1.27 defines the equation for the horizontal component of the shear center, the vertical component can be derived in the same manner. The shear flow πt can be replaced by equation 1.10 while the integral can be substituted for a summation over all the elements. The moment arm ρ is the perpendicular distance from the centroid of the cross section to the center of the shear flow diagram on a particular element.

Hand calculations of the shear center of an arbitrary cross section using the force method were comparable to the results obtained from the numerical method. The devised computer program was implemented with a script pre-processor (SPRE) which can read an input file listing the geometry of the cross section. Element orientations and properties

are then calculated using the engine of the program, TORAB (TORsional Analysis of Beams). A comparison of the shear center of a skewed channel section using both the force method and TORAB are depicted in Table 1-1. The input file used in creating the skewed channel section for the TORAB program is listed in Figure 1-7 along with an illustration of the channel in Figure 1-6. The section is broken into twelve continuous elements. By adding more elements into the system, the accuracy of the shear center computation actually decreases. The reason is that normal floating point numbers can only carry single precision. Thus, the error in storage of one of these numbers propagates when used in conjunction (arithmetically) with other numbers with similar errors. To circumvent this problem, double precision variables can be introduced which store sixteen digits. Differences in the two results can also be attributed to the Simpson numerical integration scheme used to evaluate the various inertias of each element. A more advanced numerical integration technique such as the Gaussian quadrature or even Simpson's $3/8^{th}$ method could lead to better results. The discrepancies in this particular case, however, are relatively negligible. Additional information about the TORAB program will be discussed in upcoming chapters.

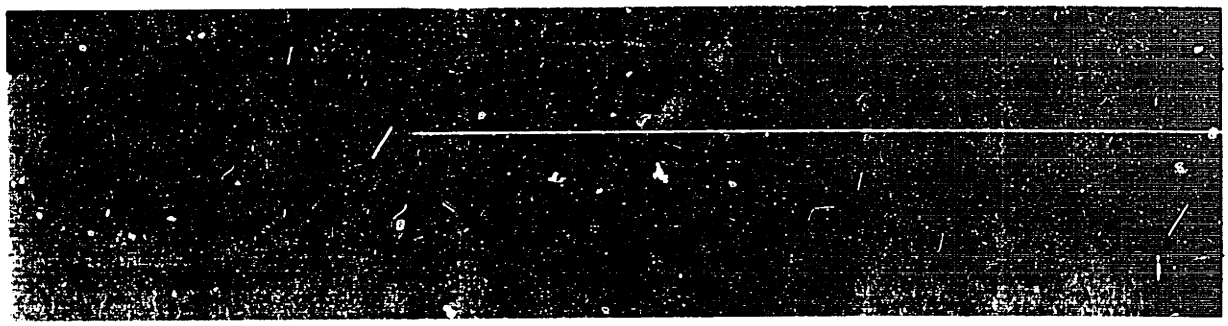

Table 1-1 Shear center calculation using Force Method and TORAB. All values are referenced from origin of section.

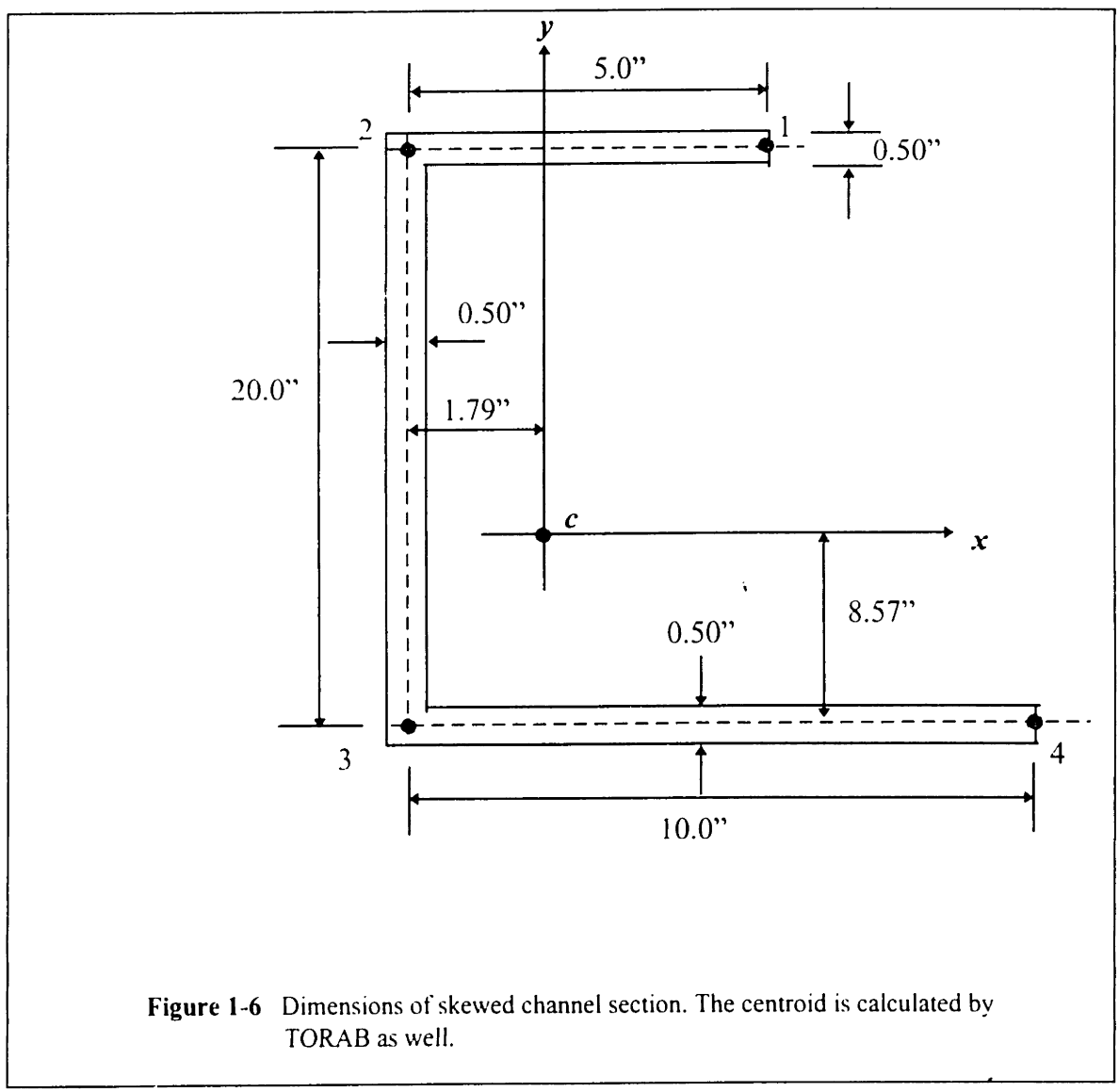

Figure 1-6 Dimensions of skewed channel section. The centroid is calculated by TORAB as well.

```
% Sample TORAB input file for skewed channel section
CROSS-SECTION
JOINT COORD
1 5. 20.
2 4.5 20.
3 4. 20.
4 3.5 20.
5 3. 20.
6 2.5 20.
7 2. 20.
8 1.5 20.
9 1.0 20.
10 0.5 20.
11 0. 20.
12 0. 0.
13 10. 0.
ELEM INCID
1 1 2
2 2 3
3 3 4
4 4 5
5 5 6
6 6 7
7 7 8
8 8 9
9 9 10
10 10 11
11 11 12
12 12 13
ELEM PROP
1 0.50
2 0.50
3 0.50
4 0.50
5 0.50
6 0.50
7 0.50
8 0.50
9 0.50
10 0.50
11 0.50
12 0.50
PRINT CENTROID
PRINT SHEAR CENTER
END
```

Figure 1-7 TORAB input file for Figure 1-6

Chapter 2

Pure Linear Torsion in Open and Closed Prismatic Sections

This chapter will describe the stress state on a cross section induced by a torsional moment M_z applied at the shear center of the section. The governing equations for pure or St. Venant's torsion will be mathematically developed using elastic theory and then be reduced from a three-state system equation to a two-state system through the use of Airy's Stress Function and Laplace's theorem. Prandtl's membrane analogy for the torsional response of a section will also be developed to abet in analyzing open and closed, thin-walled, multicontinuous cells. Similar to the shear center problem in Chapter 1, several numerical methods will be introduced to alleviate the inconveniences of solving line and surface integrals for such parameters as the torsional stiffness of a section. TORAB will be utilized to solve for these constants. Shear stresses caused by St. Venant's torsion will be analyzed separately from planar bending shear stresses so the effects of each can be isolated.

2.1 Differential representation of St. Venant's torsion

Pure torsion, as it will be referred to as from here forward, is developed from elasticity on the differential level using two basic assumptions. The first is an extension of Navier's hypothesis which states that a cross sectional plane ,prior to application of torsion, remains a plane after the torque is applied. This assumption allows the strains to remain proportional to the neutral axis. The second assumption is that Hooke's Law is valid. (i.e. stress is proportional to strain).

The stress state on one face of a differential element subjected to shearing stresses is illustrated in Figure 2-1a. The coordinate axes are referenced to the shear center of the entire section. The resulting torque M_z about the shear center can be expressed as

$$M_z = \int_0^A \left(S_{xz} y - S_{yz} x \right) dA \qquad 2.1$$

where S_{xz} and S_{yz} are the shear stresses acting on the *x*-*z* and *y*-*z* planes of the element, respectively. In Figure 2-1b a three dimensional view of the isolated element is depicted. In order for this element to be in a state of equilibrium, the $\sum F_z = 0$ or

$$S_{zx} dA_2 - \left(S_{zx} + \frac{\partial S_{zx}}{\partial x} dx \right) dA_2 + S_{zy} dA_3 - \left(S_{zy} + \frac{\partial S_{zy}}{\partial y} dy \right) dA_3 = 0 \qquad 2.2$$

which, when reduced, gives

$$\frac{\partial S_{zx}}{\partial x} + \frac{\partial S_{zy}}{\partial y} = 0 \qquad 2.3$$

By taking $\sum F_x = 0$ or from symmetry, a similar expression can be obtained

$$\frac{\partial S_{xz}}{\partial x} + \frac{\partial S_{yz}}{\partial y} = 0 \qquad 2.4$$

Finally, from summation of moments about the y and x axes, it can be shown that $S_{zx} = -S_{xz}$ and $S_{zy} = -S_{yz}$.

Some establishment of the relationship between the rotations and displacements must be created in order to interrelate the geometry, material properties, and stresses of a cross section. Timoshenko and Goodier proposed a relationship between in-plane distortions and rotation with the following equations:

$$v = x\phi \quad \text{and} \quad u = -y\phi \qquad 2.5$$

where the translational displacements in the horizontal and vertical directions are u and v, respectively. In addition to these in-plane distortions, an element will also displace an amount w out of the plane of the section in the z direction. Thus, the shearing strains on the element are equal to

$$\gamma_{xz} = \frac{\partial u}{\partial z} + \frac{\partial w}{\partial x} \quad \text{and} \quad \gamma_{yz} = \frac{\partial v}{\partial z} + \frac{\partial w}{\partial y} \qquad 2.6$$

The rate of change of the translational displacements u and v with respect to the axis of revolution of the applied torque (z-axis) can be derived by differentiating equation 2.5 with respect to z, or

$$\frac{\partial v}{\partial z} = x\frac{\partial \phi}{\partial z} = x\phi' \quad \text{and} \quad \frac{\partial u}{\partial z} = -y\frac{\partial \phi}{\partial z} = -y\phi' \qquad 2.7$$

where ϕ' is the change of the rotation per unit length. Material and geometric relationships between the shear strains, shear stresses, and the rotation of the cross section can be established by substituting equation 2.7 into 2.6 and identifying that for a

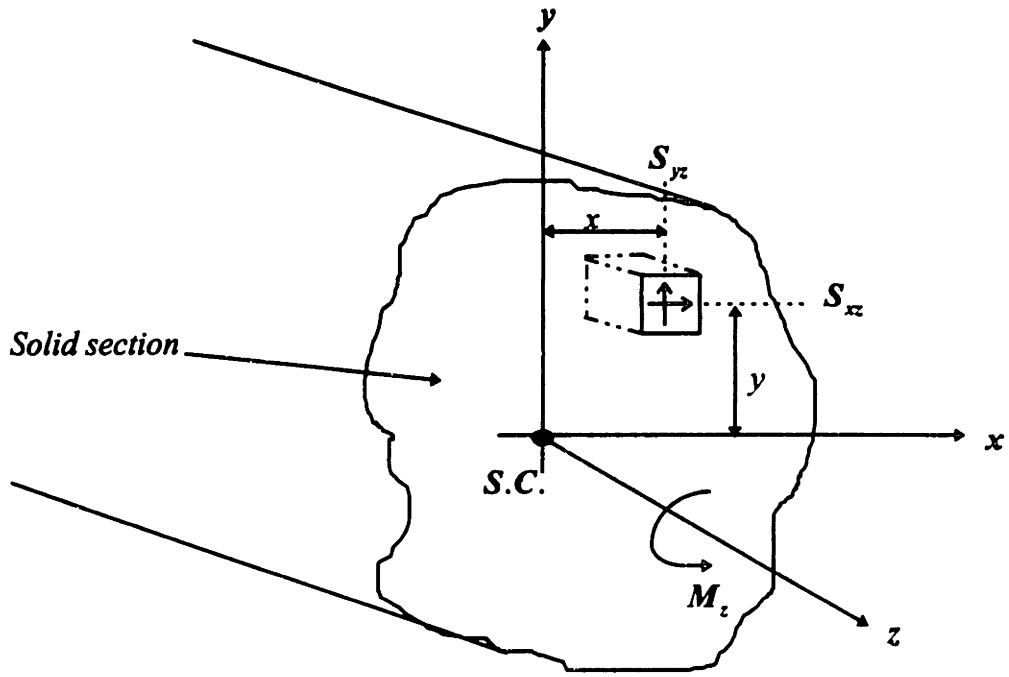

Figure 2-1a Shear stress distribution on *x-y* plane of discrete element due to external torque at shear center of cross section.

$$1 = (S_{yz} + \frac{\partial S_{yz}}{\partial z} dz) dA_1, \quad 2 = (S_{xz} + \frac{\partial S_{xz}}{\partial z} dz) dA_1$$

$$3 = (S_{zy} + \frac{\partial S_{zy}}{\partial y} dy) dA_3, \quad 4 = (S_{xy} + \frac{\partial S_{xy}}{\partial y} dy) dA_3$$

$$5 = S_{zx} dA_2, \quad 6 = S_{yx} dA_2, \quad 7 = S_{xy} dA_3$$

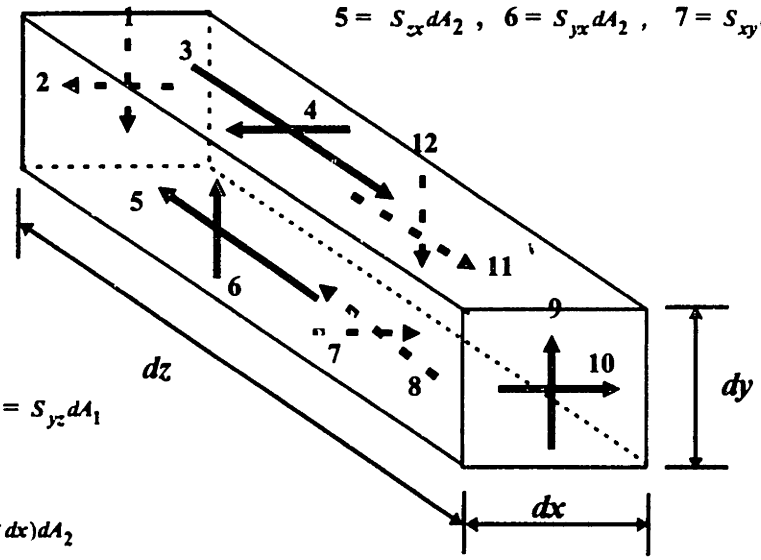

$$8 = S_{zy} dA_3, \quad 9 = S_{yz} dA_1$$

$$10 = S_{xz} dA_1$$

$$11 = (S_{zx} + \frac{\partial S_{zx}}{\partial x} dx) dA_2$$

$$12 = (S_{yx} + \frac{\partial S_{yx}}{\partial x} dx) dA_2$$

Figure 2-1b 3-D shear stress distribution from element in Figure 2-1a

linear elastic material, the strain γ can be related to the shear stress by the shear modulus or $\gamma = S / G$. Therefore,

$$\gamma_{xz} = \frac{S_{xz}}{G} = -y\phi' + \frac{\partial w}{\partial x} \qquad 2.8$$

$$\gamma_{yz} = \frac{S_{yz}}{G} = x\phi' + \frac{\partial w}{\partial y} \qquad 2.9$$

These equations can be combined into one by taking $\partial/\partial y$ of equation 2.8 and $\partial/\partial x$ of equation 2.9 and then, subtracting the two resulting equations. This leads to the expression

$$\frac{\partial S_{xz}}{\partial y} - \frac{\partial S_{yz}}{\partial x} = -2G\phi' \qquad 2.10$$

Equation 2.10 in conjunction with equation 2.1 gives an interrelationship between an external torque applied on a section and the shearing stresses and rotation that occur as a result of this torque. All that is needed to solve for the shearing stresses and rotation on a body due to an externally applied torque is the geometry of the section. Unfortunately, there are two equations and three unknowns (S_{xz}, S_{yz}, and ϕ). The need for an extra equation can be circumvented by introducing a function which relates the two shearing stresses together. This function is known as the Airy's Stress Function and was introduced by Seeley and Smith [Seeley and Smith, 1952].

2.1.1 Airy's Stress Function

The utilization of Airy's Stress Function to physically model the response of both shear stresses (S_{xz} and S_{yz}) through a single function is the force approach to rectifying

the problem of having two equations and three unknowns. This approach is explained by Connor [Connor, 1976] and will be redeveloped here so that a smooth transition into the membrane analogy can be made.

Assume that

$$S_{xz} = \frac{\partial \psi}{\partial y} \quad \text{and} \quad S_{yz} = -\frac{\partial \psi}{\partial x} \tag{2.11}$$

where $\psi(x, y)$ is function which can *possibly* identically satisfy the stress equilibrium equation listed in equation 2.4. Substituting these relationships from 2.11 into the equilibrium equation of 2.4 gives:

$$\frac{\partial^2 \psi}{\partial x \partial y} = \frac{\partial^2 \psi}{\partial y \partial x} \tag{2.12}$$

Thus, the relationship between the ψ function and the shear stresses is valid since it satisfies the equilibrium condition derived in equation 2.4. To reduce our three state variable system in equation 2.10, we can proceed to substitute the expressions for the shear stresses as a function of the Airy Stress Function (i.e., equation 2.11) into equation 2.10. This gives the following equation:

$$\frac{\partial^2 \psi}{\partial x^2} + \frac{\partial^2 \psi}{\partial y^2} = \nabla^2 \psi = -2G\phi' \tag{2.13}$$

This equation is a replication of Laplace's equation for two dimensional flow through a plate or any other two dimensional surface. A discussion about equation 2.13 will be presented in the next section. The equilibrium equation (2.1) can be modified by using equation 2.11, which gives:

$$M_z = \int_0^A \left(\frac{\partial \psi}{\partial y} y + \frac{\partial \psi}{\partial x} x \right) dA \qquad 2.14$$

Applying Green's theorem to equation 2.14 with the assumption that ψ is a harmonic function, leads to the following physical description relating the external torque to the Airy Stress Function:

$$M_z = 2\iint \psi \, dxdy \qquad 2.15$$

Equation 2.15 is significant in that the applied torque is exactly equal to twice the area under the ψ function. From equation 2.11 it can be seen that the shearing stresses are equal to the slope of the ψ function. Thus, once this ψ function can be evaluated, the shearing stresses can then be readily determined.

2.2 Laplace's equation of bidirectional flow in pure torsion

The solution of the basic torsion equation (2.13) can be obtained by creating an analogy between the element in examination and a thin membrane. Laplace's equation is used to describe the flow in a two dimensional medium. In this particular situation, it will be used to characterize the displacement field of a thin membrane. The displacement field is created as a result of a pressure being applied directly underneath the membrane. Thus, instead of solving for the abstract function ψ, we can solve for the displacement of a thin membrane under a pressure. The latter is something which can easily be derived from mechanics.

2.3 Prandtl's membrane analogy

The analogy between the Airy Stress Function and the displacement field of a thin membrane was first proposed by Prandtl [Prandtl, 1903]. This technique allows for a visualization of the ψ function by considering the inflation of a hypothetical thin membrane over the exact cross section which is subjected to a torsional moment M_z. Instead of being subjected to an external torque, the membrane will be exposed to an analogous external pressure q applied underneath it. The equilibrium of this fictitious membrane is an equation that is identical to the torsion equation in which the vertical displacement of the inflated membrane is analogous to the ψ function.

2.3.1 Analogy of Prandtl's membrane and the pure torsion problem

The cross section of an arbitrary beam is depicted in Figure 2-2a. The section has an inflated membrane placed over it which is subjected to a pressure q and has a displacement field $z(Z)$. The forces on a small element *dx-dy* of the thin membrane is illustrated in Figure 2-2b. Since the membrane is thin and has negligible bending resistance, only axial forces will preside normal to the edges of the membrane. These axial forces are denoted as S and are forces per unit length of the discrete membrane. It is imperative to mention that a body whose cross sectional dimensions are small in comparison to its longitudinal dimension is referred to as a *member* [Connor, 1976]. Unlike a member, a membrane is a two dimensional surface where one of the planar dimensions can not be neglected. Thus, the forces which act along the surface of the membrane are forces per unit length.

Transverse sections of the differential membrane along the *x* and *y* axes are depicted in Figure 2-2c. The two angles θ and $\bar{\theta}$ are obviously different since the edges dx and dy could be of different magnitudes. The summation of forces in the *z* direction must be in equilibrium or

$$\sum F_z = 0 = q dx dy - S dy \sin\theta + S dy \sin(\theta + d\theta) - \qquad 2.15$$
$$S dx \sin\bar{\theta} + S dx \sin(\bar{\theta} + d\bar{\theta})$$

Since the assumption of small strain theory is valid in linear cases, the perturbed angle from the normal is very small. Thus, the following assumption can be made

$$\sin\theta \cong \tan\theta \cong \theta = dz/dx \quad \text{and} \quad \sin\bar{\theta} \cong \tan\bar{\theta} \cong \bar{\theta} = dz/dy$$
$$\sin(\theta + d\theta) = dz/dx + (d^2z/dx^2)dx \quad \text{and} \quad \sin(\bar{\theta} + d\bar{\theta}) = dz/dy + (d^2z/dy^2)dy$$

Equation 2.15 can then be reduced to an extension of Laplace's equation by substituting the assumptions made on the angles and simplifying.

$$\frac{-q}{S} = \frac{d^2z}{dx^2} + \frac{d^2z}{dy^2} \qquad 2.16$$

2.3.2 Membrane analogy relationships

The differential equation (2.16) is similar to equation 2.13 where the displacement field *z(Z)* of the membrane is mathematically analogous to the ψ function, and the $-q/S$ term is analogous to $2G\phi'$. Since the differential equations are inherently similar in nature, the slopes of the membrane (first order change of the displacement field with respect to each side) $\partial z/\partial x$ and $\partial z/\partial y$ are analogous to the shear stresses which act along the cross section as a result of the external torque.

$$\frac{\partial z}{\partial x} \equiv \frac{\partial \psi}{\partial x} \equiv -S_{yz} \quad \text{and} \quad \frac{\partial z}{\partial y} \equiv \frac{\partial \psi}{\partial y} \equiv -S_{xz}$$

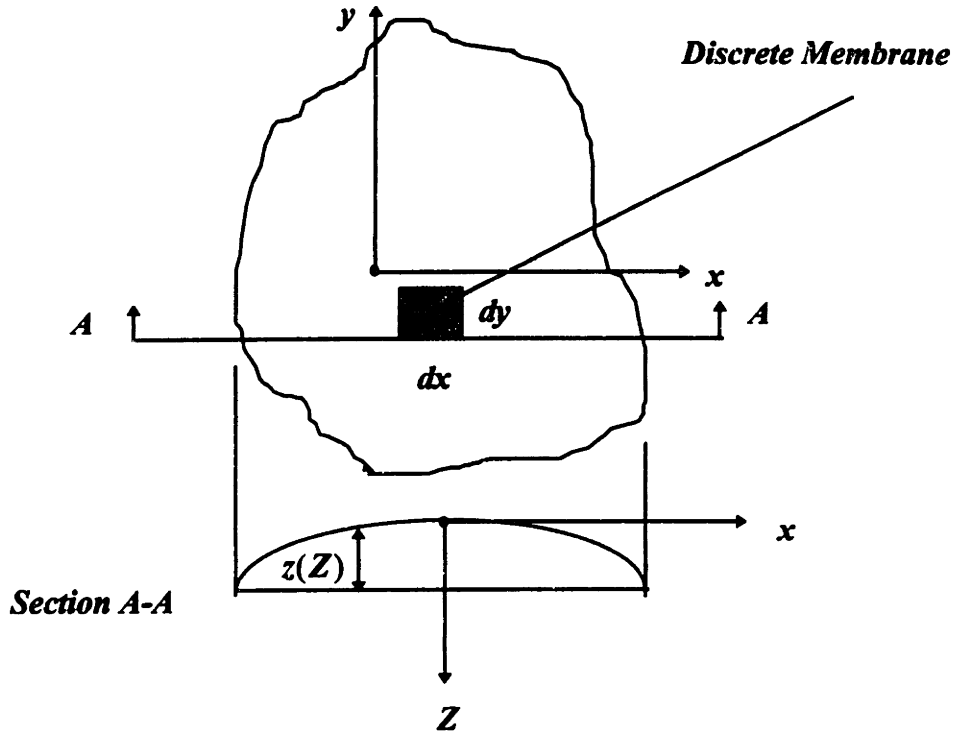

Figure 2-2a Inflated Membrane over a Solid Cross Section

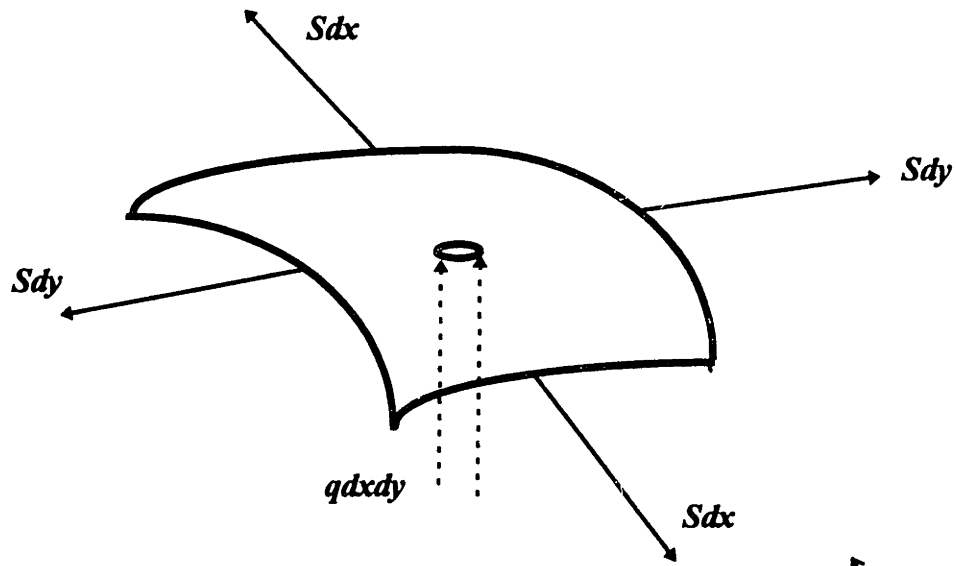

Figure 2-2b Free Body Diagram of Discrete Membrane

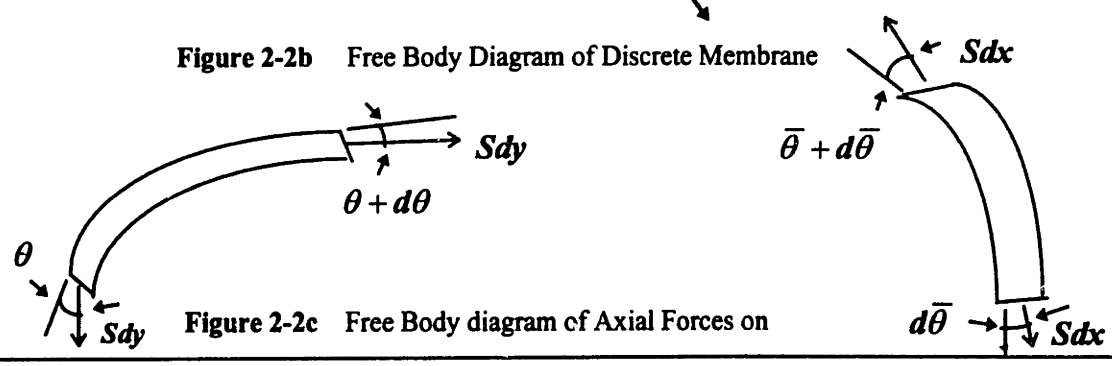

Figure 2-2c Free Body diagram of Axial Forces on

In addition to the relationship between the shear stresses and the slopes of the membrane, there is a monotonic relationship between the displacement z and the function ψ. Thus, from equation 2.15, the volume under the ψ function is analogous to the volume under the inflated membrane ($\iint z\,dxdy$). If the volume under the membrane were doubled, the value of the externally applied torque M_z can be obtained (equation 2.15). A summary of the interrelationships between the membrane and the two-state variable torsional functions is listed in Table 2-1.

Table 2-1 Membrane and Pure Torsion Relationship

$\frac{-q}{S} = \frac{d^2z}{dx^2} + \frac{d^2z}{dy^2}$	$-2G\phi' = \frac{d^2\psi}{dx^2} + \frac{d^2\psi}{dy^2}$
$\frac{\partial z}{\partial x}, \frac{\partial z}{\partial y}$	S_{xz}, S_{yz}
$V = \iint z\,dxdy$	$M_z = 2\iint \psi\,dxdy$

2.4 Solution of Laplace's equation using Prandtl's membrane

In order to obtain the solution for the displacement field of the membrane, an example must be used so a closed form solution can be derived. Since most structural cross sections are composed of flat rectangular elements (i.e., channels, tees, angles, wide-flanges, etc.) , a rectangular plate, like the one illustrated in Figure 2-3, will be used in the derivation. The height of the plate is not specified because only an in-plane section will be examined. The inflated membrane that is applied across any x-y plane of the plate is shown in Figure 2-4a with the corresponding free body diagram in Figure 2-4b. Again,

the membrane is assumed to be thin (length >> thickness) so that only axial forces prevail. This assumption also allows for the end effects of the membrane to be neglected.

The displacement $z(Z)$ of the membrane depicted in Figure 2-4b is assumed to have a parabolic distribution and a height of Z_O at its point of inflection. Thus, the shape of the displacement field can be approximated by the parabola $z(Z) = Ay^2$ where the coefficient A must be obtained from prescribed boundary conditions. Since at $y=t/2$, $Z=Z_O$, the coefficient A is

$$Z_o = At^2/4 \qquad \text{or} \qquad A = 4Z_o/t^2$$

which gives an expression for the displacement across the y-z plane of the membrane as

$$z = \frac{4Z_o}{t^2} y^2 \tag{2.16}$$

The slope of the displacement field is

$$\frac{dz}{dy} = 8\frac{Z_o}{t^2} y \tag{2.17}$$

which varies linearly since the original function was a second order function. From Table 2-1 the slope of the membrane is analogous to the shearing stresses in the same plane. Thus,

$$S_{yz} = \tau = 8\frac{Z_o}{t^2} y \tag{2.18}$$

The shearing stress is a maximum at $y=t/2$ or

$$\tau_{max} = 4Z_o/t \tag{2.19}$$

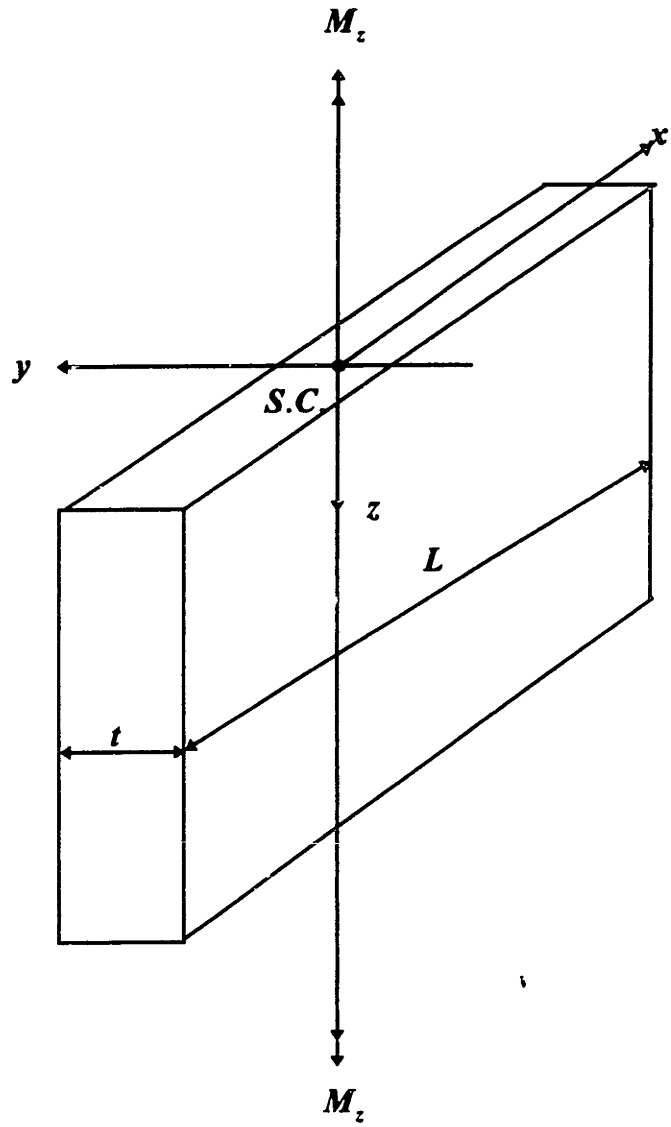

Figure 2-3 Rectangular Plate Element Subjected to External Torque

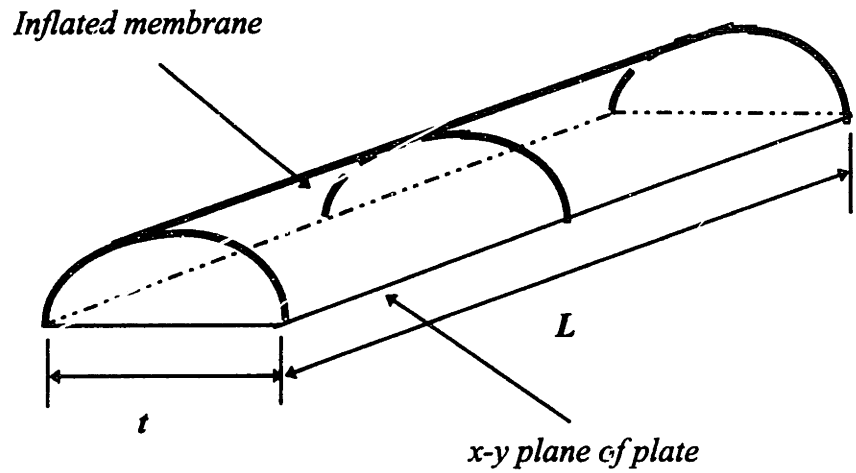

Figure 2-4a Inflated Membrane over the *x-y* plane of Plate in Figure 2-3

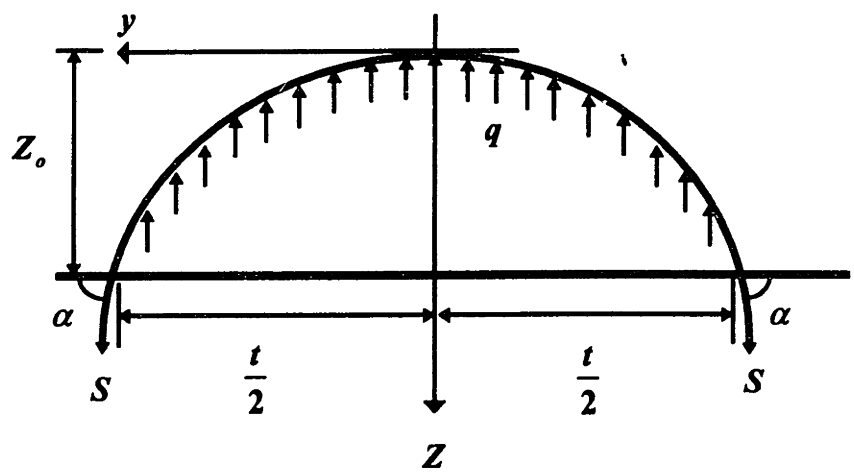

Figure 2-4b Free Body Diagram of Inflated Membrane

The shear flow can now be visualized since the characteristics of the slope of the membrane are known. Since the slope of the membrane changes its sign at $y=t/2$ and varies linearly across the thickness of the plate, the shear stress will do the same since it is analogous to the slope of the membrane. The shear flow actually changes direction at the mid-thickness of the plate which is where the tangent of the assumed displacement field is zero.

The magnitude of the shear stress is not known since the height Z_o of the membrane was assumed to be some constant. The height can be obtained by utilizing the analogy between the externally applied torque and the volume under the membrane. The volume under the membrane is $V = (2tZ_o / 3)L$ which results in a torque of $2V$. Thus, substituting and rearranging terms gives

$$Z_o = \frac{3}{4}\frac{M_z}{tL} \qquad 2.20$$

Equation 2.19 can be rewritten as

$$\tau_{max} = \frac{tM_z}{K_T} \qquad \text{where} \quad K_T = \frac{1}{3}t^3 L \qquad 2.21$$

which resembles the torsion formula for circular shafts where K_T is similar to the polar moment of inertia.

Laplace's equation has now been solved for the maximum shear stress in the cross section. However, the torsional stiffness constant K_T has to be resolved for any arbitrary cross section which entails built-up sections. Also, a basic force-rotation equation needs to be derived for numerical purposes. If this relationship can be developed, all that would need to be determined are a few innate properties of the cross section such as the shear modulus and the torsional stiffness. Thus, given the geometry of any section with an externally applied torque, the corresponding maximum shear stress

can be obtained by either looking at the force-rotation diagram or by directly solving an equation which can interrelate the shear stress on a section to its rotation.

2.5 Differential equation describing shear stress caused by pure torsion

In order to properly derive an equation that relates the external torque or shear stress to the rotation of a section, the membrane analogy summarized in Table 2-1 must be utilized again. Considering Figure 2-4b the distortion of the cross section can be obtained by looking at the equilibrium of the membrane which is inflated above it. By taking $\sum F_z = 0$,

$$qtL - 2SL\sin\alpha = 0 \qquad 2.22$$

It is important to recall that the pressure is per unit area and must be multiplied by the area to create an appropriate force, and the axial forces are per unit length of the membrane since the membrane is not a member but a plate. Assuming small strain and rotation theory, $\sin\alpha \cong dz/dy = 4Z_o/t$ at $y=t/2$. Substituting this value for the slope and the value for Z_o (2.20) into equation 2.22,

$$\frac{q}{S} = \frac{6M_z}{t^3 L} \qquad 2.23$$

From the membrane analogy summarized in Table 2.1, $q/S = 2G\phi'$ which, when substituted into equation 2.23 and isolated for M_z, yields the following

$$M_z = GK_T\phi' \qquad 2.24$$

where K_T is the torsional stiffness constant for a rectangular plate (2.21). Substituting equation 2.24 into 2.21, gives

$$\tau_{max} = Gt\phi' \qquad 2.25$$

Equation 2.24 is the force-rotation relationship that is needed to map the section's response to an external torque. This particular equation is also similar to the basic strength of materials torsion equation $\phi = TL/JG$, which can be modified to $\phi/L = \phi' = T/JG$. Numerically, the rotation at any point in the beam can be solved by analyzing the differential equation which governs the torsional response of the beam. The rotation is a function of two discrete variables: the externally applied torque and the boundary conditions on the beam. Although in the derivations the torque was assumed to be concentrated at the shear center, it can be a function of the longitudinal axis of the beam. The torque may be uniformly distributed, linearly varying, or even concentrated at different points along the beam. As mentioned previously, a force-rotation diagram can be created for different loading cases and boundary conditions since the shear modulus and torsional stiffness are constants with respect to a certain cross section. This is what equation 2.24 provides. A further discussion of the effects of pure torsion on a cross section and the incorporation of standard plots which depict the force-rotation interrelationships will be discussed after warping is introduced.

2.6 Approximation for torsional stiffness constant K_T

Use of the membrane analogy lead to the evaluation of the torsional stiffness K_T for a flat rectangular plate. This procedure, however, is very time consuming both numerically and physically especially if the cross section is quite complex. Also, when setting up the defining equations of structures or in stability investigation, the interest may not lie in the shear stresses obtained from the membrane analogy but instead, in the torsional rigidity of the members. Kollbrunner and Basler [Kollbrunner and Basler ,1966] developed an approximate equation which can be used to evaluate K_T for solid sections of any shape without having to calculate the shear stresses or rotations first.

The torsional stiffness constant is independent of the planar axes x or y just like the polar moment of inertia. For a rectangular plate, the polar moment of inertia is equal to the sum of the principal moment of inertias I_{xx} and I_{yy} where one of the inertias will be negligible since the thickness is much smaller than the length. Thus, the polar moment of inertia I_r is a good starting function for approximating K_T since both are independent of the planar axes. Kollbrunner and Basler assumed the following for K_T,

$$\beta I_r K_T = A^4 \quad \text{or} \quad K_T = A^4/\beta I_r \qquad \textbf{2.26}$$

where β is a constant which reflects the geometric arrangement of a particular cross section and A is the cross sectional area. This assumption is quite simple but very general since K_T is a function whose parameters should be independent of a particular coordinate system. The polar moment of inertia and the area satisfy this requirement. To evaluate the constant β , several shapes need to be examined. For a rectangular plate,

$$\beta = (A^4/I_r K_T) = (tL)^4/(tL^3/12 \cdot Lt^3/3) = 36$$

This expression is derived from the case where one length was presumably longer than the other. The constant β, however, should be determined from a cross section which has about the same length in every direction like a circle. A circular cross section has a β of about 40 which is a conservative assumption for any cross section. Equation 2.26 could then be expressed as:

$$K_T = A^4 / 40 I_r \qquad \textbf{2.27}$$

This formula is valid not only for cross sections with equal lengths along two mutually perpendicular directions, but also for cases where these lengths are quite different.

2.6.1 K_T for built-up solid cross sections

The previous developments were related to the behavior of a single solid element subjected to a torque of M_z. In most structures the section subjected to such a torque is composed of several such solid elements as illustrated in Figure 2-5. These built-up sections are used to absorb the torsion more efficiently since they have a much higher torsional stiffness. Assuming that each element in the cross section experiences the same rotation, the torsional response of the same section is characterized by:

$$M_{z_{Total}} = GK_T\phi' \quad \text{or} \quad \phi' = M_{z_{Total}}/GK_T \tag{2.28}$$

Since the rotations for each element j are assumed to be all equal,

$$M_{z_j}/(GK_T)_j = M_{z_{Total}}/GK_T \quad \text{or} \quad M_{z_j} = (K_{T_j}/K_T)M_{z_{Total}} \tag{2.29}$$

Equation 2.29, of course, assumes that the material is homogeneous throughout the cross section. The total applied torque $M_{z_{Total}}$ has to be equal to the sum of the torques absorbed by each individual element comprising the cross section. Therefore, summing up both sides of 2.29,

$$M_{z_{Total}} = \sum_{j=1}^{n} (K_{T_j}/K_T)M_{z_{Total}} \tag{2.30}$$

Since $M_{z_{Total}}$ is a constant,

$$K_T = \sum_{j=1}^{n} (K_{T_j}) \tag{2.31}$$

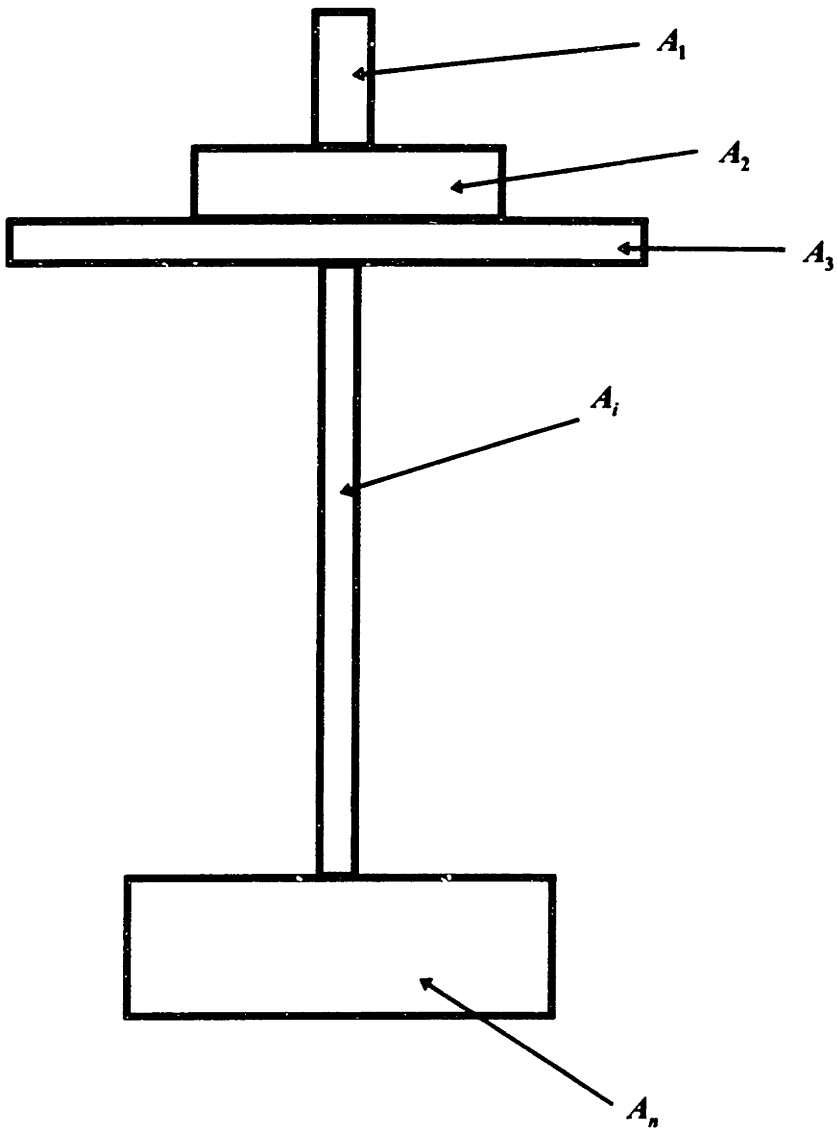

$\phi_i = \phi(i = 1,2,.....n \text{ elements})$

Figure 2-5 Built-up open cross section with assumed equal rotations

which signifies that the total torsional stiffness of the entire section is equal to the sum of the torsional stiffness of each element. Substituting equation 2.31 into 2.27 gives,

$$K_T \cong \frac{1}{40}\sum_{j=1}^{n}\frac{A_j^4}{I_{r_j}} \qquad 2.32$$

TORAB has the ability to determine the torsional stiffness for any cross section using equation 2.32. This constant is obviously needed to determine the torsional response of a beam.

2.7 Pure torsion on closed thin-walled cell sections

The membrane analogy that was used to develop an expression for the torsional stiffness constant of open and solid sections can also be extended for closed sections as well. Closed sections are more appropriate when torsion needs to be resisted since they possess a higher stiffness in the twisting direction of the section. Since these sections are thin-walled, they are hollow between the edges of opposite walls. The membrane analogy must reflect this by accounting for the fact that there are no shear stresses between the walls.

To proceed with adapting the membrane analogy to closed thin-walled sections, an arbitrary closed thin-walled section will be examined in detail (Figure 2-6). The section is assumed to be thin-walled which implies that the shear stress across the thickness of the element is constant. Bredt [Bredt, 1902] showed that this assumption was not true since the slope at the ends of a fictitious membrane placed above the section was always greater than the slope at the inner boundary. This difference in slope leads to an additional shear stress of $\Delta\tau$ which produces an extra torsional moment ΔM_z. Vlasow and Kolbrunner [Vlasow and Kolbrunner, 1961] argued that this extra torque could be ignored since the lever arm belonging to ΔM_z is the thickness of the wall which is relatively small compared to the other cross section dimensions. As a rule of thumb,

Vlasow proposed that the error in calculating the shear stresses for a hollow cross section with a constant wall thickness is less than 10% when the effective area of the cross section is less than one fifth the area enclosed by the wall center line.

Figure 2-6 depicts a thin-walled closed cell with an external torque applied at its shear center. The corresponding membrane associated with this cell changes its slope twice due to the distribution of the shear stresses throughout the section. As stated in Table 2-1 the slopes of the membrane are directly related to the shear stresses in the actual cross section. Thus, the slope of the membrane positioned across the thickness of the section is constant while the remaining portion spanning the hollow area is zero since there is no shear stress there. Using the membrane analogy,

$$\tau = Z_o/t \quad \text{or} \quad Z_o = \pi t$$

For equilibrium to hold, the externally applied torque M_z has to balance the moments caused by the shear flow around the cross section or

$$M_z = \pi t \oint_S \rho \, ds \qquad 2.33$$

where the line integral is taken around the surface S (the perimeter of the cross section) and ρ is the perpendicular distance from the shear center to the centerline of each individual element. The shear flow πt is a measure of force per unit length and is independent of its location on the surface since it is constant (from the assumption about thin-walled cells). From geometry the area enclosed by the ds element is related to the line integral in equation 2.33 by the following equation:

$$dA = \frac{1}{2} ds\rho \quad \text{or} \quad 2dA = \rho ds$$

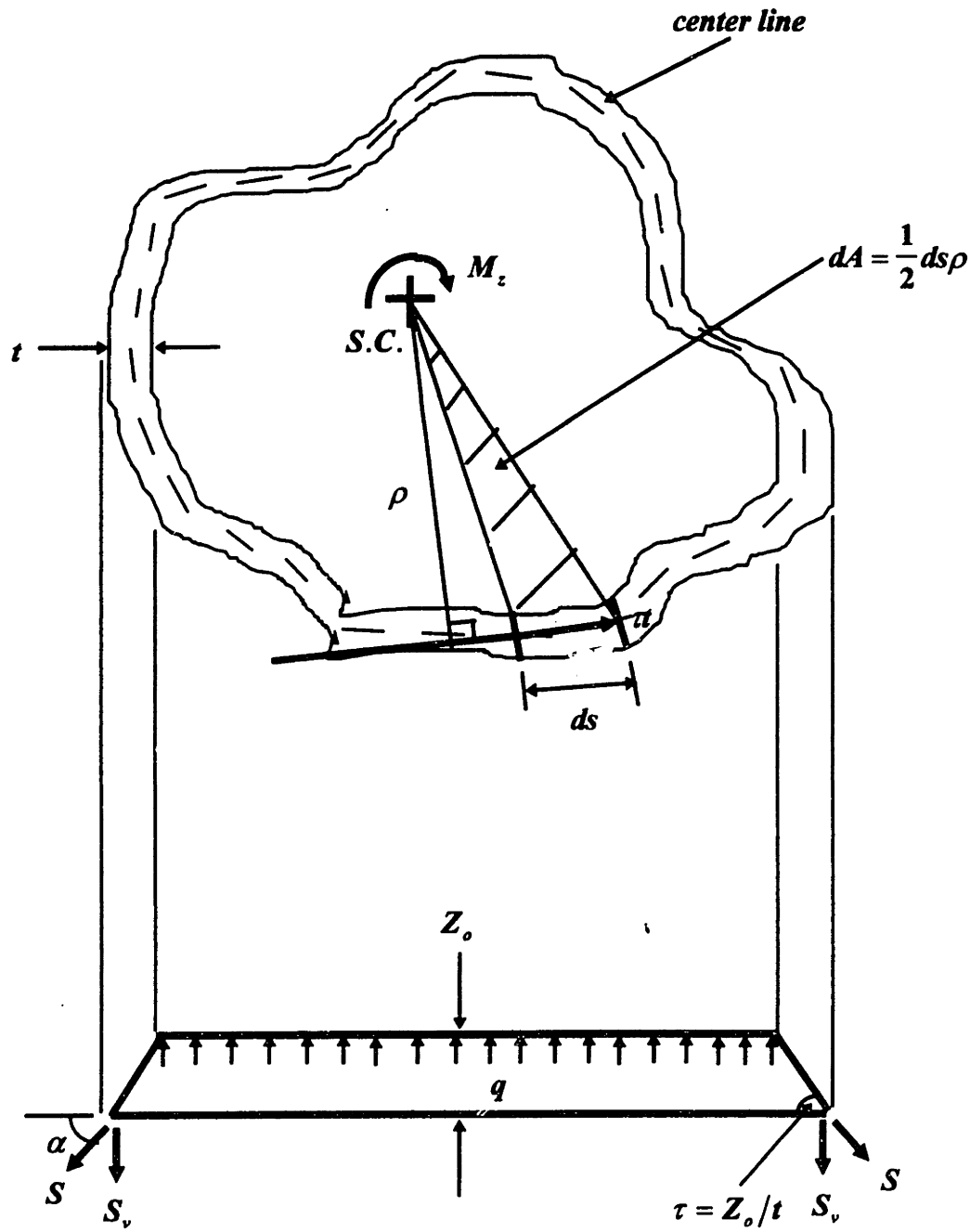

Figure 2-6 Membrane of a thin-walled closed cross section

Integrating both sides of equation 2.33 states that the $\oint_S \rho\, ds$ is equivalent to $2A_O$ where A_O is the area enclosed by the thin-walled cross section. Using this fact, equation 2.33 can be rewritten as

$$M_z = 2\pi t A_o \qquad 2.34$$

The primary goal in the development of an equation which defines the pure torsional response of a closed thin-walled cell is to maintain the integrity of equation 2.28. By conforming to the same functional parameters as 2.28, the application of closed thin-walled and open sections to a pure torsional load can be identified without any changes in the structure of an algorithm. Since the rotation, of which the solution will be discussed in later chapters, and the shear modulus can readily be obtained for thin-walled sections, all that is required is a closed form relationship defining the torsional stiffness K_T. The summation of forces in the z-direction must be in equilibrium for the membrane in Figure 2-6 so:

$$\sum F_z = 0 \quad \text{or} \quad qA_o = \oint_S S_v\, ds \qquad 2.35$$

where, from Figure 2-6, $S_v = S\sin\alpha = S Z_o/t = S\tau$. The slope of the membrane (or the shear stress in the section) is a linear term which depends only on the thickness and the height of the inflated membrane. The thickness and the shear stress are inversely related since as the thickness decreases, the shear stress increases. Since a constant shear stress distribution was assumed in the wall, the force S along with the height of the membrane will also be constants. Thus, equation 2.35 can be expressed as:

$$\frac{q}{S} = \frac{Z_o}{A_o}\oint_S \frac{ds}{t} \qquad 2.36$$

From the membrane analogy summary in Table 2-1, the right hand side of the Laplacian equations signifies that $q/S = 2G\phi'$. Also, from equations 2.34 through 2.36, it can be shown that $Z_o = M_z/2A_o$ which, when substituted into equation 2.36 and simplified, yields:

$$M_z = \left(\frac{4A_o^2}{\oint_S \frac{ds}{t}} \right) G\phi' \qquad 2.37$$

The form of this equation is identical to that of equation 2.28 if K_T is defined as:

$$K_T = \frac{4A_o^2}{\oint_S \frac{ds}{t}} \qquad 2.38$$

which gives $M_z = GK_T\phi'$. Thus, the pure torsional response of a thin-walled closed cell is governed by the same equation as a solid rectangular element. Substituting the value for the externally applied torque from equation 2.37 into 2.34, the shear stress in the section is defined as:

$$\tau = \left(\frac{GK_T}{2A_o t} \right) \phi' \qquad 2.39$$

2.7.1 Pure torsion on multicontinuous cells

Multicontinuous cells are prevalently seen as box girders which are essential in bridge construction. These particular cells are simply a group of closed, thin-walled, single cells attached to each other with no separation. Since each individual cell

obviously affects the behavior of an adjacent cell, the determination of the shear stresses can not be made directly as in the case of the single cell. The sectional stresses are indeterminate and thus, require the development of special relationships between each cell. These cells can be thought of as spans of a continuously supported beam where the boundaries of adjacent cells are prescribed boundary conditions or supports.

To attack the boundary problem, the shear flow in a multicell section (Figure 2-7) has to be carefully inspected. Any multicell section has to be continuous which implies that the wall thickness of adjacent boundary elements must be the same. Most box sections have the same thickness around its perimeter for economical and practical reasons. Although the webs or flanges of these sections can be tapered, it will not be considered in this section or in TORAB. The summation of forces in the z-direction of the membrane derived in section 2.7 (equation 2.35) can be rewritten as

$$\oint_S \tau \, ds = 2M_z A_o / K_T \qquad \textbf{2.40}$$

if the term S_v is replaced by $S\tau$ $(= SZ_o/t)$ and $G\phi'$ replaced by M_z/K_T. The line integral now represents the flow of stress around a single cell and A_o is the area enclosed by each cell. In Figure 2-7 cells 1 and 2 share a common boundary element labeled C. The shear stress flow in each cell is assumed to be acting counterclockwise which will be designated as the positive direction. Since the shear stress contribution from cell 1 (τ_1) is resisting the shear stress in cell 2 (τ_2), the net shear stress acting on the boundary is simply the difference between the two stresses. By defining the shear stress τ as q/t, where q is the shear flow, equation 2.40 can be applied to cell 1 as follows:

$$q_1 \oint_1 \frac{ds}{t} - q_2 \int_1^2 \frac{ds}{t} = 2\left(M_z/K_T\right)A_{o_1} \qquad \textbf{2.41}$$

where the line integral sums up the stresses around cell 1 and the definite integral represents the shear stress of the wall which is adjacent to cells 1 and 2 (segment C in

Figure 2-7). The term A_{o_1} is the enclosed area o cell 1. This particular example can be related to Kirchoff's law of voltages which states that the sum of the voltages around a loop in a circuit has to be equal to the sum of the externally applied voltages on that circuit. Each multicontinuous cell can be thought of as a loop in the circuit where the moments caused by the shear stresses are the internal voltages while the external torque is the externally applied voltage. Also, similar to Kirchoff's law, all boundary segments must equilibrate the voltages coming from all cells which share this segment.

In general equation 2.41 can be applied to a series of interconnected multicells which possess several adjacent boundary segments.

$$q_j \oint_j \frac{ds}{t} - \sum_k q_k \int_{jk} \frac{ds}{t} = 2\left(M_z / K_T\right) A_{o_j} \qquad 2.42$$

where the line integral represents the total shear stress along the entire cell j, and k are the number of cells which are adjacent to cell j. If there are n cells in the system, equation 2.42 will produce n simultaneous equations of the form

$$q_i = \overline{C}_i \left(M_z / K_T\right) \qquad 2.43$$

where $\overline{C}_i$ is a vector of constants obtained after solving 2.42 for q. The solution of 2.42 can not be directly obtained since the value of the torsional stiffness constant K_T is unknown during the solution process. Therefore, once the constant vector $\overline{C}_i$ is obtained, the torsional stiffness constant can be expressed in terms of this vector. Using the membrane analogy, the externally applied torque is equivalent to twice the volume under the membrane. Thus,

$$M_z = 2\sum_{i=1}^{n} q_i A_i = 2\sum_{i=1}^{n} \overline{C}_i (M_z / K_T) A_i \qquad 2.44$$

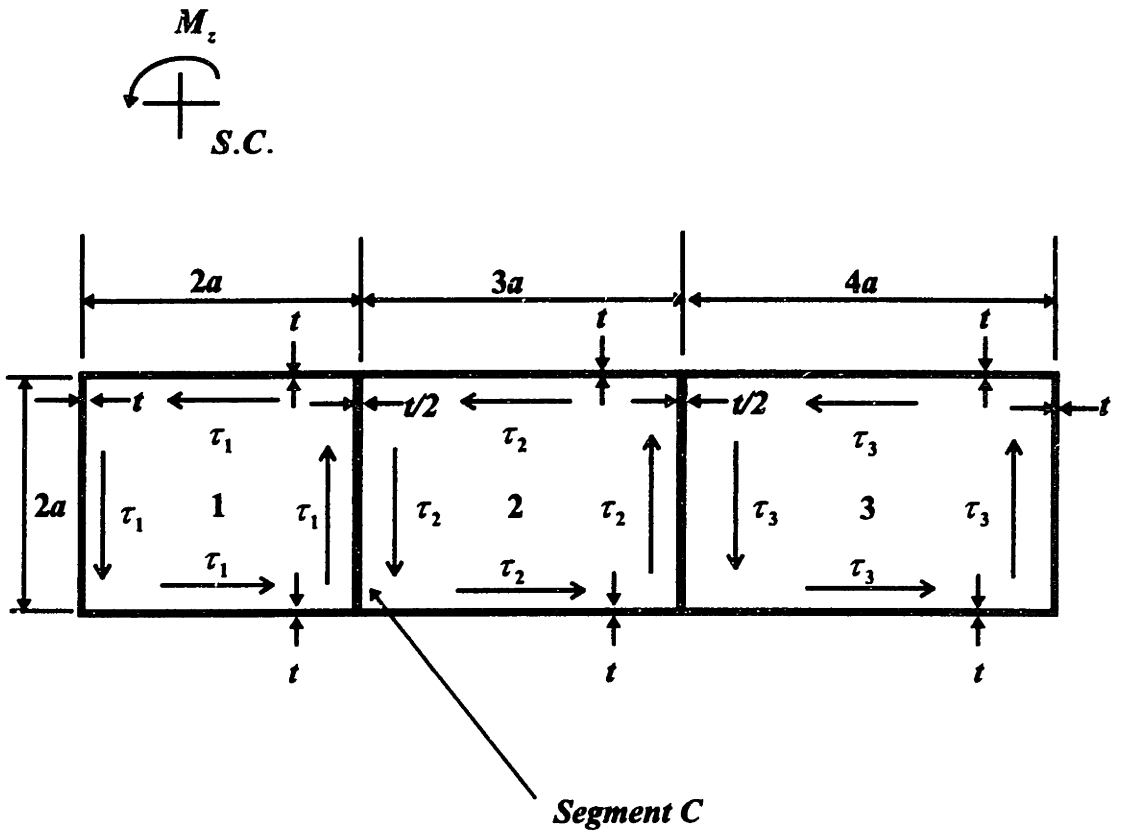

Figure 2-7 Shear stress distribution in a 3-span multicell section. CCW is taken as the positive sense for stress and rotation.

Since the torque is a constant, it can be taken out of the summation which gives

$$K_T = 2\sum_{i=1}^{n} \overline{C}_i A_i \qquad 2.45$$

The analysis of multicontinuous cell systems requires only the geometry and the loading of the system. The solution for the rotation of the system is not required since the ratio of $G\phi' = M_z / K_T$ was used to eliminate that particular unknown. However, the unknown was eliminated by introducing another unknown which could be solved for in a more systematic manner. Since the torsional stiffness for any arbitrary section (open or closed thin-walled) is already being calculated for the pure torsion problem, the algorithm which produces the constant needs to be slightly altered to encompass single or multicontinuous cells. The algorithm has to be passed a flag which tells it if a closed thin-walled section is being analyzed. If this is the case, the algorithm needs to revert to another solution process which specifically handles closed thin-walled sections.

Solid rectangular elements found in open cross sections follow Kollbrunner and Basler's equation (2.27) which is derived from relating the polar moment of inertia to a factor β. The form of this equation has its rudimentary basis from the membrane which was imposed on the solid rectangular element. Since the membrane changes slope along its length (parabolic nature), the shear stress also changes parabolically. In the thin-walled case the shear stress is assumed to remain constant across the thickness of the section. Thus, the membrane behaves linearly. The major difference in the computation of the torsional stiffness lies in the shear force distribution in the membrane. With the open section, the shear force is finite since the forces only act at an angle at the ends of the membrane. In the closed thin-walled section a summation of the forces along the surface of the section must be taken since the surface is not defined like the rectangular elements comprising the open structural sections. Thus, the equilibrium of forces in the

z-direction of the membrane produce a different expression for the torsional stiffness constant.

The use of TORAB to analyze single and multicontinuous cells will be discussed in later chapters with specific examples. The simultaneous equations are stored using normal matrix techniques. The solution of the linear equation $\tilde{A}\bar{X} = \bar{B}$ is solved using Gaussian elimination with partial pivoting. When enormous multicell systems are analyzed, more powerful computational techniques are necessary to solve for the unknown stresses such as an active column storage algorithm or the conjugate gradient method. These topics, however, are beyond the scope of this thesis. Once the unknown values of $q\,(=\tau/t)$ are obtained from the solution of equation 2.42, the stresses in the cells are evaluated by simply multiplying by the thickness of the cross section. For the boundary segments, the shearing stresses are equal to the difference between each adjoining cell shear stress value τ_j and τ_k or:

$$\tau_{jk} = 2\left(\tau_j - \tau_k\right)\left(M_z/K_T\right)l \qquad \textbf{2.46}$$

where l is a unit of length obtained after solving the linear equations in 2.42. The factor of two is to account for the shear stress on each side of the boundary element. When the stresses are obtained, it is important to understand the signs that are associated with the magnitudes. If the sign is negative, the stress is acting clockwise (negative sense) which indicates the initial assumption was incorrect.

2.7.2 Advantages of membrane analogy in analysis of multicell sections under pure torsion

The most advantageous facet of using the formulation presented in equation 2.42 is that it allows for a direct combination of bending stresses caused by planar bending forces. If planar bending shear stresses are applied to a multicell section, a similar formulation can be derived using equation 1.10. The only obstacle lies in the fact that equation 1.10 is applicable for thin-walled open cross sections whereas multicell sections

are closed. If the equation was directly applied to a closed cell section, a free edge would be required for the integral to evaluate the first moment of areas Q_x and Q_y (1.9). In the instance of a closed cell, there is no free surface and thus the integration $\int_0^s$ is not valid in determining the shear flow. To utilize equation 1.10, an imaginary cut is made at some location on the cell, or in the case of multicells, enough cuts are made to determine the bending shear flow around each of the cells. When the structure is cut, however, the shear flows become discontinuous at the edges. In order to restore compatibility, an unknown shear flow(s) is/are applied at the cut(s) to close the cut.

The constraint equation which ensures compatibility can be compared to a Lagrange multiplier. This particular type of multiplier includes the constraint equation in the solution equation similar to the inclusion of enforced displacements in the formulation of finite element equations. The compatibility equation is that the shear deformation, integrated around each cell j, must equal zero or

$$\oint_j \gamma \, ds = 0 \qquad \textbf{2.47}$$

This constraint or Lagrange multiplier can be compared to Kirchoff's law of currents where the sum of the currents around a loop must be equal to zero. The shearing strain $\gamma = \tau/G$ or $\gamma = q/tG$ where q is the shear flow which is equal to the sum of the shear flow in the open section (q_o) and the redundant or indeterminate shear flow applied to close the cut (q_r). Substituting these values into 2.47 gives,

$$\oint_j \frac{q_o}{Gt} ds + q_r \oint_j \frac{ds}{Gt} - \sum_k q_k \int_{jk} \frac{ds}{Gt} = 0 \qquad \textbf{2.48}$$

where the summation component represents the adjacent cells which share common boundaries. The above equation is almost exactly analogous to equation 2.42 for pure torsion. The surface integrals ds/t are evaluated by simply dividing each individual

element's length by its thickness. By establishing this relationship between plane bending shear stresses and pure torsional shear stresses, one algorithm could solve for the stresses caused by each phenomena and then simply superimpose them. Along with solving for the shear stresses of the open section q_o (which is done using equation 1.10), the redundant or indeterminate shear stresses that are applied to close the section must also be solved for. Thus, the linear equation $\tilde{A}\bar{X} = \bar{B}$ which needs to be solved in this particular case has $\tilde{A}$ as the matrix containing the coefficients of the redundant shear stresses, $\bar{X}$ as a vector containing the redundant shear stresses, and $\bar{B}$ as a vector containing the constants derived from the shear stresses of the open cross section (i.e. $\oint_j q_o/GT\,ds$). For the situation of torsional shear stresses, the matrix $\tilde{A}$ contains the coefficients of the shearing stresses around each cell, $\bar{X}$ contains the actual shear stresses, and $\bar{B}$ contains the right hand side of 2.42. It is important to note that the bending shear stresses vary around each individual cell since the first moment of area changes with respect to the local y-axis. This is the reason why q_o is inside the integral.

TORAB was not equipped to handle bending shear stresses, but a more advanced computer program could easily incorporate the aforementioned theory. It is the belief of the author that this relationship derived from the membrane theory has not been properly automated in any commercial programs. However, the simplification of the mechanics of pure torsion to a more sensible numerical scheme (TORAB) should be a stepping point to introduce pure torsion into everyday structural analysis.

Chapter 3

Warping Torsion in Open and Closed Prismatic Sections

In chapter 2 the distributions of shearing stresses due to an applied torque M_z at the shear center on solid, thin-walled open and closed cross sections were analyzed. The displacements that were acting on the section were in the plane of the section while the out of plane displacement was assumed to be unrestrained. If the out of plane displacements are restrained or altered, normal and shear stresses will be induced into the beam. These normal and shear stresses are referred to as warping normal and warping shear stresses, respectively. The warping shear stresses will provide an additional torsional restraining moment similar to the moment caused by the shear flow when only pure torsion was applied. This moment, defined as the warping torsional moment, in conjunction with the pure torsional moment maintain equilibrium for the beam. Functional warping parameters of the cross section like the normalized unit warping function and the warping statical moment will be developed analytically for a general cross section and then be evaluated using a numerical procedure. An equation relating the warping normal and shear stresses to these functions and the rotation of the beam will also be evaluated. TORAB will also be utilized to solve for the aforementioned functional parameters.

3.1 Significance of warping torsion; Assumptions made in theory

A prismatic member exhibits two ways to resist twist. The first results in a circulatory shear flow in the cross section while the second yields shear stresses resulting from the change in axial stresses. The first contribution was discussed in Chapter 2 and is referred to as pure torsion. The latter phenomena is denoted as warping torsion and is usually negligible in most cases. Design methods such as the ASD (Allowable Stress Design) account for warping torsion by allowing local corrections in certain members such as slender members with compact solid or hollow cross sections. Warping torsion is a fairly new subject that was not fully realized until the past fifty years. The mechanics behind it are fairly sophisticated and require the development of an unique coordinate system in order to keep track of the sign conventions for force and rotation.

When dealing with warping torsion, the assumption of plane sections remaining plane no longer holds valid. For structural components, however, the web extension of the section is assumed not to experience any planar rotation. The reason for this is that all flanges can then be assumed to deflect laterally an equal amount. Thus, it is assumed the web is thick enough compared to the flanges so that it does not bend during twisting as a result of the high torsional resistance of the flanges. Kubo and Johnston [Kubo and Johnston , 1956] showed that except for thin-web plate girders, neglecting lateral bending in the web does not affect the warping response of the entire section. If an external torque is applied through the shear center of a cross section, in and out of plane displacements will occur. The in-plane displacements contribute to the closed shear flow (pure torsion) while the out of plane displacements pertain to the warping of the section. If these particular displacements are somehow restrained or altered along the axis of the section, the existing axial stresses will undergo a perturbation which results in extra shear stresses being produced.

3.2 Warping moment in a general open cross section

It is much easier to represent the displacements (in and out of plane) of an open cross section using curvilinear coordinates rather than Cartesian. Thus, the expressions for the shearing strains must be rewritten to reflect this new curvilinear system. From the shearing strains, a relationship between the normal and shear stresses and the rotation of the section can be developed which in turn, leads to a closed form expression for the moment induced by the section to abet in resisting the externally applied torque.

The same stress block depicted in Figure 1-4 can be used to derive the basic warping equations except that all strains and displacements will be referenced with respect to the arc coordinate s. From equation 2.6 the shearing strain in the y-z plane of a differential element was defined as the change in position of the element with respect to the z and y axes. If the out of plane displacement w is measured in terms of the arc length (along the longitudinal surface of the element) s, the shearing strain can be written as

$$\gamma = \frac{\partial w}{\partial s} + \frac{\partial v}{\partial z} \qquad 3.1$$

The displacement v along the curvilinear coordinate s needs to be expressed in terms of displacements acting in the x- and y-directions and the rotation around an axis which is parallel to the member axis z. In order to accomplish this, a new set of coordinate labels (ξ, η, ϕ) will be used to denote the respective displacements mentioned above. To clarify this reference system, Figure 3-1 depicts the side view of the discrete element from Figure 1-4 with the direction of the in-plane displacement v. This particular displacement must be put in terms of the ξ, η, ϕ system which can be though of as the local x-y-z coordinate frame. Although the shearing strain in the y-z plane was chosen to express the displacements in the ξ, η, ϕ system, the derivation could proceed using the shearing strain in the x-z plane as well. In that case, the displacement in question would be u.

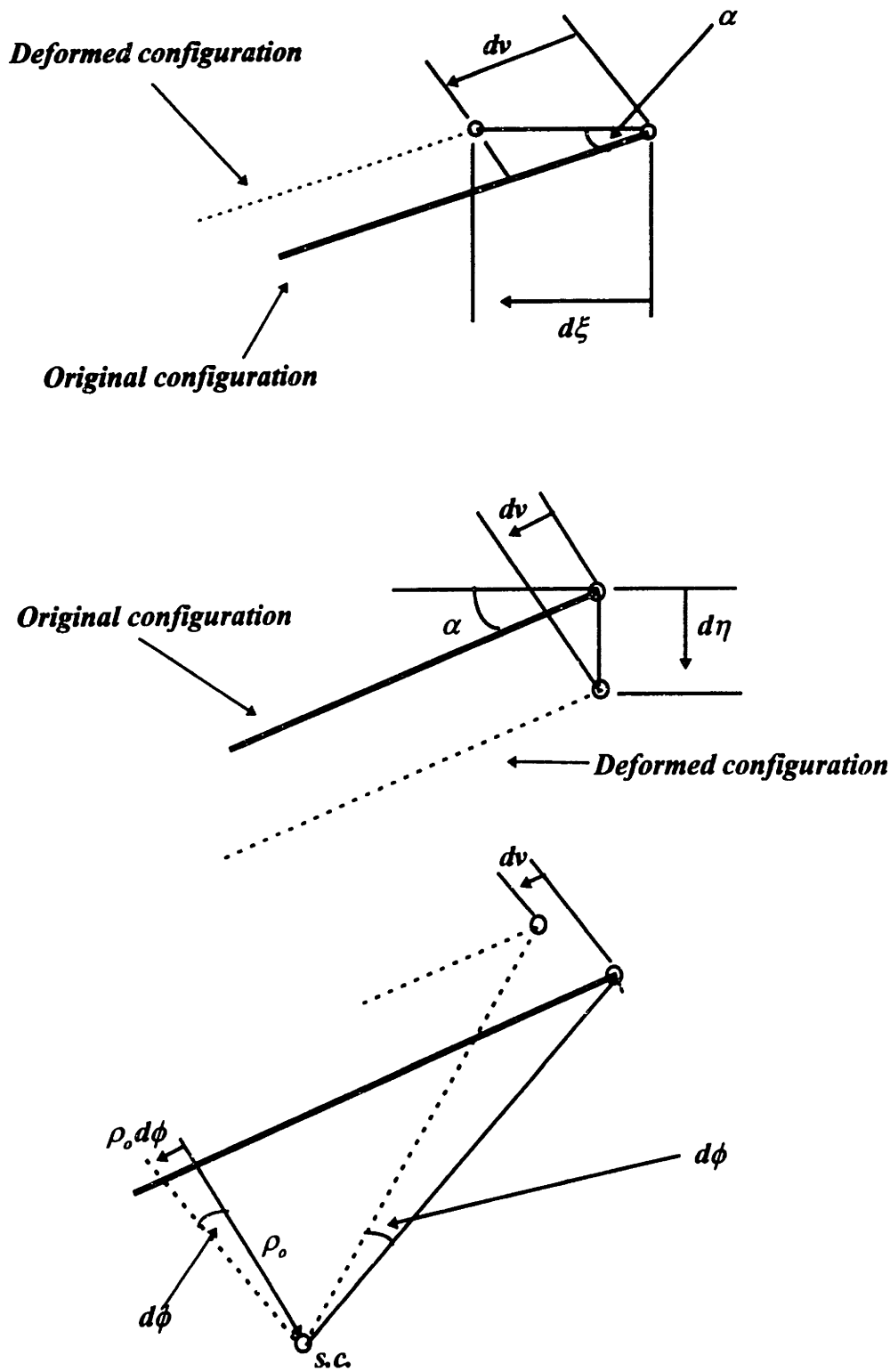

Figure 3-1 Deformations and displacements of a discrete thin-walled element. The first two pictures show the v displacement along the x and y surfaces, respectively. The last picture illustrates the relationship between the displacement v and the rotation ϕ.

The angle α represents the inclination between the positive x-axis and the positive tangential direction measured counterclockwise. Thus, the tangential displacement v can now be written in terms of the local translational and rotational degrees of freedom

$$dv = d\xi \cos\alpha, \quad dv = d\eta \sin\alpha, \quad dv = \rho_o d\phi \qquad \textbf{(a)}$$

The distance ρ_o is the perpendicular distance from the shear center of the cross section to the tangent of the discrete element. The sign of this distance can be chosen to be anything as long as it is consistent. Heins and Yoo [Heins and Yoo , 1974] suggested that this value should be positive if the shear center is to the left of the element when viewing it from node j to node k where node j represents the starting point of the element and node k the ending point. This particular notation is well suited for numerical purposes since the orientation of all the elements comprising the cross section can be defined with respect to the shear center. Superimposing the contributions of the tangential displacement v from the two translational and one rotational directions,

$$dv = d\xi \cos\alpha + d\eta \sin\alpha + \rho_o d\phi \qquad \textbf{3.2}$$

Since ξ, η, and ϕ are functions of the coordinates s and z while α and ρ_o do not depend on z, the contribution of the displacement v in the y-z shear strain can be expressed as:

$$\frac{\partial v}{\partial z} = \frac{\partial \xi}{\partial z}\cos\alpha + \frac{\partial \eta}{\partial z}\sin\alpha + \rho_o \frac{\partial \phi}{\partial z} \qquad \textbf{3.3}$$

In the instance of pure torsion only, there are no axial forces or bending moments being induced on the cross section. Thus, the displacements in the ξ and η directions are zero which reduces equation 3.3 to the following:

$$\frac{\partial v}{\partial z} = \rho_o \frac{\partial \phi}{\partial z} \qquad \textbf{3.4}$$

The formulation of 3.4 has some intrinsic assumptions built into it. The first assumption is that the integrity of the cross sectional shape has to be preserved. This means that the functions $\xi(s,z)$, $\eta(s,z)$, and $\phi(s,z)$ have to assume equal values at all points of the cross section and must not depend on the cross sectional coordinate s. In other words these functions vary over the length of the beam but are representative for the entire cross section. The second assumption assumes negligible shear deformation which means the shearing strain in equation 3.1 is zero. Although Timoshenko [Timoshenko , 1945] developed a similar formulation with shear deformation included, that topic will not be covered here. With this assumption equation 3.1 can be rewritten as:

$$\frac{\partial w}{\partial s} = -\frac{\partial v}{\partial z} = -\rho_o \frac{\partial \phi}{\partial z} = -\rho_o \phi' \qquad \textbf{3.5}$$

The final assumption is that Hooke's law holds valid which means that the first derivative of the displacements are related to the stresses by Young's modulus or $\sigma = E\,\partial w/\partial z$.

3.2.1 Relationship of unit warping to tangential displacement

The tangential displacement v is related to the out of plane displacement w by equation 3.5. Rewriting this equation to isolate w gives,

$$dw = -\rho_o \phi'\, ds \qquad \textbf{(a)}$$

Integrating equation (a) over the surface of the section results in the following:

$$w = -\phi' \int_0^s \rho_o \, ds + \overline{w}_o(z) \qquad 3.6$$

where w is the out of plane displacement or warping of a particular element in the cross section. $\overline{w}_o$ is the constant of integration that is undetermined as of yet. This expression clearly shows that plane cross sections do not necessarily remain plane when the section is subjected to pure twist. The cross section warps according to the longitudinal displacement w. Since we are dealing with structural cross sections which are comprised of rectangular elements, the warping w is, at most, distributed linearly across the section. If the tangential distance ρ_o is not constant (i.e. for curved surfaces), the warping w would be a function of the surface function governing the shape of the element. In this case ρ_o would have to be left in the integral in equation 3.6. Defining a new constant w_o as the unit warping with respect to the shear center,

$$w_o = \int_0^s \rho_o \, ds \qquad 3.7$$

equation 3.6 can be expressed as:

$$w = -\phi' w_o + \overline{w}_o \qquad 3.8$$

The relationship between the rotation and warping of an element in a section is defined in 3.8. From the shear strain in a plane of the section, the out of plane and in-plane displacements were expressed in terms of a coordinate system that only varied along the length of the beam and not along the cross section. This transformation of coordinate system established a relationship between the rotation and out of plane displacement or warping of the section (3.8). The objective, however, is to establish how much stress (normal and shear) is being produced by this warping. In order to determine the contribution of warping to the overall stress in a section, the constant of integration

$\overline{w}_o$ must be evaluated. Also, the relationship between shearing and normal stresses and the unit warping with respect to some point must be established.

3.2.2 Normal warping and shear stress; open form differential equation

One of the assumptions encompassed into equation 3.4 is that the strains are related linearly to the stresses. Thus, the longitudinal stress can be expressed as:

$$\sigma_z = E\varepsilon_z \qquad \textbf{(a)}$$

where the strain in the longitudinal direction is simply $\partial w/\partial z$. This longitudinal stress is referred to as the warping normal stress. Substituting equation 3.8 into Hooke's law, the warping normal stress can be written as:

$$\sigma_z = E\frac{\partial w}{\partial z} = (\overline{w}_o' - w_o\phi'')E \qquad \textbf{3.9}$$

It is important to note that the rotation as well as the constant of integration $\overline{w}_o$ are a function of the longitudinal axis (z) of the beam. From the stress block depicted in Figure 1-4, the horizontal shearing stresses have to be in equilibrium with the normal stresses in all directions of the element in order to maintain equilibrium. Thus, integrating equation 1.4 (which is derived from reducing the equilibrium of the stress block) over the surface of the element, the shear flow is given as:

$$\tau t = -\int_0^s t\frac{\partial \sigma_z}{\partial z}ds \qquad \textbf{3.10}$$

The problem with equation 3.9 is that the unit warping is not well defined in terms of the geometry of the cross section which is tangible. By exploiting some basic geometric

relationships and using equilibrium, the unit warping and the constant of integration can be combined into one function which describes the warping geometry over the entire cross section. A similar process can be applied to equation 3.10 after a suitable expression for the normal warping stress is derived.

3.2.3 Normalized unit warping function of the cross section

In order to better understand the physical nature of the unit warping of each element, equation 3.9 needs to have a closed form solution for the constant of integration $\overline{w}_o(z)$. Also, a function which describes the warping of the geometry as a whole rather than each element (like the unit warping does) is desired. To accomplish this, 3.9 needs to be rewritten as to entail geometric properties of the cross section which are already known or can be derived using simple numerical techniques. For example, the tangential distance from the shear center to some element in the cross section (ρ_o) can be expressed in terms of the shear center coordinates or

$$\rho_o = \rho + Y_o \frac{dx}{ds} - X_o \frac{dy}{ds} \qquad 3.11$$

where X_o and Y_o are the shear center coordinates and ρ is the perpendicular distance from the centroid of the cross section to a tangent drawn at any point (x,y). Substituting 3.11 into 3.7 gives:

$$w_o = \int_0^s \rho\, ds + Y_o \int_{x_1}^{x} dx - X_o \int_{y_1}^{y} dy \qquad 3.12$$

where x_1 and y_1 are the coordinate distances to the starting surface of the section referenced to the centroid. Defining w as the unit warping with respect to the centroid (whereas w_O is the unit warping with respect to the shear center) as:

$$w = \int_0^s \rho \, ds \qquad 3.13$$

Equation 3.12 can now be simplified by integrating over the boundaries and substituting 3.13 where suitable:

$$w_o = Y_o x - Y_o x_1 - X_o y + X_o y_1 + w \qquad 3.14$$

Equation 3.14 still includes the unit warping w of each element with respect to the centroid of the entire cross section. The problem with this term is that it carries a constant of integration $\overline{w}_o(z)$ which is still undetermined. However, this term can be evaluated by looking at the equilibrium of a stress block under a torsional moment. The stress state on this particular element is assumed to be caused only by the application of a torque M_z. Therefore, the resultant longitudinal axial force N and moments caused by planar bending M_X and M_Y are zero. Thus, from mechanics [Seeley and Smith, 1952],

$$\begin{aligned} N &= \int_0^b \sigma_z t \, ds = 0 \\ M_x &= \int_0^b \sigma_z y t \, ds = 0 \\ M_y &= \int_0^b \sigma_z x t \, ds = 0 \end{aligned} \qquad 3.14$$

where the integration is across the entire length of the section since each element comprising the section contributes some moment and axial force. Also, for convenience, the reference axes will be taken as the principal centroidal axes. The normal warping stress from equation 3.9 can then be substituted into the three equations in 3.14. Noting from mechanics that

$$\int_0^b xt\,ds = \int_0^b yt\,ds = \int_0^b xyt\,ds = 0; \quad \int_0^b t\,ds = A; \quad \int_0^b x^2 t\,ds = I_y; \quad \int_0^b y^2 t\,ds = I_x; \qquad \textbf{(a)}$$

and from equations 1.24 and 1.25,

$$\int_0^b wxt\,ds = I_{wx} \quad \textbf{and} \quad \int_0^b wyt\,ds = I_{wy} \qquad \textbf{(b)}$$

two of the three equations from 3.14 can be reduced. The moment equations (M_X and M_y, respectively) give:

$$\phi''\left(-X_o I_x + I_{wy}\right) = 0 \quad \textbf{and} \quad \phi''\left(Y_o I_y + I_{wx}\right) = 0 \qquad \textbf{(c)}$$

In order for the equations in (c) to be non-trivial, ϕ can not be equal to zero which means that the part of the equations in the parenthesis must be equal to zero. Therefore, the shear center can be written as:

$$X_o = \frac{I_{wy}}{I_x} \quad \textbf{and} \quad Y_o = \frac{-I_{wx}}{I_y} \qquad \textbf{(d)}$$

which is the same expression derived in Chapter 1 using the equilibrium of a stress block under bending forces only (no axial or torsional forces). Thus, the center of twist is identical to the shear center of a cross section. This conclusion was first realized by Maillart and Eggenschwyler [Maillart and Eggenschwyler, 1921].

After substituting 3.9 into the axial equation in 3.14, the resulting equation becomes:

$$\overline{w}_o' \int_0^b t\,ds - \phi'' \int_0^b w_o t\,ds = 0 \quad \textbf{or} \quad \overline{w}_o' = \frac{\phi''}{A} \int_0^b w_o t\,ds \qquad \textbf{3.15}$$

where $\overline{w}_o'(z)$ is the derivative of the constant of integration obtained from integrating equation 3.7. Substituting 3.15 into the equation for the warping normal stress (3.9),

$$\sigma_z = EW_n\phi'' \qquad \textbf{3.16}$$

where W_n is defined as:

$$W_n = \frac{1}{A}\int_0^b w_o t\, ds - w_o \qquad \textbf{3.17}$$

W_n is defined as the normalized unit warping of the cross section. This equation is extremely powerful in the way it relates the unit warping function of each element comprising the cross section to the entire warping function. The unit warping of each element (w_O) can be obtained through equation 3.7. It can be readily seen that w_O is, at most, a linear function as long as the moment arm from the shear center ρ_O is constant. Thus, for structural sections with curved elements, the computation of 3.17 becomes more complex. Heins and Evick [Heins and Evick , 1973] discuss the solution of non-prismatic curved girders using the Fourier series method. This concept, however, will not be discussed here.

If the cross section is thought of in an eclectic sense, the computation of 3.17 can be done through a numerical integration procedure. Each element in the cross section is a subset of the spatial domain of the entire cross section. By storing the spatial information of each element (i.e., joint coordinates, local and global orientations, etc.), it is possible to define a warping sub-function which can relate the unit warping at any point in the cross section to an overall warping function. Another words, the warping sub-function can be though of as a weighting factor which normalizes the unit warping of each element in the section. By establishing the warping sub-function, a simple calculation of the unit warping at various points is all that is needed to calculate the overall normalized unit

warping. The numerical solution process of the normalized unit warping function and other similar torsional functions will be discussed in section 3.3.

3.2.4 Warping statical moment and warping constant

The expression for the shear flow caused by warping (3.10) can be simplified by differentiating the normal warping stress with respect to the longitudinal axis of the beam. Thus,

$$\frac{d\sigma_z}{dz} = EW_n\phi''' \qquad \textbf{(a)}$$

It is important to recall that the normalized unit warping function does not vary along the longitudinal axis of the beam since the cross section is assumed to preserve its shape throughout the length of the beam. Substituting equation (a) into 3.10, the shear flow can be expressed as:

$$\tau t = -ES_w\phi''' \qquad \textbf{3.18}$$

where S_w is referred to as the warping statical moment of the cross section and is defined as:

$$S_w = \int_0^s W_n t\, ds \qquad \textbf{3.19}$$

The surface integral around the cross section in equation 3.10 does not apply to the rotation of the beam. The reason for this is the assumption stated in Chapter 2 that all the elements in the cross section rotate an equal amount. Thus, the rotation, or any derivatives, are not a function of the cross section and may be pulled out of the integral.

The warping moment can be determined by summing the moments about the z-axis of the cross section. The shear flow (3.18) produces moments which can be found by multiplying the moment arms of each element by the shear flow through each element or

$$M_z = \int_0^b \rho_o(\tau t)\, ds \qquad \textbf{(b)}$$

Substituting equations 3.18 and 3.19 into the moment equilibrium equation (b) and integrating gives:

$$M_z = -EI_w\phi''' \qquad \textbf{3.20}$$

where I_w is called the warping constant and is defined as:

$$I_w = \int_0^b W_n^2 t\, ds \qquad \textbf{3.21}$$

The warping moment is an innate characteristic of every beam. It abets to resist any externally applied torque in combination with the moment caused by pure torsion. As can be seen, equations 3.16, 3.18, and 3.20 have been derived as to entail geometric properties that are inherent to any cross sectional shape. The rotation, which will be discussed in the next chapter, is the only item which is a function of the longitudinal axis of the beam rather than its cross section. Thus, the normalized unit warping function, warping statical moment, and the warping constant can be evaluated by either directly solving the integrals or through numerical integration techniques.

3.2.5 Normal warping stress as a function of the bimoment

An analogy between flexure and warping torsion can be established which is extremely useful when boundary conditions need to be defined in order to solve for the rotations along the beam. In Bernoulli beam theory the moment curvature relationship is defined as:

$$M(z) = -EIv''(z) \qquad \textbf{(a)}$$

where $v(z)$ is the displacement function and $M(z)$ is the variation of the bending moment. The beam is assumed to have a constant flexural rigidity. A similar expression exists in torsional analysis by simply rewriting equation 3.20 as:

$$Bi(z) = EI_w\phi'' \qquad \textbf{3.22}$$

where Bi is referred to as the bimoment of the beam. In ordinary flexural analysis the bending moment is a function of the second derivative of the displacement. Similarly, in torsional analysis the bimoment is a function of the second derivative of the rotation or the out of plane displacements. If the derivative of the governing bending moment equation is taken, the shearing forces acting on the beam can be determined since the shear function is the first order change of the moment. Analogously, the derivative of the bimoment (3.22) yields the warping moment expressed in equation 3.20. Hence, the warping moment M_z corresponds to the shear force in a beam subjected to pure flexure. Substituting the equation for the bimoment (3.22) into the equation for the normal warping stress (3.16) gives:

$$\sigma_z = \frac{BiW_n}{I_w} \qquad \textbf{3.23}$$

which is similar to the plain bending stress equation *MC/I*.

There is also a relationship between the load and the warping moment in torsion similar to the relationship of the load and shear force for a member under pure bending. The equilibrium condition for a discrete element length *dz* acted upon by a distributed torsional load m_Z is written as:

$$-M_z + m_z dz + \left(M_z + \frac{\partial M_z}{\partial z} dz \right) = 0 \quad \text{or} \quad m_z = -M_z' \qquad 3.24$$

Thus, the derivative of the warping moment gives the equation for the loading on the member. The relationships between the planar bending and warping equations are summarized in Table 3-1. When multicontinuous cells were analyzed in Chapter 2, a similar interrelationship was observed between the equations governing pure bending and pure torsion. The advantage of establishing these links is that a single algorithm can be devised to handle bending and torsion at one time. Since the differential equation in 3.22 is similar to that of its flexural counterpart, only the warping constant and the moment of inertia about the axis under analysis needs to be passed to evaluate both the bimoment and the bending moment. The forms of the differential equation are identical so only one numerical solution procedure is required. The solution process will be discussed in detail in the next chapter.

3.3 Numerical solution of warping torsional properties

The determination of the warping torsional properties W_n, S_w, and I_w can be obtained by considering the cross section to be composed of interconnected rectangular plate elements [Heins and Seaburg, 1963]. The same concept was implemented in Chapters 1 and 2 when a numerical solution for the shear center and the torsional stiffness were derived. This assumption is accurate for structural cross sections which are mostly composed of rectangular plate elements.

If a plate element of length L_{ij} and thickness t_{ij} is considered (Figure 1-5a), the perpendicular distance from the shear center to the tangent line between the end points of the element is constant (i.e. the element is not curved). Thus, the technique used to calculate the parameters I_{wx} and I_{wy} in Chapter 1 can be utilized to calculate the warping properties here. The determination of the geometric properties I_{wx} and I_{wy} required a general relationship for w ($= \int_0^s \rho\, ds$) between points w_i and w_j. This term was, at most, linear since

	ϕ	
v'	ϕ'	u'
$M_y = -EI_{yy}v''$	$Bi = EI_w\phi''$	$M_x = -EI_{xx}u''$
$Q_y = -EI_{yy}v'''$	$M_z = -EI_w\phi'''$	$Q_x = -EI_{xx}u'''$
$p_y = EI_{yy}v''''$	$m_z = EI_w\phi''''$	$p_x = EI_{xx}u''''$

Table 3-1 Relationship of a member under pure flexure and warping torsion

the perpendicular distance from the centroid to the tangent line through the two points on the element was constant. A similar relationship can be developed for w_O which is required to determine W_n and thus, S_W and I_W. Equation 1.21 gave an expression for w relative to the centroid. w_O can be expressed similarly except that it is referenced relative to the shear center. Therefore,

$$w_o = \sum \rho_o L$$

The expression $\int_0^b w_o t\, ds$ in equation 3.17 can then be evaluated for an element *ij* and is given by the expression:

$$\int_0^b w_o t\, ds = \sum t_{ij} L_{ij} \left(w_{o_i} + w_{o_j} \right) / 2 \qquad \textbf{3.25}$$

From Figure 1-5b it can be seen that the function *w*, at most, varies linearly over the element. Since w_O is analogous to *w* except for the reference point, the distribution of the unit warping across each element can be taken as the average of the unit warping values at the start and end of the element. The unit warping at a specified point *j* in an element is given by:

$$w_{o_j} = \rho_{o_j} L_{ij} \qquad \textbf{3.26}$$

Substituting 3.25 into 3.17 gives:

$$W_{n_i} = \frac{1}{2A} \sum_0^n \left(w_{o_i} + w_{o_j} \right) t_{ij} L_{ij} - w_{o_i} \qquad \textbf{3.27}$$

Equation 3.27 is the normalized unit warping at point *i* for any element *ij*. The term $W_{n_i} = \frac{1}{2A} \sum_0^n \left(w_{o_i} + w_{o_j} \right) t_{ij} L_{ij}$ is the sum effect of the unit warping of all the elements in the cross section. This term is called the warping sub-function. This particular term weighs or normalizes the unit warping w_O at any point *i* in the element.

3.3.1 Assumptions and techniques used to numerically evaluate the normalized unit warping

By replacing the surface integral in 3.17 with an equivalent summation, the normalized unit warping function can be evaluated numerically over a series of points. There are some techniques, however, that must be implemented to numerically solve for the normalized unit warping of the section. First, the unit warping at the starting point (any open point in the section) is assumed to be zero. Secondly, the unit warping at one end of an element is a function of the unit warping across the element ($\rho_o L_{ij}$) and the unit warping at the other end of the element. Thus, by assuming a starting point to have a unit warping of zero, the unit warping at the point on the other end of the element containing the designated starting point is evaluated by simply linearly adding the unit warping across the element with the starting unit warping value.

To simplify things, it maybe easier to visualize the normalized warping as a current flowing through the elements of the section. For example, Figure 3-2 depicts a wide-flanged cross section with a fictitious current flow going through the elements. The wide-flanged section is broken into five interconnected rectangular elements as shown in the figure. If the unit warping at point 1 is assumed to be zero, the unit warping at point 2 can readily be found by evaluating the unit warping across element 1 and adding it to the unit warping at point 1. As can be seen by the direction of the arrow (current flow), the unit warping at point 3 is related to point 2 and the unit warping across element 2. Thus, the same procedure can be applied to find the unit warping at point 3. A problem arises, however, when the unit warping at point 5 or 6 needs to be determined. Since the direction of the flow in elements 4 and 5 are assumed to go from points 6 and 5 to points 3 and 2, respectively, the process used to determine the unit warping at the other points must be reversed. For example, to evaluate the unit warping at point 6, the unit warping across the element must be determined along with the unit warping at point 3. Since the flow goes from point 6 to 3, the unit warping at point 6 is the difference between the unit warping at point 3 and the unit warping across element 4. Table 3-2 summarizes the

numerical procedure to calculate the unit warping at each point and subsequently, the normalized unit warping at each point. The table basically helps to visualize the parameters needed for equation 3.27.

3.3.2 TORAB's capabilities in evaluating the normalized unit warping

Conceptually, the aforementioned process is fairly easy to implement for basic structural cross sections. When built-up sections are utilized, however, a fair amount of "bookkeeping" is necessary. A flow pattern must be kept which means constructing a scheme that allows TORAB to be able to decide if the unit warping at one end of an element needs to be added or subtracted from the unit warping across the element. TORAB actually creates its own flow pattern by taking the starting joint coordinate as the origin of the flow. Thus, according to the joint coordinate input given in the input file, the starting joint is automatically registered as the first joint coordinate. The next

Point	ρ_o	L_{ij}	$\rho_o L_{ij}$	w_o	$t_{ij}L_{ij}$	$\left(w_{o_i}+w_{o_j}\right)t_{ij}L_{ij}$	W_{n_i}
1				0			$bh/4$
	$h/2$	$b/2$	$bh/4$		$bt/2$	$b^2ht/8$	
2				$bh/4$			0
	0	h	0		wh	$bh^2w/2$	
3				$bh/4$			0
	$h/2$	$b/2$	$bh/4$		$bt/2$	$3b^2ht/8$	
4				$bh/2$			$-bh/4$
5				$bh/2$			$-bh/4$
	$-h/2$	$b/2$	$-bh/4$		$bt/2$	$3b^2ht/8$	
2				$bh/4$			0
6				0			$bh/4$
	$h/2$	$b/2$	$bh/4$		$bt/2$	$b^2ht/8$	
3				$bh/4$			0
				$\sum$	$(2tb+wh)$	$\left(b^2ht+bh^2w/2\right)$	

Known quantity

Table 3-2 Numerical evaluation of normalized unit warping

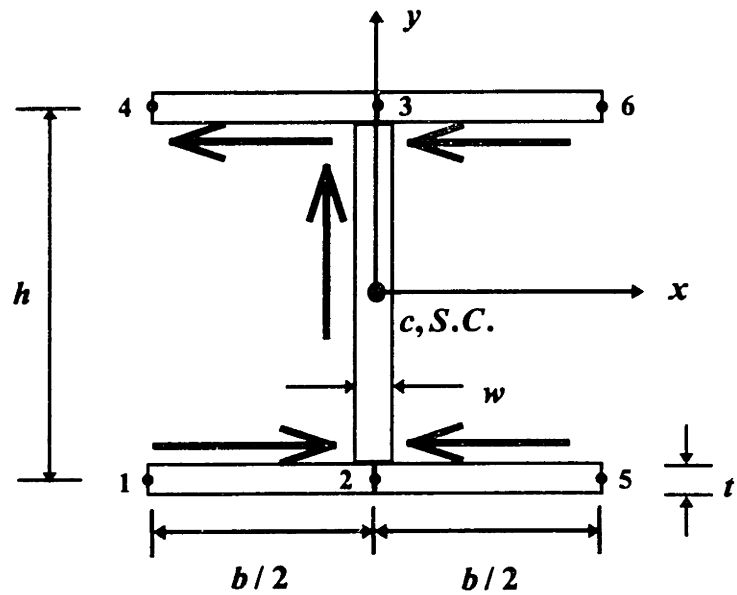

Figure 3-2 Fictitious current flow through meshed wide-flanged section

problem arises when the joint coordinate scheme is not in any specific pattern. If this problem occurs, TORAB will automatically regenerate the joint numbering scheme and keep an internal record of the actual joint numbering for the user's purpose. This technique is similar to the bandwidth reduction procedure which attempts to minimize the bandwidth of a matrix by renumbering the joint coordinates internally.

From Table 3-2 it can be seen that the sum of the terms in column seven divided by twice the sum of the terms in column six gives the warping sub-function or the term

$$W_{n_{sub-function}} = \frac{1}{2A}\sum_{0}^{n}\left(w_{o_i} + w_{o_j}\right)t_{ij}L_{ij} \qquad \text{(a)}$$

Thus, column eight, the normalized unit warping, is simply the difference between the warping sub-function and the unit warping at each point. TORAB finds the warping sub-function in this manner, but does not require a significant amount of "bookkeeping" to find the necessary values. Through the use of C and C++ tools such as pointers, structures, and classes, each element in the cross section knows what elements are

connected to it and how to go about getting information (i.e. where the flow through the element starts) it does not have. Although procedures such as a renumbering scheme are redundant, they will prove much more useful when the actual differential equations of warping and pure torsion need to be resolved. More of TORAB's internal abilities will be discussed in the next few chapters.

3.3.3 Numerical determination of the warping constant and the warping statical moment

After outlining a definitive method to numerically compute the normalized unit warping function, a similar expression for equation 3.21 (the warping constant I_w) can be defined. The warping constant is simply the integral of the square of the normalized unit warping curve across the entire cross section. Since this curve is, at most, linear as long as the distance ρ_o remains constant, the general W_n relative to W_{n_i} and W_{n_j} of element length L_{ij} can be written as:

$$W_n = W_{n_i} + \left[\left(W_{n_j} - W_n\right)_i / L_{ij}\right] s \qquad 3.28$$

Equation 3.28 is just a linear interpolation for any point W_n on the line $W_n(s)$ (see Figure 1-5b). Substituting 3.28 into equation 3.21 for *one element* and integrating using Simpson's 1/3rd integration method gives:

$$\int_0^{L_{ij}} (W_n)^2 t \, ds = \frac{1}{3} L_{ij} t_{ij} \left(W_{n_i}^2 + W_{n_j} W_{n_i} + W_{n_j}^2\right) \qquad 3.29$$

For the entire cross section, the warping constants can be summed up for each individual element or:

$$I_w = \frac{1}{3}\sum_{0}^{n}\left(W_{n_i}^2 + W_{n_j}W_{n_i} + W_{n_j}^2\right)t_{ij}L_{ij} \qquad \textbf{3.30}$$

The warping statical moment S_w from equation 3.19 can now be discretized through the utilization of equation 3.27. Since S_w is the area underneath the normalized unit warping curve, the term $\int_0^s t\,ds$ in 3.19 equals the area of the cross section which cancels out the area constant in equation 3.27. Thus, the warping statical moment can be written as:

$$S_w = \frac{1}{2}\sum_{0}^{n}\left(w_{n_i} + w_{n_j}\right)t_{ij}L_{ij} \qquad \textbf{3.31}$$

It is imperative to note that the S_w is not a constant, like the warping constant, but a variable across the entire cross section. The minimum and maximum for the function may change over each element comprising the section. Also, since the function is the integral of the normalized unit warping curve, this particular function will vary, at most, parabolically over an element since the unit warping curve is, at most, a linear curve. For example, in a wide-flanged section with equivalent flanges , S_w will be zero at the edge of the flanges and a maximum at the mid-span. Obviously, the magnitude of S_w will be zero along the length of the web since the value of the normalized unit warping function is zero (see Table 3-2). A detailed examination of the numerical algorithm TORAB uses to calculate S_w and I_w can be found in subsequent chapters along with specific examples.

Chapter 4

Combination of Pure and Warping Torsion

In the prior chapters, the action of a section subjected to a torque M_z which produced pure torsional stresses and warping torsional stresses was examined. Under certain boundary conditions both or only one of these aforementioned stresses may develop to resist the external torque. This chapter will discuss the combined influence of the internal torques and their solution. It is assumed that the section under examination is prismatic and straight. In order to solve the differential equations which govern the torsional behavior of the beam, a closed and approximate solution using the finite difference method will be examined.

4.1 Governing differential equation for combined torsional resistance

The combined torsional resistance of a section is comprised of the pure torsional resisting torque and the warping resisting torque. Thus, the sum effects are

$$M_z = M_z^{Pure} + M_z^{Warp} \qquad 4.1$$

The torque caused by pure torsion is equal to $GK_T\phi'$ (2.24) while that produced by warping torsion is equal to $-EI_w\phi'''$ (3.20). Substituting these equations into 4.1 gives:

$$M_z = GK_T\phi' - EI_w\phi''' \qquad 4.2$$

where M_z is an external concentrated torque. If a uniform torque m_z (torque per unit length) is applied along the length of the beam, a relationship between M_z and m_z can be established. A free body diagram would show that $m_z = -dM_z/dz$ which, when substituted into 4.2, gives:

$$m_z = EI_w\phi^{iv} - GK_T\phi'' \qquad 4.3$$

4.1.1 Solution of combined torsional resistance equation

The solution of equation 4.2 must be broken down into two parts since it is a non-homogeneous differential equation. These parts entail a homogeneous and a particular solution. Equation 4.2 is modified as follows to provide a path for a standard solution process:

$$\phi''' - \frac{GK_T}{EI_w}\phi' = -\frac{M_z}{EI_w} \qquad 4.4$$

Let $\lambda^2 = GK_T/EI_w$ and $M_z/EI_w = 0$ in order to solve for the homogeneous part of the solution. Thus, equation 4.4 can be rewritten as:

$$\phi''' - \lambda^2\phi' = 0 \qquad 4.5$$

Equation 4.5 is basically a replica of a standard first order differential equation except that the derivatives are of a higher order. To solve 4.5, assume the solution is of the form

$$\phi_H = e^{mz} \qquad (a)$$

Taking the appropriate derivatives of (a) corresponding to equation 4.5 and substituting them back into 4.5 gives the following characteristic equation:

$$m(m^2 - \lambda^2) = 0 \qquad \textbf{(b)}$$

where the roots of (b) are

$$m = 0, \pm\lambda \qquad \textbf{(c)}$$

The total homogeneous solution can then be expressed as:

$$\phi_H = c_1 e^0 + c_2 e^{\lambda z} + c_3 e^{-\lambda z} \qquad \textbf{(d)}$$

The particular solution of 4.2 can be obtained by assuming that $\phi_p = AZ$ where A is some constant that can be determined by substituting the assumed particular equation into 4.4. Thus, the particular solution is

$$\phi_p = \frac{M_z}{\lambda^2 EI_w} Z \qquad \textbf{(e)}$$

The total solution is the sum of $\phi_H + \phi_p$ or

$$\phi = c_1 e^0 + c_2 e^{\lambda z} + c_3 e^{-\lambda z} + \frac{M_z}{\lambda^2 EI_w} Z \qquad \textbf{4.6}$$

The exponential terms can be written as hyperbolic functions, and the constants can be regrouped to give the following equation:

$$\phi = A + B\cosh\lambda z + C\sinh\lambda z + \frac{M_z}{\lambda^2 EI_w} Z \qquad 4.7$$

Equation 4.6 was rewritten using trigonometric functions so that the graph and limits of the rotation can easily be obtained. The solution of equation 4.3 can be obtained in a similar manner. The only differences are that the homogeneous equation has four roots and the particular solution is obtained by assuming $\phi_p = AZ^2 + BZ^3$. In hyperbolic form, the solution to equation 4.3 is

$$\phi = A + BZ + C\cosh\lambda z + D\sinh\lambda z - \frac{m_z}{2\lambda^2 EI_w} Z^2 \qquad 4.8$$

4.1.2 Support types and corresponding boundary conditions

Since 4.7 and 4.8 are differential equations of order three and four, respectively, an equivalent amount of boundary conditions are necessary to properly solve for the torsional rotational response. These restraints, however, should be chosen such that the physical problem is modeled correctly in a mathematical sense. According to the LRFD code, clause A2.2, two basic types of restraint construction are permitted: Type FR (fully restrained) which is the typical "rigid frame" construction and Type PR (partially restrained) which entails "simple" or "conventional" framing [Chen and Jolissaint, 1983]. The latter type of restraint boils down to pinned and roller connections which carry a negligible amount of flexure and "semi-rigid" connections which can resist flexure to some extent (i.e. partial moment release). The ASD has its own classification of torsional restraints listed in clause A2.2. The ASD defines three types of restraint construction: Type 1 which is equivalent to Type FR in the LRFD code, Type 2 which is "simple" or "conventional" framing, and Type 3 which is "semi-rigid" framing. ASD Types 2 and 3 are encompassed by the LRFD's definition of Type PR.

The correlation of "simple" and "rigid" framing with torsional restraints is illustrated in Figure 4-1a and 4-1b. The situation in which there is zero deflection and zero moment (pinned support) corresponds torsionally to $\phi = 0$ and $d^2\phi/dz^2 = 0$. Ojalvo [Ojalvo, 1975] suggested that the rotation is zero if and only if the simple connection extends over a significant portion of the beam depth. Figure 4-1b depicts a rigid connection where zero deflection and zero slope translates torsionally to $\phi = 0$ and $d\phi/dz = 0$. Hotchkiss [Hotchkiss, 1966] states that the ends of the beams must be boxed in order for the connection to be classified as rigid or torsionally fixed. Boxing is the process of providing welding stiffener plates between the toes of flanges and extending them along the beam for a length equivalent to the beam's depth. A plan view of the plate configuration is illustrated in Figure 4-1b. These plates ensure that there is no deflection or rotation at the joint. If the column has flexible flanges, column stiffeners should be provided in a similar manner (plates B in Figure 4-1b). Several research studies have been conducted on torsional restraints at I-section joints by Vacharajittiphan and Trahair [Vacharajittiphan and Trahair , 1974], but few have been done on other section types.

The aforementioned support types have associated boundary conditions which are summarized in Table 4-1. Although partially restrained supports (partial moment releases) are very typical in structural problems, only Type 1 and Type 2 restraints will be discussed here due to the complexity of partial flexural restraining supports.

Table 4-1 Torsional boundary conditions for simple and rigid connections

$\phi = 0$		$\phi' = 0$
$\phi = 0$		$Bi = 0$
$Bi = 0$		$\phi''' = 0$
$\phi = 0$	$\phi'_{r(ight)} = \phi'_{l(eft)}$	$Bi_{r(ight)} = Bi_{l(eft)}$
$\phi_r = \phi_l$	$\phi'_{r(ight)} = \phi'_{l(eft)}$	$Bi_{r(ight)} = Bi_{l(eft)}$

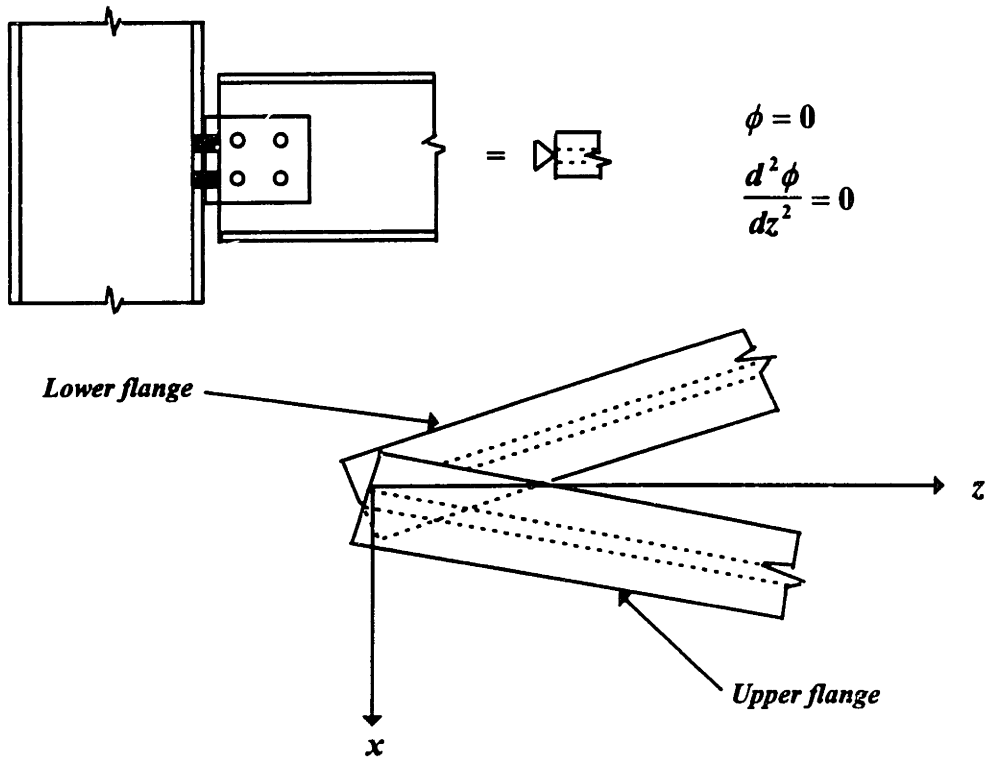

Figure 4-1a AISC Type 2 simple framing connection; $M_z=M_{pure}+M_{warp}$ and $M_{flexure}=0$

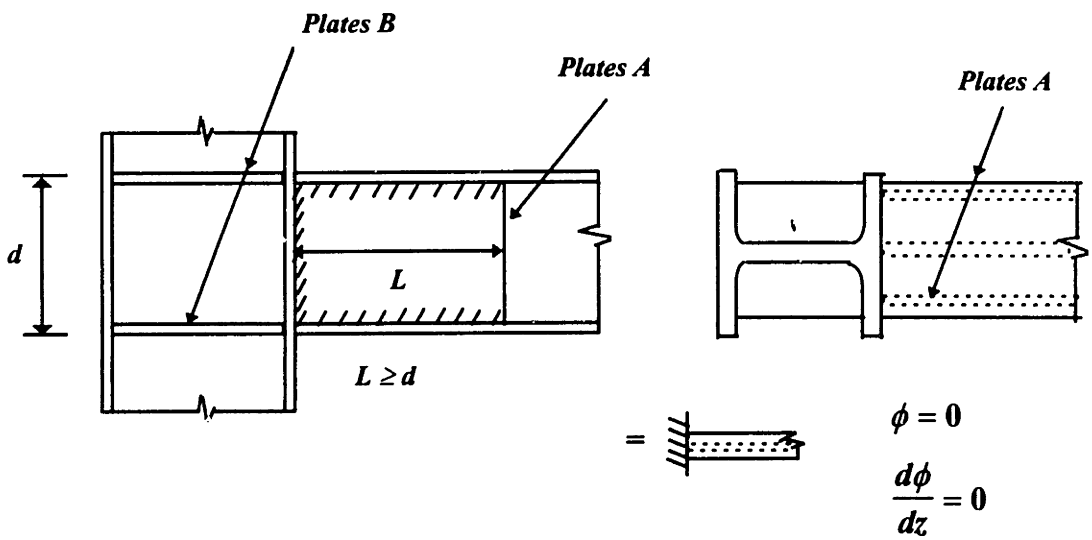

Figure 4-1b AISC Type 1 rigid framing connection with boxing; $M_z=M_{warp}$ and $M_{pure}=0$

4.2 Closed form solution of governing torsional differential equation

In order to solve either equations 4.7 or 4.8, the unknown constants inherent to each equation must be appropriately determined using Table 4-1. To understand how to implement Table 4-1, a simple cantilever beam of length L subjected to a concentrated torque of M_z at the free end of the beam will be examined. Suppose that the global axis along the length of the beam is the z-axis and the fixed end of the beam is at $Z=0$ while the free end is at $Z=L$. The boundary conditions for this beam are at $Z=0$, $\phi = \phi' = 0$ and at $Z=L$, $\phi'' = 0$. Since a concentrated torque is being applied, equation 4.7 needs to be evaluated with the above boundary conditions. Taking the appropriate derivatives of 4.7 and applying the boundary conditions gives:

$$Z = 0, \phi = 0 \qquad 0 = A + B \tag{1}$$

$$Z = 0, \phi' = 0 \qquad 0 = \lambda C + M_z/GK_T \tag{2}$$

$$Z = L, \phi'' = 0 \qquad 0 = \lambda^2 B \cosh \lambda L + \lambda^2 C \sinh \lambda L \tag{3}$$

The solution of these linearly independent equations for the constants A,B, and C gives:

$$A = -B, \qquad C = -M_z/GK_T\,\lambda, \qquad B = \left(M_z/GK_T\lambda\right)\tanh \lambda L \tag{4}$$

Substitution of these constants in equation 4.7 yields a closed form solution for the function describing the torsional rotation at any point along the beam.

$$\phi = \frac{M_z}{GK_T\lambda}\left[\lambda z - \sinh \lambda z + \tanh \lambda L(\cosh \lambda z - 1)\right] \tag{4.9}$$

The derivatives of equation 4.9 can then be evaluated. These derivatives, listed in equation 4.10, are required for the determination of the stresses caused by pure and warping torsion (2.25 ,3.16, and 3.18).

$$\phi' = \frac{M_z}{GK_T}\left[1 - \cosh \lambda z + \tanh \lambda L \sinh \lambda z\right]$$

$$\phi'' = \frac{M_z \lambda}{GK_T}\left[-\sinh \lambda z + \tanh \lambda L \cosh \lambda z\right] \qquad \textbf{4.10}$$

$$\phi''' = \frac{M_z \lambda^2}{GK_T}\left[-\cosh \lambda z + \tanh \lambda L \sinh \lambda z\right]$$

Thus, for a given length and material properties, the pure torsional and warping stresses can be evaluated at any point along the span of the beam. It is interesting to note that for this particular example the warping stresses are zero at the free edge of the beam. This can obviously be proven from the boundary condition (no warping shear at the free end), but physically, it should also make sense. The out-of-plane displacements w at the free edge are uninhibited from following their normal path. Thus, there will be no corresponding secondary force transmitted through the longitudinal axis of the beam to account for any restraint on these displacements. Another important point is that the warping and pure torsional stresses vary across the cross section. This is due to the fact that the normalized unit warping function W_n and the statical warping moment S_w vary across the elements comprising the cross section. For example, if the beam given in the example above had a wide-flanged cross section, the normal and shear stresses caused by warping would be zero in the web since W_n and S_w are both zero along the web. The normal warping stress can be proven to be zero in the web if the analogy between the bimoment and bending moment (3.23) is examined. A detailed discussion about the relationship between normal and shear stresses caused by pure flexure and torsion will be discussed in the next chapter.

4.3 Torsional charts dimensionalizing force-rotation relationships

Since it is rather complicated to develop a numerical scheme or algorithm to solve for the torsional response of a beam under any given boundary condition and load case, Heins and Seaburg [Heins and Seaburg, 1963] developed several torsional charts which would allow for an engineer to graphically determine the rotation and its successive derivatives at any point in the beam. These charts are the force-rotation diagrams that were discussed in Chapter 2. The rotation and its derivatives are always a function of $K_T, M_z, G,$ and λ. Hence, the equations in 4.9 and 4.10 can be written as:

$$\begin{aligned} F(\phi^n) &= \phi \frac{GK_T}{M_Z} \lambda \\ F(\phi^n) &= \phi' \frac{GK_T}{M_Z} \\ F(\phi^n) &= \phi'' \frac{GK_T}{M_Z \lambda} \\ F(\phi^n) &= \phi''' \frac{GK_T}{M_Z \lambda^2} \end{aligned} \qquad \textbf{4.11}$$

where $F(\phi^n)$ (n=0,1,2,3) contains the values of the contents in the brackets [] from equations 4.9 and 4.10. Although these charts can prove to be advantageous, they reveal nothing about the type of cross section being used. Thus, in order to evaluate the stresses in the beam, one must still proceed to calculate the centroid, shear center, warping constant, statical warping moment, and the normalized warping function.

As can be seen by the equations in 4.11, a common thread lies in the evaluation of the terms λL and λz. Heins and Seaburg state that a reasonable range for λL is from a minimum of 2 to a maximum of 5. Thus, to properly construct a chart which generalizes the torsional behavior of a beam under certain constraints and loading, it is necessary to evaluate the situation for a motley assortment of lengths and material properties. Usually, equation 4.11 is evaluated for λL's of 2.0, 3.0, 4.0, and 5.0 and any value which is

required in between is simply interpolated. The horizontal axis represents the fraction of the span length which is being examined (i.e. Z/L). The vertical axis represents the range of the function $F(\phi'')$. Since this function contains the values for all the bracketed [] equations in 4.9 and 4.10 (i.e. the rotation function and its three successive derivatives), the range needs to be calculated so it can properly depict the rotation response for any ordinary value of λL. Kuo and Heins [Kuo and Heins, 1971] acquired a significant amount of research from bridge and highway developers which contained values for λ used in standard practices as well as expected rotational values. It is important to understand that these charts only represent what is found in actual, modern torsional problems. If an unorthodox torque or material property is used, the charts will not produce an accurate answer. In that case a closed or approximate solution to equations 4.7 or 4.8 is required.

The force-rotation graph for the cantilevered beam under a concentrated torque at the free end is illustrated in Figure 4-2. To procure similar graphs with different loading cases and boundary conditions, the appropriate differential equation (4.7 or 4.8) would have to be solved and rearranged into the form given in equation 4.11. A graph similar to that in Figure 4-2 depicts the force-rotation relationship for a cantilevered beam subjected to a uniform distributed torsional loading (Figure 4-3). Again, the range for the values of λL's are chosen from experience gathered from actual observations.

4.4 Approximate solution to governing torsional differential equations using finite difference

An alternate method for solving the basic differential equations (4.7 and 4.8) can be obtained by use of finite difference equations. The application of such a formulation gives a discrete solution rather than a closed form continuous function. Although accuracy can be lost by pursuing a discrete formulation, with enough mesh points (i.e. a smaller step size), the solution can be very precise. The finite difference approach used here will be the central difference approach. The goal of this approach is to transform the

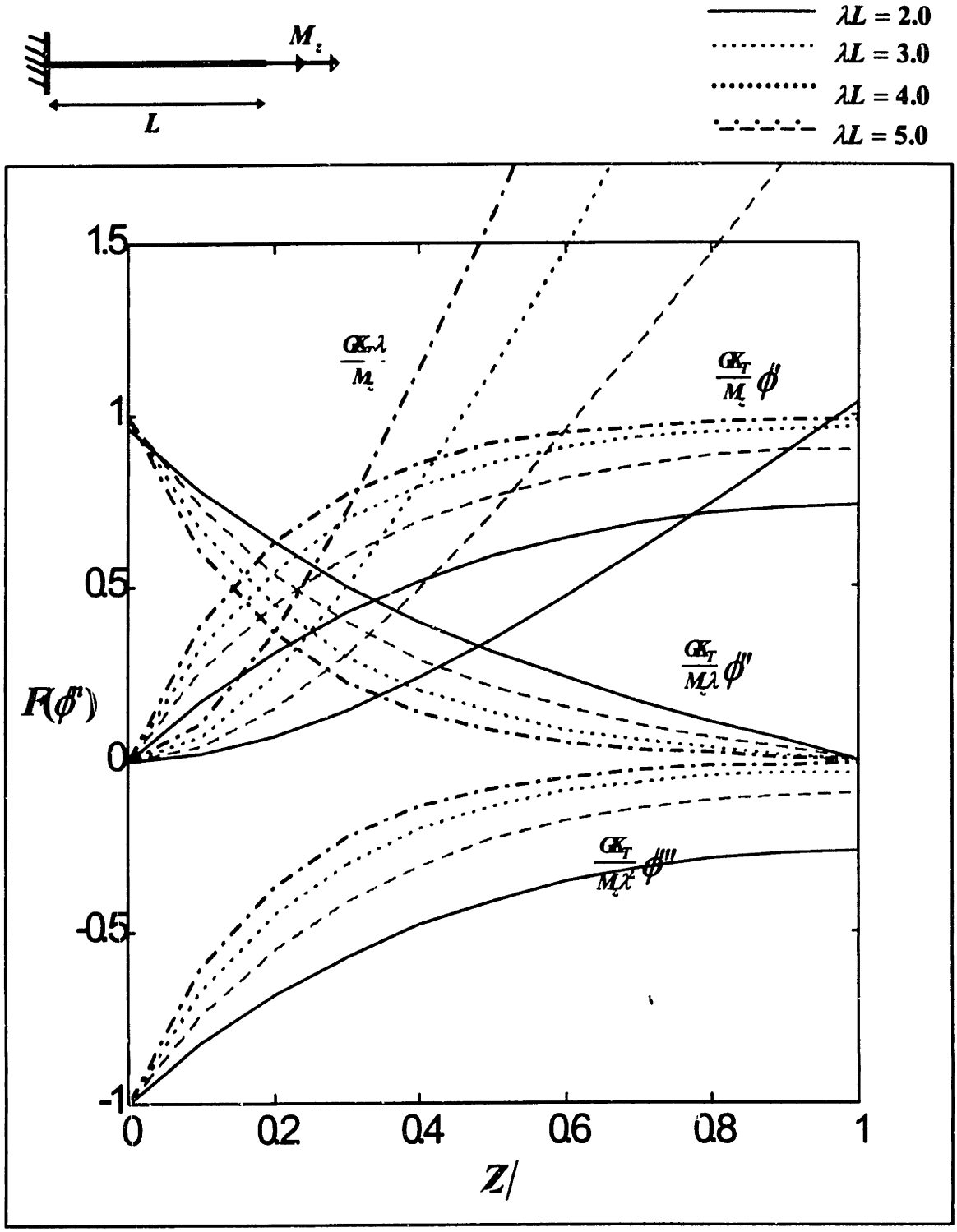

Figure 4-2 Force-rotation torsional chart for cantilever beam with concentrated torque

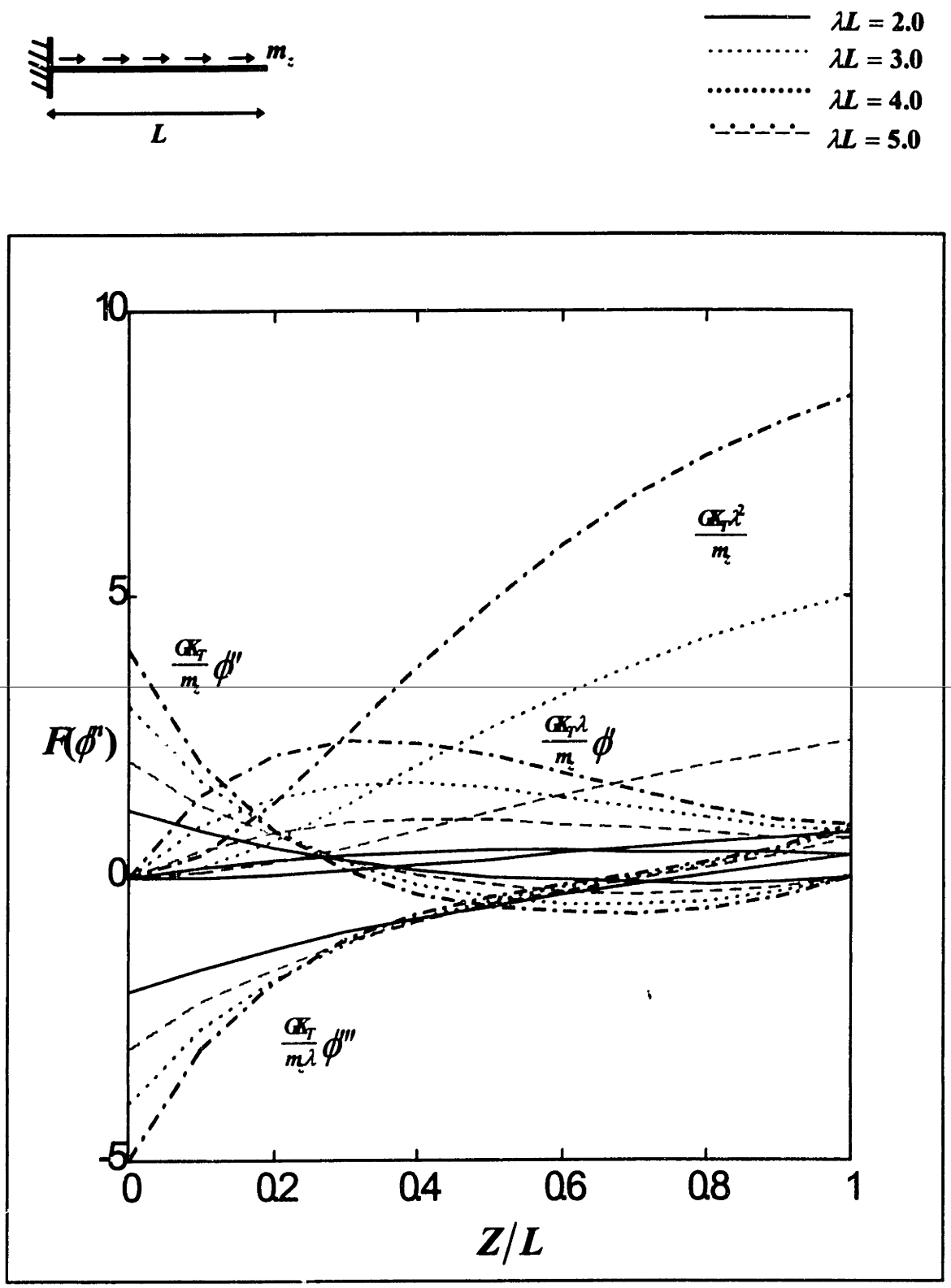

Figure 4-3 Force-rotation torsional chart for cantilever beam with distributed torque

differential equations into a set of simultaneous algebraic equations that can be solved using standard linear decomposition techniques. One good facet of the matrix containing the coefficients of the linearly independent equations is that it is tridiagonal. This sparse but organized matrix is rather easy to store and decompose.

4.4.1 Solution for torsional rotation using central difference method

The finite difference equations for the torsional rotation ϕ can be formulated by first considering the solutions for ϕ that are known at specified mesh points. The number of mesh points, of course, is dependent upon the accuracy required for the solution. In Figure 4-4 a portion of a beam which has been meshed into x amount of points with a spacing of h between each point is shown. Assume that the quantities ϕ_{n-1}, ϕ_n, and ϕ_{n+1} are known where n is a specific node on the beam. Since there are three known data points in the mesh, a parabolic curve can be passed through to simulate the actual behavior of the rotation function. The curve is of the form:

$$\bar{\phi} = AZ^2 + BZ + C \qquad \textbf{4.12}$$

This equation has to satisfy the conditions that at $Z = 0$, $Z = +h$, and $Z = -h$, $\bar{\phi}$ equals ϕ_n, ϕ_{n+1}, and ϕ_{n-1}, respectively. Using these three prescribed boundary conditions, the coefficients in equation 4.12 can be resolved by solving three simultaneous equations.

- at $Z = 0$, $\bar{\phi} = \phi_n$ or $\phi_n = A(0) + B(0) + C$ **(i)**
- at $Z = +h$, $\bar{\phi} = \phi_{n+1}$ or $\phi_{n+1} = Ah^2 + Bh + C$ **(ii)**
- at $Z = -h$, $\bar{\phi} = \phi_{n-1}$ or $\phi_{n-1} = Ah^2 - Bh + C$ **(iii)**

The solution of the expressions (i), (ii), and (iii) for the coefficients A, B, and C yield:

$$A = \frac{(\phi_{n-1} - 2\phi_n + \phi_{n+1})}{2h^2}$$

$$B = \frac{(\phi_{n+1} - \phi_{n-1})}{2h} \qquad 4.13$$

$$C = \phi_n$$

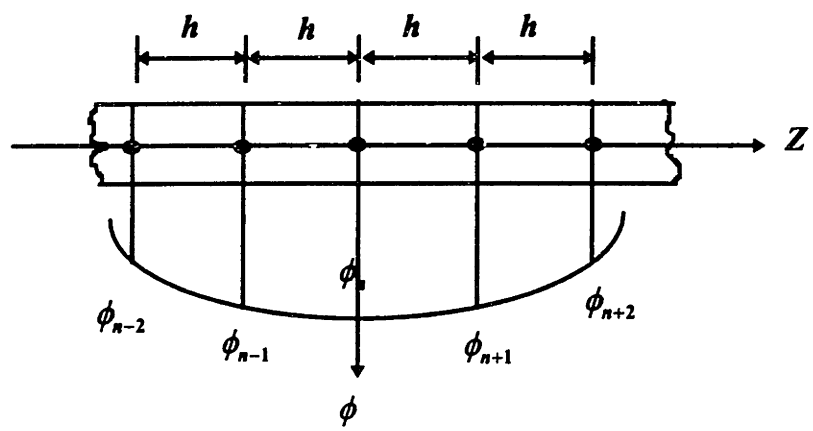

Figure 4-4 Mesh points for finite difference equations

Substituting the constants in equation 4.13 into 4.12, the rotation can be written as:

$$\bar{\phi} = \frac{(\phi_{n-1} - 2\phi_n + \phi_{n+1})}{2h^2} Z^2 + \frac{(\phi_{n+1} - \phi_{n-1})}{2h} Z + \phi_n \qquad 4.14$$

The first two derivatives of 4.14 at the point $Z = 0$ are:

$$\overline{\phi'}\Big|_{z=0} = \frac{(\phi_{n+1} - \phi_{n-1})}{2h} \qquad 4.15$$

$$\overline{\phi''}\Big|_{z=0} = \frac{(\phi_{n-1} - 2\phi_n + \phi_{n+1})}{h^2} \qquad 4.16$$

Although the determination of the third derivative (and the fourth derivative in cases of distributed loading) is required, higher derivatives of equation 4.14 result in zero

quantities. In order to circumvent this problem, additional mesh points (ϕ_{n-2} and ϕ_{n+2}) are added as shown in Figure 4-4. The third derivative can be written as:

$$\overline{\phi'''}\Big|_{z=0} = \frac{d}{dz}(\overline{\phi''}) = \frac{1}{h^2}\left[\phi'_{n+1} - 2\phi'_n + \phi'_{n-1}\right] \qquad 4.17$$

However, ϕ' at a given point, as given by equation 4.15, is ϕ at the right minus ϕ at the left of the given point divided by $2h$. Therefore, 4.17 can be rewritten and simplified as:

$$\overline{\phi'''}\Big|_{z=0} = \left[\phi_{n+2} - 2\phi_{n+1} + 2\phi_{n-1} - \phi_{n-2}\right]/2h^3 \qquad 4.18$$

Following a similar procedure, the fourth derivative can be obtained by taking the second derivative of equation 4.16 or

$$\overline{\phi}^{iv}\Big|_{z=0} = \frac{d^2}{dz^2}(\overline{\phi''}) = \frac{1}{h^2}\left[\phi''_{n+1} - 2\phi''_n + \phi''_{n-1}\right] \qquad 4.19$$

From the central difference procedure or equation 4.16, the second derivative of ϕ is given for a point as the sum of the two adjacent nodes minus twice the center divided by h^2. Therefore, equation 4.19 can be reduced by substituting equation 4.16 wherever there is a ϕ'' to yield:

$$\overline{\phi}^{iv}\Big|_{z=0} = \left[\phi_{n-2} - 4\phi_{n-1} + 6\phi_n - 4\phi_{n+1} + \phi_{n+2}\right]/h^4 \qquad 4.20$$

4.4.2 Establishment of mesh patterns in tridiagonal form for finite difference equations (concentrated torque)

The necessary derivatives of the torsional rotation in finite difference form were calculated in section 4.3.1. These equations can now be used to represent the governing

differential equation for pure and warping torsion in combination (4.2 and 4.3). For the case of a concentrated torque (4.2), the first and third derivatives can be replaced by equations 4.15 and 4.18 and simplified to yield:

$$\frac{2M_{\cdot}h}{GK_T} = (\phi_{n+1} - \phi_{n-1}) - \beta(\phi_{n+2} - 2\phi_{n+1} + 2\phi_{n-1} - \phi_{n-2}) \qquad \textbf{4.21}$$

where

$$\beta = EI_w / h^2 GK_T$$

Equation 4.21 can be represented as a mesh pattern by collecting terms together to give:

$$\left[(\beta) \quad (-1-2\beta) \quad (0) \quad (1+2\beta) \quad (-\beta)\right]\tilde{\phi} = \frac{2M_{\cdot}h}{GK_T} \qquad \textbf{4.22}$$

where $\tilde{\phi}$ is a column vector equal to:

$$\tilde{\phi} = \left[\phi_{n-2} \quad \phi_{n-1} \quad \phi_n \quad \phi_{n+1} \quad \phi_{n+2}\right]^T \qquad \textbf{4.23}$$

When written for each mesh point, equation 4.22 produces a well-conditioned system of linear simultaneous equations having strong pivotal elements. To establish these equations, the appropriate boundary modifications must be incorporated into 4.22 to determine the difference equations for mesh points adjacent to boundary points. From section 4.1.2 it was assumed that the torsional restraints used in practice were either rigid (fixed) or "simple" (pinned). Suppose a beam with one end is torsionally fixed as shown in Figure 4-5. From Table 4-1 a torsionally fixed end translates into the rotation and the slope equaling zero. This condition expressed in central differences at point 1 (using equation 4.15) is:

$$\phi_1' = 0 = (\phi_2 - \phi_0)/2h \quad \text{or} \quad \phi_2 = \phi_0 \tag{a}$$

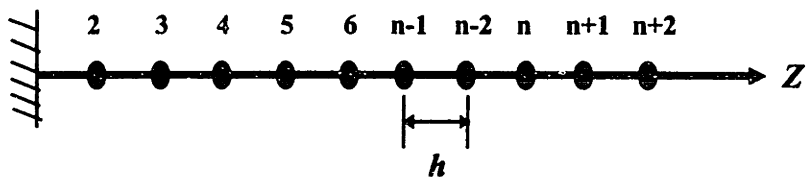

Figure 4-5 General central difference mesh notation

Substituting the relation obtained in (a) into the mesh pattern in 4.22 with the constraint $\phi_1 = 0$, gives the mesh equation for $n = 2$ (i.e. node 2):

$$n = 2 \qquad [\beta \quad 1+2\beta \quad -\beta]\tilde{\tilde{\phi}} = \frac{2M_z h}{GK_T} \tag{b}$$

where the column vector $\tilde{\tilde{\phi}}$ is

$$\tilde{\tilde{\phi}} = [\phi_2 \quad \phi_3 \quad \phi_4]^T \tag{c}$$

It is important to note that the ϕ_0 term is not in (b) because it combines with ϕ_2 due to (a). Thus, $\phi_{2Total} = \phi_2 + \phi_0 = 0 + \beta$. Also, the term ϕ_1 is not in (b) because it is inherently zero from the boundary condition associated with a torsionally fixed support.

The equations for the rest of the mesh points can be found in a similar fashion. Of course, the mesh equations for the right end must be evaluated carefully since another boundary condition exists. Suppose that Figure 4-5 was a complete beam, meshed into nine points, and that the right end was free. The *natural* boundary conditions associated with a free end are $\phi_9'' = \phi_9''' = 0$. One problem that arises in creating the mesh pattern in

equation 4.22 is that the terms ϕ_{10} and ϕ_{11} show up. These terms have to be written in terms of rotations that are physically on the beam. In order to accomplish this, the boundary conditions must be utilized. Hence,

$$\phi_9'' = 0 = \frac{\left(\phi_8 - 2\phi_9 + \phi_{10}\right)}{h^2} \quad \text{or} \quad \phi_{10} = 2\phi_9 - \phi_8 \tag{d}$$

$$\phi_9''' = 0 = \frac{\left(\phi_{11} - 2\phi_{10} + 2\phi_8 - \phi_7\right)}{2h^3} \quad \text{or} \quad \phi_{11} = 4\phi_9 - 4\phi_8 + \phi_7 \tag{e}$$

In matrix form, the mesh pattern for a cantilevered beam (discretized into nine points) with a torsionally rigid left end and a free right end is given as:

$$\tilde{R} = \begin{bmatrix} \beta & 1+2\beta & -\beta & 0 & 0 & 0 & 0 & 0 \\ -1-2\beta & 0 & 1+2\beta & -\beta & 0 & 0 & 0 & 0 \\ \beta & -1-2\beta & 0 & 1+2\beta & -\beta & 0 & 0 & 0 \\ 0 & \beta & -1-2\beta & 0 & 1+2\beta & -\beta & 0 & 0 \\ 0 & 0 & \beta & -1-2\beta & 0 & 1+2\beta & -\beta & 0 \\ 0 & 0 & 0 & \beta & -1-2\beta & 0 & 1+2\beta & -\beta \\ 0 & 0 & 0 & 0 & \beta & -1-2\beta & \beta & 1 \\ 0 & 0 & 0 & 0 & 0 & 0 & -2 & 2 \end{bmatrix} \tag{f}$$

Notice how the matrix $\tilde{R}$ is an 8x8 matrix as opposed to a 9x9 matrix. The reason is that the first point (i.e. $n = 1$) is given as an *essential* boundary condition which is $\phi_1 = \phi_1' = 0$. This boundary condition is built into the other mesh point equations. If it was physically inserted into the matrix given in (f), the matrix would be singular. To actually solve for the torsional rotations at each mesh point, the equation $\tilde{R}\vec{\phi} = \vec{L}$ must be evaluated where the matrices $\vec{\phi}$ and $\vec{L}$ are:

$$\vec{\phi} = \begin{bmatrix} \phi_2 & \phi_3 & \phi_4 & \phi_5 & \phi_6 & \phi_7 & \phi_8 & \phi_9 \end{bmatrix}^T \tag{g}$$

$$\bar{L} = \frac{2M_z h}{GK_T}\begin{bmatrix}1 & 1 & 1 & 1 & 1 & 1 & 1 & 1\end{bmatrix}^T \qquad \textbf{(h)}$$

The load vector $\bar{L}$ is the same at each point because there is only one concentrated torque M_z applied at the end of the beam. Thus, the torque at any point in the beam is the same for equilibrium to hold. If the torque varied across the beam, it would have to be reflected at each mesh point in the load vector $\bar{L}$.

The solution to the equation depicted in (f) (or any other one like it) can be easily obtained since the $\tilde{R}$ matrix is tridiagonal. Since the matrix consists solely of a band of entries three columns wide along the diagonal, the decomposition process is very short. A standard Gaussian procedure can be used to solve for the torsional rotations in the system. One key point is that the $\tilde{R}$ matrix is not *always* symmetric which means that standard solution procedures such as LDL^T decomposition will not work since the lower and upper triangles are not identical. Expedient storage procedures can be used to store the tridiagonal matrices which can help precipitate the solution process.

4.4.3 Establishment of mesh patterns in tridiagonal form for finite difference equations (distributed torque)

A procedure similar to the one given in section 4.3.2 can be applied to a beam subjected to a distributed torque instead of a concentrated one. In this case equation 4.8 must be expressed in finite difference form by substituting the expressions for ϕ^{iv} and ϕ'' in equations 4.20 and 4.18 into 4.8. This substitution gives:

$$\frac{m_z}{GK_T}h^2 = \left[\phi_{n+2} - 4\phi_{n+1} + 6\phi_n - 4\phi_{n-1} + \phi_{n-2}\right]\beta - \left[\phi_{n+1} - 2\phi_n + \phi_{n-1}\right] \qquad 4.24$$

where the value β is:

$$\beta = EI_w / h^2 GK_T$$

The mesh pattern for the uniform distributed loading case is:

$$\left[(\beta) \quad (-1-4\beta) \quad (2+6\beta) \quad (-1-4\beta) \quad (\beta)\right]\tilde{\phi} = \frac{m_z h^2}{GK_T} \qquad \textbf{4.25}$$

where $\tilde{\phi}$ is the same column vector given in equation 4.23. The derivation of a series of simultaneous equations to represent all the mesh points on a particular beam depend, of course, on the boundary conditions on both ends. The process, however, is exactly the same as for the concentrated torque example.

To properly demonstrate the situation for a distributed torque as well as incorporate a "simple" support, a beam with conventional (pinned) supports at both ends subjected to a uniform distributed torque across the entire length will be examined. Assume that nine mesh points are used (evenly spaced at a distance h) just like in the example in section 4.3.2. According to Table 4-1, a "torsionally pinned" support signifies that the rotation and corresponding bimoment (i.e. $\phi_{boundary}$, $\phi''_{boundary}$) are zero. These boundary conditions translate into

$$\phi_1 = \phi_9 = \phi_1'' = \phi_9'' = 0 \qquad \textbf{(a)}$$

if it is assumed that point 1 is the constraint at the left end while point 9 is the constraint at the opposite end. In order to derive the first mesh equation for point 2 (i.e. $n = 2$), it is necessary to determine the value of ϕ_0 (i.e. $\phi_{n-2}\big|_{n=2}$). From equation 4.16,

$$\phi_1'' = 0 = \frac{\phi_0 - 2\phi_1 + \phi_2}{h^2} \qquad \text{or} \qquad \phi_0 = -\phi_2 \qquad \textbf{(b)}$$

Thus, substituting (b) into the mesh pattern in equation 4.25 and collecting like terms gives the finite difference equation for node 2:

$$n=2 \qquad \begin{bmatrix} 2+5\beta & -1-4\beta & \beta \end{bmatrix} \tilde{\tilde{\phi}} = \frac{m_z h^2}{GK_T} \tag{c}$$

where the column vector $\tilde{\tilde{\phi}}$ is

$$\tilde{\tilde{\phi}} = \begin{bmatrix} \phi_2 & \phi_3 & \phi_4 \end{bmatrix}^T \tag{d}$$

Since this beam has identical torsional restraints on both ends, it is symmetric. Thus, the evaluation of the difference equations on the right side of the beam will entail following the exact procedure given above. The $\tilde{R}$ matrix for this case is as follows:

$$\tilde{R} = \begin{bmatrix} 2+5\beta & -1-4\beta & \beta & 0 & 0 & 0 & 0 \\ -1-4\beta & 2+6\beta & -1-4\beta & \beta & 0 & 0 & 0 \\ \beta & -1-4\beta & 2+6\beta & -1-4\beta & \beta & 0 & 0 \\ 0 & \beta & -1-4\beta & 2+6\beta & -1-4\beta & \beta & 0 \\ 0 & 0 & \beta & -1-4\beta & 2+6\beta & -1-4\beta & \beta \\ 0 & 0 & 0 & \beta & -1-4\beta & 2+6\beta & -1-4\beta \\ 0 & 0 & 0 & 0 & \beta & -1-4\beta & 2+5\beta \end{bmatrix} \tag{e}$$

Here, the $\tilde{R}$ matrix is a 7x7 matrix as opposed to an 8x8 matrix when the beam was cantilevered. Although the same number of mesh points were used in both examples, this particular case has two *essential* boundary conditions: the pinned supports on both ends. These constraints are built into the other mesh point equations. If they were included in the $\tilde{R}$ matrix as a separate entity, the matrix would be singular. To directly solve for the

rotations on the beam, the equation $\tilde{R}\bar{\phi} = \bar{L}$ must be evaluated where the matrices $\bar{\phi}$ and $\bar{L}$ are:

$$\bar{\phi} = \begin{bmatrix} \phi_2 & \phi_3 & \phi_4 & \phi_5 & \phi_6 & \phi_7 & \phi_8 \end{bmatrix}^T \quad \text{(f)}$$

$$\bar{L} = \frac{m_i h^2}{GK_T}\begin{bmatrix} 1 & 1 & 1 & 1 & 1 & 1 & 1 \end{bmatrix}^T \quad \text{(g)}$$

4.5 Comparison of finite difference solution to exact closed form solution

It is impractical to solve the governing torsional differential equations (4.7 and 4.8) in a closed form since the number of realistic combinations of boundary conditions and loading patterns are much too large. Since all combinations can not be accounted for, a neural network would have to be created in which the "black box" would have to be taught how to solve a new problem using relational information it already knows from past situations. A much easier way to tackle the solution process is to use the finite difference method mentioned in section 4.3. It can be shown that in order to achieve convergence to the real solution (i.e. the closed form solution of 4.7 or 4.8), the number of required discrete mesh points is quite small.

Figures 4-6 and 4-7 contrast the difference obtained in using the finite difference method to obtain the torsional rotational response of a system. Figure 4-6 simulates the case in which the beam is torsionally pinned at both ends and subjected to a uniformly distributed torque. Figure 4-7 is the case of a cantilevered beam with a simple concentrated torque at the free end. The finite difference solutions were obtained using TORAB. The automation process for the finite difference solution is quite straightforward since there exits only two essential and one natural boundary condition. Thus, the $\tilde{R}$ matrices can be assembled rather easily since the effects of the free, pinned, and fixed constraints on the difference equations are known in advance. All that needs to be automated is the load vector $\bar{L}$ which can vary from a concentrated torque placed

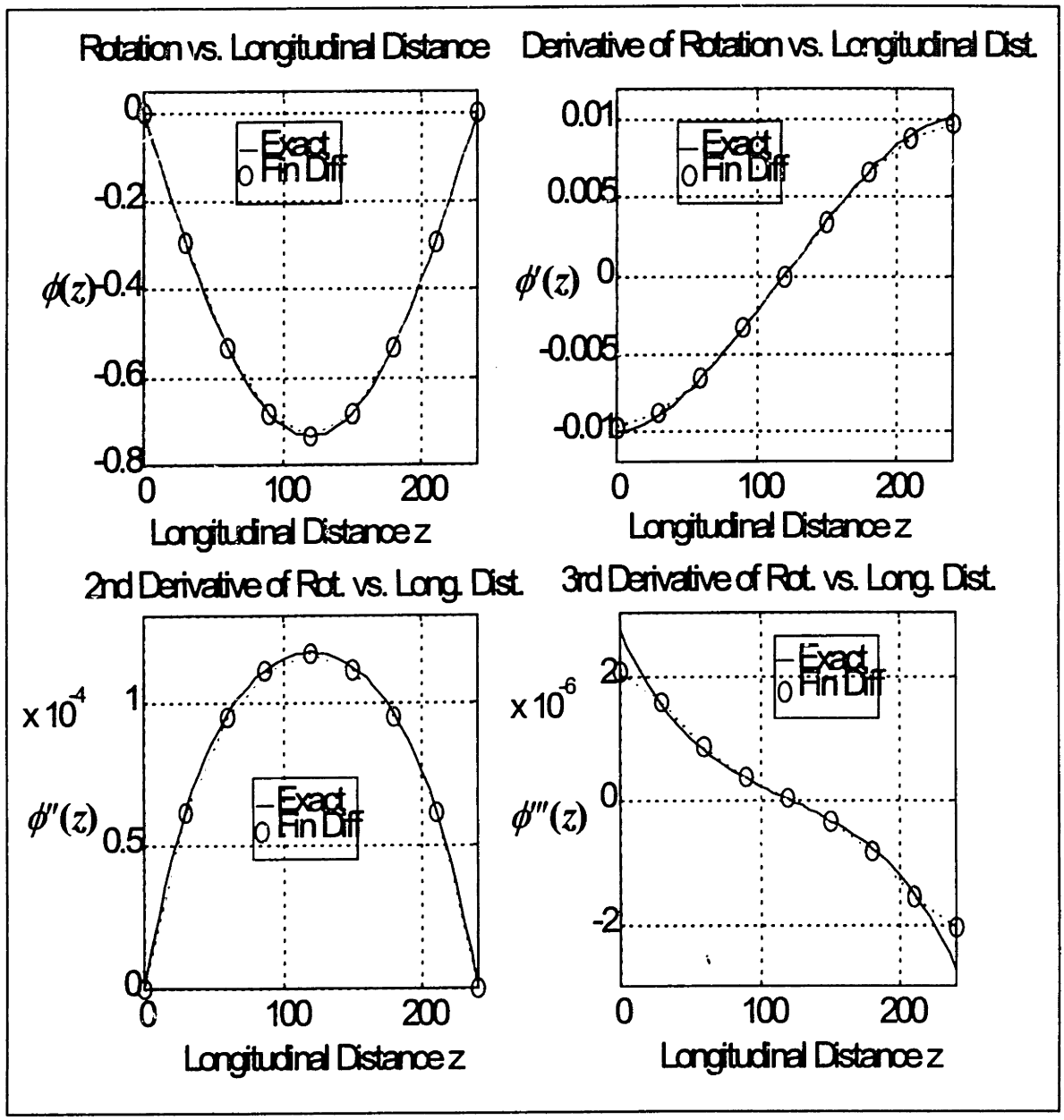

Figure 4-6 Comparison of exact solution of rotation and successive derivatives to that of finite central difference method for a pin-pin beam with distributed torque (m_z = -3 k•in/in, L=240", h=30", G=11.2 X 10^3 Ksi, E=30.0 X 10^3 Ksi, K_T=1.82 in^4, I_w=1881.0 in^6)

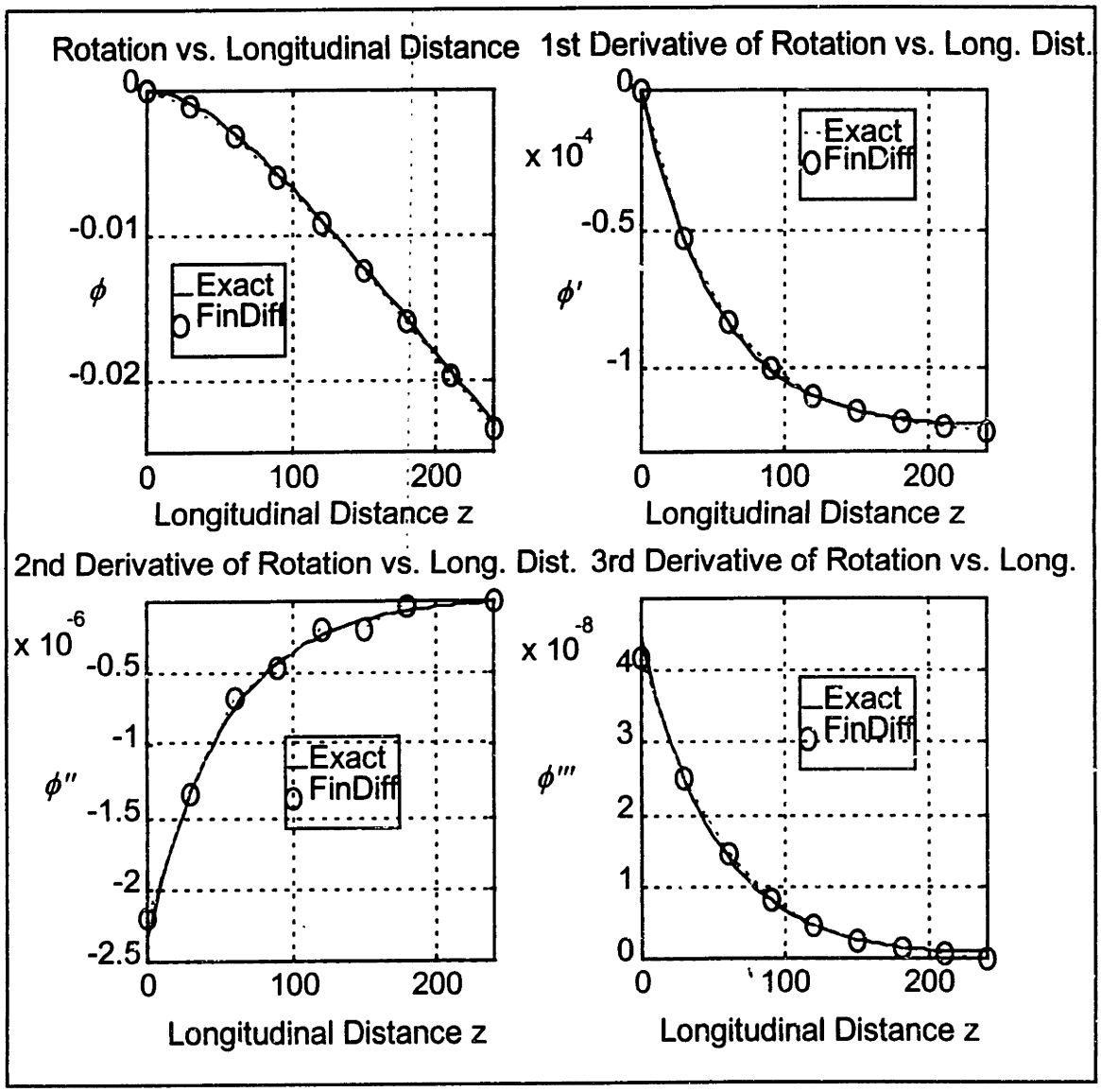

Figure 4-7 Comparison of exact solution of rotation and successive derivatives to that of finite central difference method for a cantilevered beam with a concentrated torque at free end (M_z = -2.5 k•in, L=240", h=30", G=11.2 X 10^3 Ksi, E=30.0 X 10^3 Ksi, K_T=1.82 in^4, I_w=1881.0 in^6)

anywhere on the beam to a linearly distributed torque along a certain portion of the beam. A discussion of the procedure TORAB undergoes to determine $\tilde{R}$ and $\bar{L}$ can be found in Chapter 5.

Figures 4-6 and 4-7 also illustrate the differences between the first, second, and third derivatives of the rotation obtained from the finite difference and exact solutions. The finite difference solution used contained nine mesh points. Heins and Looney [Heins and Looney, 1967] stated that accurate solutions could only be obtained if a fine mesh was used. However, the problems in Figures 4-6 and 4-7 were run through TORAB under coarser meshes (six nodes) and the results slightly differed from the nine node mesh. Since these matrices are rather small and extremely sparse, it is not computationally expensive to set up a fine mesh if absolute accuracy is of top priority.

Chapter 5

Implementation of numerical algorithm to solve the torsional response of a beam (TORAB)

The focus of this chapter is to discuss a devised scheme which can properly and accurately handle the entire torsional problem of a beam. This scheme would entail the tedious and problematic tasks of calculating the centroid, shear centers, warping properties, etc. for any cross section as well as the evaluation of the resulting warping and pure torsional shear and normal stresses. The responses for both open and closed cross sections (i.e. continuous and multicontinuous cells) can be determined using a simple text input file. TORAB (*TOR*sional *A*nalysis of *B*eams) is written in the C and C++ architectures for both the PC and UNIX platforms. It is also equipped with a MATLAB® interface which produces a MATALB® file that graphically displays such things as the distribution of the normalized warping function and the statical warping moment.

5.1 User interface for defining a cross section in TORAB

The torsional properties for a given cross section were numerically calculated in Chapters 2 and 3. These properties entail the torsional stiffness K_T, the normalized unit warping function W_n, the statical warping moment S_w, the warping constant I_w, and the shear center X_o and Y_o. Although the determination of these properties are rather straightforward when looking at the problem in a physical basis, the computer has no idea about the shape of the cross section, the elements that comprise it, or the orientation of the joints. In order to 'feed" the computer the relevant information it needs to determine the characteristics of the cross section, an input language was created as an interface medium. This input language is a simple text language that is comprised of a series of

phrases which may be used in combination with each other. A listing of all the commands in the language can be found in Appendix A.

5.1.1 Joint and element orientation for cross sections

The frame of reference which TORAB utilizes throughout the analysis is based upon the joint coordinates provided by the user. The cross section, as described in Chapters 1 and 2, is comprised of smaller rectangular elements of which the starting and ending coordinates must be supplied by the user. Since flat rectangular elements constitute most structural sections, TORAB *is not* equipped to handle sections which embody curvilinear surfaces. Adding curvilinear elements would completely change the numerical derivations described in Chapters 1 through 3 since the tangential distance ρ or ρ_o would not be constant. The cross section in question is divided into parts by the user and not by TORAB. The process of meshing the cross section either for accuracy or convenience is beyond the scope of this thesis and the code behind it.

The joint coordinates can be numbered in any order. The joint number is succeeded by the x and y coordinates, respectively. Each element has two joints associated with it, but joints may be shared among adjacent elements. These joints, obviously, should not be listed twice. Once the joint coordinates have been listed, the element connectivity information must be ascertained. The elements can be numbered in any order where the element number is succeeded by the starting and ending joint numbers, respectively. As discussed in section 3.3.1, the internal flow used to evaluate the normalized warping sub-function ($W_{n_{sub-function}}$) is decided by the starting and ending joints. The flow is automatically designated to travel into the direction of the ending joint.

TORAB creates a frame of reference for the cross section by sorting out the joint coordinates provided in the input file. TORAB looks for the joint which has the minimum abscissa and ordinate and designates that as the origin for the entire cross section. Thus, the centroid and shear center is referenced from the newly created origin. The reason the frame of reference was chosen in this particular manner was that the cross

section did not have to be scaled from an actual design, plan, or blueprint. An alternate command, labeled **FRAME**, is also included so that the user can create a "dummy node" which would simulate an origin the user desired. However, the author recommends that the origin should be a point which is physically on the section so that frame of reference is entirely encompassed by the section itself.

The storage scheme used to organize the joint coordinates, element connectivity, and the frame of reference is done with classes and structures. Since there can be an arbitrary amount of joints and elements, the class (`Class SectionInfo`), which is assigned to hold all this information, has the ability to dynamically allocate memory every time a new element needs to be created. Of course, the amount of memory is solely limited by the hardware on which TORAB is being run on. Element connectivity is processed by the same class through a technique called *doubly linked listing* [Johnsonbaugh and Kalin, 1993]. This linked list is simply an array of structures where each structure contains all the information about a particular element (i.e. length, joint coordinates, thickness, etc.). The fact that the elements in the cross section are placed in a linked list allows for TORAB to grasp the orientation of each element with respect to adjacent elements. If TORAB sees that two elements share the same joint coordinates (adjacent elements), it will place the element (element 2), whose unique joint number is spatially greater than the other element's (element 1) unique joint number, in the slot in the list directly to the right of element 1. Not only does this allow for TORAB to understand element orientations, but it also arranges the elements in an order which would make the calculations of the torsional properties much simpler. As can be seen by equations 3.27 and 3.29 and Table 3-2, it is imperative to know how the elements are interconnected by geometry.

Figure 5-1 illustrates how the doubly linked list behaves. If a simple array of structures were used, it would be much more difficult to insert and move elements in the array when a new one was added. It must be recalled that the elements comprising the cross section may be defined in any order. Thus, with a linked list, a new link can be created to insert a new element into the list without interrupting the continuity of the other linked elements. The linked list can be traversed in both directions since the links

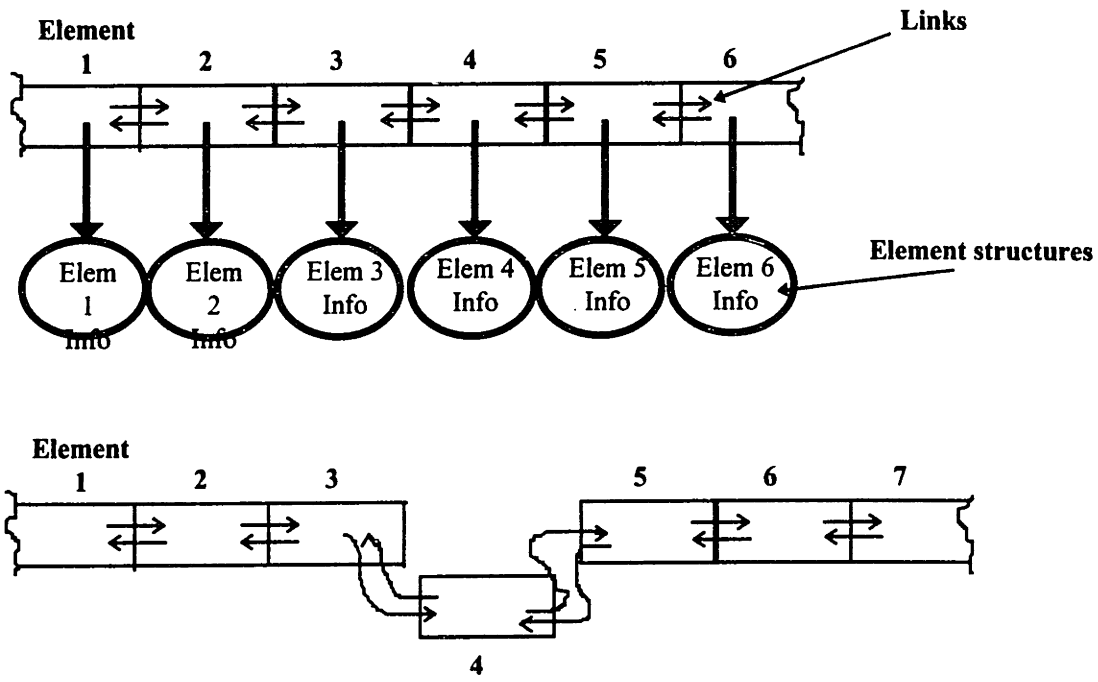

Figure 5-1 Doubly linked list used to store element structures as they are read from the input file

point in both directions. An additional comment must also be made on the element structures themselves. These structures are quite complex in regards to their contents. They include dynamically allocated arrays which hold such information as joint coordinates, element number, orientation, thickness, local centroids, and elemental offsets. In order to manage memory, these arrays within the structures are allocated during *run-time*, not *compile-time*. This technique is used to safeguard against cross sections which need to be defined by several elements.

5.1.2 Local vs. global; element offsets and local centroids

TORAB calculates the local geometric properties of elements as well as their global counterparts. For example, the local centroid of each individual element is evaluated and stored in the element structure (Figure 5-1). The reason for this is that it alleviates the computational effort needed to derive the global geometric properties of the

entire cross section which is a function of the geometric properties of each individual element. When the global centroid is calculated, the areas of each element along with the distance from the centroid of each element from the origin (in each direction) needs to be determined. These local values are also used to calculate the local moment of inertias I_x, I_y, and I_{xy} for each element.

Element offsets can also be defined in TORAB with the command **ELEM OFFSET** followed by the amount of offset necessary in the *y-direction only*. The offset option is provided so that the user can shift the position of the joint coordinate with respect to the element thickness. The default for the offset is zero which means that the joint is placed at the mid-surface of the element. Figure 5-2 graphically depicts how the offset command can be used.

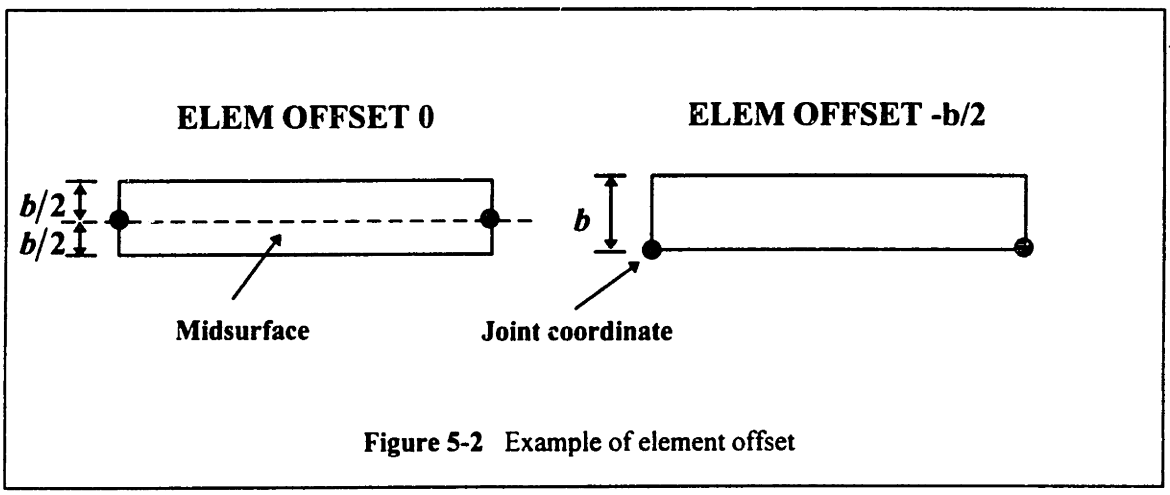

Figure 5-2 Example of element offset

5.1.3 Elemental properties

The thickness of each element can be defined under the command **ELEM PROP**. This command is to be used after the definition of the elemental connectivity so TORAB can properly place the thickness of each element in the correct structure. The correct usage of this command entails listing the element number followed by the thickness. TORAB reads everything in double precision so the thickness can be a very precise number if necessary. Tapered elements can not be used in TORAB since the tangential

distance from the centroid or shear center to the element mid-surface becomes a function of the degree of taper rather than a constant. This would change the expressions for the torsional properties derived in the previous chapters. Although this problem can be included into the formulation for the torsional properties of a cross section, the concept is not applicable to structural cross sections used in practice today.

5.1.4 Distinction between closed cells and ordinary cross sections

Closed continuous and multicontinuous cells are treated slightly different than typical open cross sections. The quintessential reason for this is that the solution process used in determining the torsional stiffness K_T involves solving the simultaneous equations obtained from equation 2.39. To distinguish between cell elements and ordinary elements, the command **CELL** is used instead of the command **ELEM INCID** which is used for defining the element connectivity for a single cross section (see Figure 1-7). Following the **CELL** command, the cell number, the height, and the width must be listed in that order. TORAB will understand when the user has completed listing all the cells in the box section since it incessantly searches for a new command that will take it out of the command process routine it is currently in. This is true for any command which needs to be terminated (i.e. joint coordinate listing, element incidences, element properties, etc.). The thickness for the cells is listed under the command **CELL PROP** in the input file. It should be recalled that the boundary thickness between elements must be the same to preserve cell continuity. The information related to each cell is stored in a structure similar to that of an ordinary element. Allocation of new memory is performed when new cells are added to the box section. All cell structures are still a part of the higher class in which these structures as well as the element structures are stored (`Class SectionInfo`). This is so TORAB can treat either an element or a cell as a separate object rather than just a part of the cross section. It abets to establish a hierarchy among the elements or cells and the cross section itself.

5.2 User interface for defining a beam for analysis in TORAB

In order to start the input for the cross section, the command **CROSS SECTION** must be listed before any other command. Similarly, to begin the input for the beam itself, the command **BEAM** must be given after the end of the cross section input. After the **BEAM** command, the joints along the beam and the support conditions must be given using the commands **JOINTS** and **SUPPORT**. An example of the usage of the aforementioned commands is given in Figure 5-3. It should be noted that the **SUPPORT** command (listed in Appendix A) can maintain the following values:

⇒ **FREE** (no shear or bimoment)

⇒ **PINNED** (no deflection)

⇒ **FIXED** (no deflection or rotation)

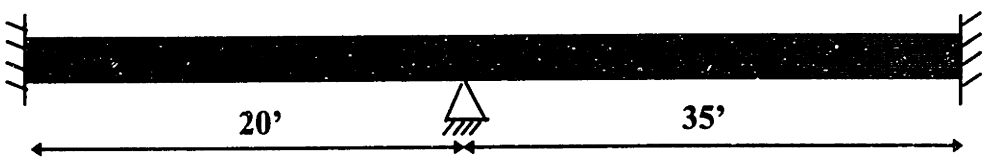


```
...
...
BEAM
JOINTS
1 0.0
2 20.0
3 55.0
SUPPORT
1 FIXED
2 PINNED
3 FIXED
...
...
...
```

Figure 5-3 Sample continuous beam with TORAB input file

5.3 Evaluation of torsional properties using TORAB

The torsional properties of a cross section, including the normalized warping function, warping constant, torsional stiffness, and warping statical moment, can be evaluated using the equations derived in Chapters 2 and 3. The implementation of these equations in a computer algorithm usually would require some "bookkeeping", but with the use of a *class architecture*, the "bookkeeping" can be eliminated. Since the warping statical moment and the warping constant are a function of the normalized unit warping function, the primary goal for TORAB is to first evaluate the normalized unit warping function at the discrete nodes provided by the user.

Through object-oriented programming, each element in the cross section has the ability to understand its geometric disposition with respect to all other elements. The doubly linked list described in section 5.1.1 abets in giving each element its own identity and at the same time, establishes a relationship with other elements. Thus, after obtaining the origin for the cross section (section 5.1.1) and the global coordinate axis system (i.e. frame of reference), information such as the distance from the centroid or the shear center to the mid-line of an element can be obtained by *each element itself.* These pieces of information are vital to acquiring the normalized warping function and sub-function. Each element has its own structure which carries all the information pertinent to that particular element. With this information, the element can further proceed to calculate any other distance, angle, etc. so that it can determine its contribution to a specific global property. A flow chart depicting this object-oriented relationship between the local elemental properties and the global cross sectional properties is shown in Figure 5-4.

5.3.1 Evaluation of torsional stiffness of a cross section in TORAB

Since each element in the cross section (including built-up sections) is assumed to be rectangular, the resolution of equations 2.27 or 2.32 can be made by simply evaluating

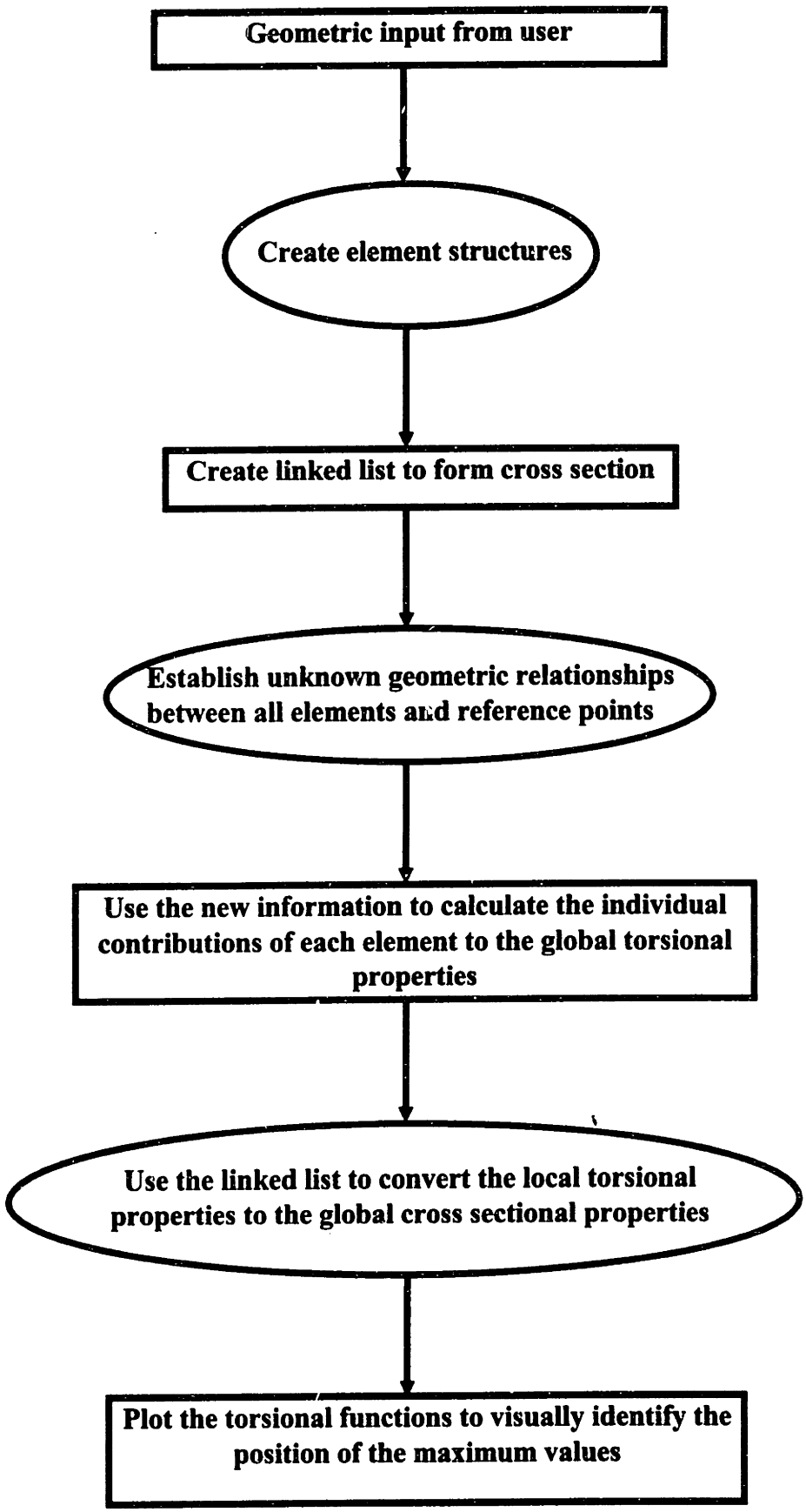

Figure 5-4 Flow chart of TORAB's torsional properties

the polar moment of inertia I_r. For a rectangular section the moment of inertia along the minor axis is negligible since the thickness is small compared to the depth of the section. Since each element already knows its major moment of inertia (and thus, the polar moment of inertia) with reference to the principal axes of the cross section, equation 2.27 or 2.32 can be evaluated to find the total torsional stiffness. The area of each element can be individually evaluated by the element itself since it already knows its own dimensions. Class functions such as `Element.Area()` and `Element.GetPolarInertia()` are used by the element to obtain the aforementioned properties. Once these properties are calculated, they are stored in the element's structure.

5.3.2 Evaluation of normalized warping function of a cross section in TORAB

In order to evaluate the normalized warping at a discrete point in the cross section, the determination of the warping sub-function is necessary. The process through which this value is determined is listed in Table 3-2. Since TORAB automatically creates a flow pattern between the joints (from the starting and ending joint coordinates of an element), it is left to the individual elements to decide whether to add or subtract the warping across itself from one joint to the next. The initial warping is automatically set to zero at joint coordinate one. This, of course, means that if the user does not assign joint coordinate one to be one of the open joints where the warping is zero, TORAB will do so internally. Since each element knows the direction of the flow across it, the element can determine whether it should add or subtract the warping from the starting joint by simply checking its structure and seeing which end is the starting end. To get the variation in warping across the element, the area of the element, the distance from the shear center to the mid- or tangent line of each element ρ_o, and the sign of ρ_o need to be calculated. The sign of ρ_o is assumed to be positive if while looking at the element from the starting joint to the ending joint, the shear center falls on the left hand side. TORAB can determine this numerically by using an algorithm called the convex hull [Sedgewick,

1992]. This algorithm determines the relative orientation of a vector to a specific point on a two-dimensional plane. The details of this algorithm are actually quite complex and will not be discussed in this thesis.

After the area and the magnitude and sign of ρ_o are determined for each element, Table 3-2 can be processed by simply traversing through the linked list and following the correct flow in the cross section. The goal is to first determine the warping sub-function which, from Table 3-2, is column seven divided by twice the value obtained in column six. The value in column six is the area of the entire cross section which TORAB already knows from the contributions of each element. Column seven is evaluated from the process described in the above paragraph. After the warping sub-function is obtained, the normalized unit warping W_{n_i} at each joint i in the cross section can be determined by subtracting the unit warping w_{o_i} at each joint i from the warping sub-function. Of course, the normalized unit warping at each joint is stored in the structure of the element which possesses those joints. If one joint is common to more than one element, the unit normalized warping *is not* stored in all common elements. Each element structure possesses several other structures which contain linked lists of various information. This organizational network is referred to as a substructural network. In this case each element structure has a pointer to the joint coordinate linked list which contains information relative to each joint such as the unit normalized warping and the warping statical moment. It should be noted that the information provided in all linked lists are dynamically allocated at run time. Although extended memory is not a problem for computers today, larger or more detailed problems are being examined where there may be over a thousand types of cross sections used.

5.3.3 Evaluation of statical warping moment and warping constant of a cross section in TORAB

Once the unit normalized warping function is evaluated at each joint in the cross section, the statical warping moment S_w and the warping constant I_w can be easily obtained through equations 3.30 and 3.31. A simple traversal through the linked list of

elements of the cross section is required to pick up the values of the normalized warping function, substitute them into the appropriate equations, and sum up the results over all the elements. The contribution to the warping constant from each element is stored in the individual element structure. Since the statical warping moment is the integral of the normalized unit warping function, the value of the moment can vary at the discrete joints along the cross section. Thus, the value of S_w at each joint is stored in the joint linked list which can be accessed by each individual element.

5.4 Graphical interface of torsional properties using MATLAB® and TORAB

In order to determine the maximum values of the normalized unit warping function and the statical warping moment, a listing of the values along various points on the cross section is needed. The maximum values of these properties are required so that the maximum values of the normal and shear stresses caused from warping can be obtained (equations 3.16 and 3.18). Although the maximum value of these properties illustrate where the maximum stresses on the cross section will be, it does not give insight to where the maximum stresses along the beam are. Since the warping normal and shear stresses are also a function of the rotation which, in turn, is a function of the longitudinal distance along the beam, the maximum values of the torsional properties can only portray the maximum stresses *on the cross section.*

TORAB has the capabilities to interface with MATLAB® by creating `.m` files that contain information for plotting the normalized unit warping and statical moment functions. There is no command that is required to create these plot files. The name of the `.m` file that is created is identical to that of the input file name used in TORAB. TORAB plots the cross section (in two separate plots) with the normalized unit warping and statical moment superimposed on top. The user can now visually see where the maximum values of these two functions lie on the cross section. The magnitudes of the functions are also displayed along with the exact location of the maximum values. Of course, with the command **PRINT RESULTS** (all print commands are described in

Appendix A), a text output for the same results can also be obtained. A sample plot of the two warping properties for the skewed channel cross section in Figure 1-6 is illustrated in Figure 5-5. It is apparent from Figure 5-5 that the location of the minimum values of the normalized unit warping function corresponds to the maximum values of the statical warping moment.

5.5 Location of maximum stress combination using TORAB

Although the locations of the maximum normal and shear stress caused by warping can be found, these locations will most likely not coincide with each other or the location of the maximum pure torsional shear stress. Since the shear stress on the cross section caused by pure torsion is a function of the shear modulus and the thickness, the stress does not vary along the length of the section but rather along the thickness. Thus, by finding the location of the maximum value of the statical warping moment, the location of the maximum combined shear stress on the cross section is also known. The value of the pure torsional and warping shear stresses are then added together at that point.

The shear and normal torsional stresses also vary along the length of the beam since the rotation and its derivatives change. However, assuming the cross section does not vary, only specific points along the length of the beam need to be evaluated for the values of the rotation and its derivatives to find the maximum. TORAB divides the beam into fifty discrete points (including the supports) and finds the maximum value among those points. There is no storage problem here since the values at only one point need to be stored and compared against a new one. Any information related to the beam is stored in a class called `Class BeamInfo` which contains structures entailing information about the beam. Most of this information is final results such as the location and magnitudes of the maximum stresses.

When a beam is subjected to planar bending forces which produce planar normal and shear stresses, these stresses must also be correctly added to the stresses caused by torsion. The location of the maximum values of the planar normal and shear stresses will probably lie at a different spot than their torsional counterparts. For wide-flange sections

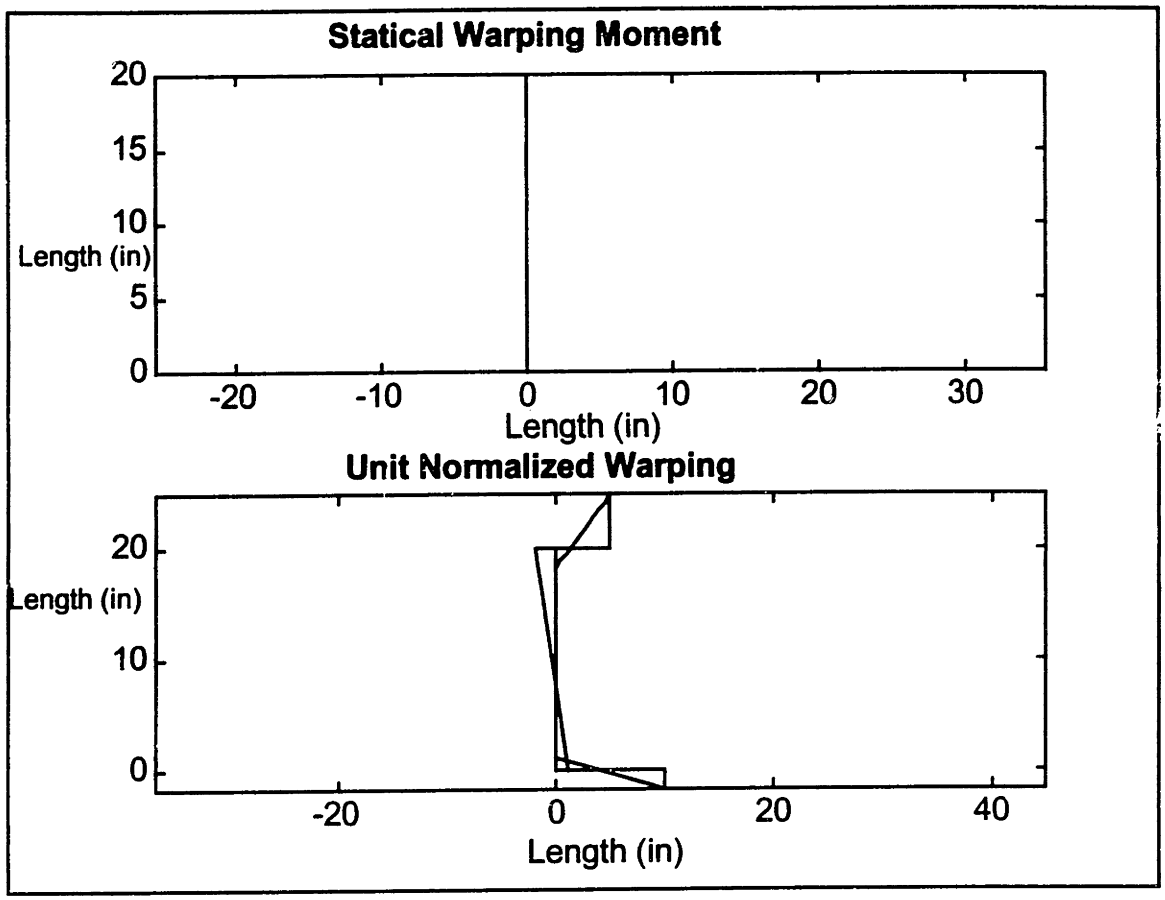

Figure 5-5 Normalized unit warping and statical warping moment plots of skewed channel

the normal stresses caused by warping and pure bending are both at their maximum values at the edges of the flanges. Likewise, there are always two flange tips where these stresses add regardless of the directions of the applied torsional and bending moments. Thus, for wide-flange cross sections, the normal warping and bending stresses should always be added to determine the maximum longitudinal stress on the cross section. Also, for wide-flange sections, the maximum values of the shear stresses caused by warping, pure torsion, and planar bending in the flanges will always add at some point regardless of the direction of the applied torsional moment and vertical shear to give the maximum shear stress in the flange. For the web, the maximum value of the planar shear stress adds to the value of the shear stress caused by pure torsion in the web, regardless of the direction of loading, to give the maximum shear stress in the web. For other types of structural cross sections such as channels and Z shapes, it is impossible to provide general

rules for the magnitude of the maximum combined stresses. It is necessary, for these shapes, to consider the directions of the applied loading and to check the combined stresses at several locations in both the flange and the web.

TORAB summarizes the stresses in the output with the commands **PRINT STRESSES ALL** or **PRINT STRESSES MAXIMUM**. The former command prints the combined normal and shear stresses caused from pure and warping torsion at all fifty points along the beam. Only the maximum stresses on the flange and the web are reported for those points. The latter command prints the maximum combined normal and shear stress for the whole beam along with the location. This command also separates the information into the maximum combined normal and shear stresses for the flange and the web.

5.6 Solution of torsional rotation and successive derivatives in TORAB

In order to determine the stresses caused by pure and warping torsion, it is necessary to obtain the value of the torsional rotation along the longitudinal span of the beam. The numerical procedure to calculate the torsional rotation and its derivatives were explained in Chapter 4. The mesh equations given in equations 4.22 and 4.25 are "hardcoded" in memory since the only general types of loads available are concentrated and distributed. If the distributed torque is not uniform (i.e., linearly varying), the right hand side of equation 4.25g must be changed to reflect the variation in m_z. Since the boundary constraints affect the finite difference equations and thus, the $\tilde{R}$ matrix in equations 4.23f and 4.25e, these constraints must be pre-calculated so the assemblage of the $\tilde{R}$ matrix becomes simpler. TORAB uses the constraints listed in Table 4-1 and creates the difference equations for the mesh points affected by the boundary conditions. Thus, when TORAB realizes (from the input file) that a specific joint is constrained in some manner, it pulls the appropriate finite difference equation associated with the constraint and substitutes it into the correct position in the $\tilde{R}$ matrix. TORAB is capable of determining if the beam presented by the user has symmetric boundary conditions. If this

is the case, it will only calculate one triangular part of the square $\tilde{R}$ matrix and simply transpose those entries to fill the other triangle.

The solution to the set of finite difference equations , $\tilde{R}\vec{\phi} = \vec{L}$ where $\vec{\phi}$ and $\vec{L}$ are the rotation and load vectors, respectively, is resolved using a standard Gaussian solver with partial pivoting. Since the $\tilde{R}$ matrix may not be symmetric, it is not possible to use solvers such as LDL^T since the lower and upper triangles of the $\tilde{R}$ matrix are not the transpose of each other. However, the $\tilde{R}$ matrix is tridiagonal which allows TORAB to only store the blocked bandwidth. This bandwidth is, at maximum, three entries wide. The rest of the matrix is just filled with zeroes. The Gaussian solver used is slightly altered to accommodate the sparseness of the matrix and the elements being stored.

After the rotations are obtained, TORAB uses equations 4.15 through 4.20 to solve for the derivatives of the rotation at each mesh point. TORAB goes through a loop and applies those equations for every mesh point on the beam. If a mesh point coincides with a boundary point, TORAB will automatically be informed by the structure in the beam class which keeps track of mesh points that are boundary constraints. Therefore, instead of applying one of the equations from 4.15 to 4.20, the correct boundary condition will be substituted. All of the values for the rotations and its successive derivatives are stored in linked lists pointed to by pointers stored in the beam class `Class BeamInfo`.

Chapter 6

Conclusion

The problem of torsion in structural problems is very complicated and extremely time consuming if accurate results are to be obtained. Linear torsion is often avoided in most analyses since the amount of computation required to solve for the torsional properties, rotations, and stresses does not compensate for the information acquired. The focus of this paper, however, was to create a numerical forum in which the computation is simplified by converting the differential equations and line and surface integrals into discrete, closed form expressions.

The most complicated aspect of torsional analysis is the fact that structural cross sections may be open, closed, continuous, or even built-up. Since these cross sections may vary from one beam to the next, it is difficult to calculate the shear center for each section, especially since the shear center is difficult to quantify in a numerical sense. In this paper, it was shown that the shear center was a function of the tangential distance from the mid-line of each element in the cross section to the centroid. By quantifying this value, it was possible to express the shear center in terms of the geometric inertial properties of a cross section. The Force Method was used to compare the results of the numerical scheme with an unorthodox cross section.

The concept of pure or St. Venant's torsion was examined and developed using elastic theory. The Airy's Stress Function was introduced to express the governing differential equation for pure torsion in terms of a Laplace based equation for bidirectional flow. With the aid of Prandtl's membrane analogy, the Laplace equation for pure torsion was proven to be analogous to a thin membrane inflated by some pressure. The effects of this membrane subjected to a pressure could easily be obtained. Thus, with the help of the analogy, it was discovered that the slope of the displacement field of the membrane

caused by the pressure was exactly equal to the shear stresses imposed on the cross section by the pure torsion. It was also shown that the volume underneath the inflated membrane was equal to the torque developed by the cross section to resist the external torque. A numerical scheme was developed to calculate the torsional stiffness constant for any cross section. For built-up sections, it was proven that the total torsional stiffness was simply the sum of the torsional stiffness for each individual section. Continuous and multicontinuous cells, such as box sections, were also introduced. Since these sections are indeterminate, a separate algorithm was utilized to solve for the torsional stiffness and shear stresses. Redundant forces were imposed to create a cut in the original section so it could be treated as an ordinary open, thin-walled section. A set of simultaneous equations were introduced and solved to get both the torsional stiffness of the entire section as well as the shear stresses through the elements of the section. Boundary elements were treated separately since the stresses in adjacent cells sharing the boundary element needed to be vectorally added.

The phenomena of warping torsion and the effects it has on the existing axial forces in a beam were also examined. Warping was shown to be an out of plane effect arising when the out of plane displacements are somehow constrained. The normal and shear stresses caused by warping were related to the torsional rotation of the beam and several warping properties. These warping properties, including the normalized unit warping, the statical warping moment, and the warping constant, were very abstract quantities that were difficult to obtain even by hand. However, by isolating and quantifying parts of the equations related to these properties, it was discovered that a key parameter in numerically decomposing these properties lied in the tangential distance from the shear center to the mid-line of an element in the cross section. The integration of this quantity over the surface of all the elements in the section was done using Simpson's $1/3^{rd}$ integration technique. Thus, the normal and shear stresses could now be obtained using a numerical procedure.

The combination of pure and warping torsion created a fourth order differential equation whose closed-form solution, depending on the loading, was undesirable. In order to bypass the differential equation, the finite difference method was introduced, and

the beam was decomposed into several discrete points to accommodate the method. A mesh equation was developed for each point by rewriting the derivatives of the torsional rotation at that point as a function of the torsional rotations at other points. The boundary conditions were also included in the formulation as they affect the finite difference equations for certain points. The equations were then assembled into matrix form and solved using an altered Gaussian elimination scheme. Since the matrix containing the coefficients of the difference equations was tridiagonal, storage was not a problem.

Finally, a computer program (TORAB) was created to assemble the whole torsion process together. With a simple text input file, the user could create a cross section of any shape and a beam with arbitrary continuous supports and loading. TORAB has the ability to determine the centroid and shear center and graphically display the warping properties inherent to a specific cross section. TORAB will also solve for the torsional rotations on the beam and determine the maximum combined pure and warping stresses on the cross section and along the longitudinal axis on the beam. It will separate the cross section into flanges and webs and will also report the maximum stresses on each component. Created in an object-oriented environment, TORAB treats the cross section as a group of individual elements of which each is autonomous of the next. Each element is capable of deriving its orientation, area, relative distances, etc. and passing this information to the cross section. All of the elements are placed in a doubly linked list of structures which allows the cross section to easily traverse the list and find any information it needs. The joint coordinates and any final results are also kept in the same manner.

Appendix A

This appendix contains a brief synopsis of all the commands available in TORAB.

CROSS-SECTION

Used at the very beginning of the input file before any data for the cross section is given

JOINT COORD

Used for the cross section to specify the nodes desired by the user to configure the cross section. The syntax for specifying a joint is the joint number followed by the x and y coordinates.

ELEM INCID

Used to create actual elements by connecting joints. In order to create an element, the element number followed by the starting and ending joint numbers must be listed.

ELEM PROP

Used to specify the thickness of an element. The correct usage for this command is to first list the element number followed by the thickness of the element.

PRINT CENTROID

Prints the coordinates of the centroid in the output file.

PRINT SHEAR CENTER

Prints the coordinates of the shear center in the output file.

FRAME

User can specify an alternate origin for the cross section. The syntax for this command is to list the x and y coordinate for the new origin.

ELEM OFFSET

Used to shift the position of the joint coordinates with respect to the thickness of the element. Only the y-coordinate of the joint can be shifted.

CELL

Used to create continuous or multicontinuous cell sections. The command is followed by the cell number, cell height, and cell width. Used in place of ELEM INCID when cell sections are desired.

CELL PROP

Used to designate the thickness of the cells. Since each cell has four segments, the user

can provide a thickness for each segment by listing the cell number followed by the four values. All boundary segments must share the same thickness for continuity purposes. TORAB will inform the user if this is not the case.

BEAM

Used to start the data for the beam under investigation.

JOINTS

Used to specify the joints where support are located. The command is followed by the joint number and the longitudinal distance from the left end of the beam.

SUPPORT

Used to designate the type of support at each joint. The command is followed by the joint number where the support lies and the type of support desired. The three types of supports available are: **FREE**, **FIXED**, and **PINNED**.

CONSTANTS

The modulus of elasticity and the shear modulus are listed after this command.

LOADING

Used to specify the torsional loading on the beam. The first piece of information listed is the type of loading: **CONCENTRATED** or **DISTRIBUTED**. For a concentrated load the distance from the left end of the beam where the torque is applied and the magnitude of the torque is required. For a distributed load the starting and ending distances (measured from the left end of the beam) of the load followed by the magnitude at the start and end are required.

PRINT RESULTS

Prints all values of the torsional properties (i.e. unit normalized warping function, warping statical moment, warping constant, torsional stiffness) at each joint in the cross section where applicable. The results are printed in an output file under the same name as the input file but with a *.anl* extension.

PRINT STRESSES ALL

This command prints the combined normal and shear stresses caused from pure and warping torsion at all fifty points along the beam. Only the maximum stresses on the flange and the web are reported for those points.

PRINT STRESSES MAXIMUM

This command prints the maximum combined normal and shear stress for the whole beam along with the location. This command also separates the information into the maximum combined normal and shear stresses for the flange and the web.

PRINT ROTATIONS

Prints the torsional rotation at all fifty points along the beam.

END

Signifies the end of the input file.

Bibliography

[1] American Institute of Steel Construction. *Torsional Analysis of Steel Members*. American Institute of Steel Construction, Inc., Pub. No. T114, Chicago, IL., 1983.

[2] Bathe, Klaus-Jurgen. *Finite Element Procedures*. Prentice Hall, Englewood Cliffs, New Jersey, 1996.

[3] Bell, L.C and Heins, C.P. "The Solution of Curved Bridge Systems Using the Slope-Deflection Fourier Series Method". *Civil Engineering Report No. 19*, June 1968.

[4] Chopra, Steven and Canale, Raymond. *Numerical Methods for Engineers*. McGraw-Hill, Inc., 1988.

[5] Chu, K.H. and Johnson R.B. "Torsion in Beams with Open Sections". *Journal of Structural Div.*, ASCE, Vol. 100, No. ST7, July 1974.

[6] Connor, Jerome J. *Structural Analysis*. Ronald Press, 1976.

[7] Eggenschwyler, A. and Maillart, R. *Zur Frage der Biegung*. Schweiz, Germany, 1921.

[8] Evick, D.R. and Heins, C.P. "Torsional Analysis of Partially Coverplated Wide-Flange Structural Beams". *Civil Engineering Report*, University of Maryland, College Park, Maryland, December, 1973.

[9] Hanselman, Duane and Littlefield, Bruce. *Mastering MATLAB®*. Prentice-Hall, New Jersey, 1996.

[10] Heins, C.P. *Bending and Torsional Design in Structural Members*. D.C. Heath and Company, Lexington, 1975.

[11] Heins, C.P. and Kuo, J.T. "Composite Beams in Torsion". *Journal of Structural Division*, ASCE, Vol. 98, No. ST 5, May 1972.

[12] Heins, C.P. and Seaburg, P.A. "Torsion Analysis of Rolled Steel Sections". Bethlehem Steel Co., Bethlehem, Pa., 1963.

[13] Hotchkiss, J.G. "Torsion of Rolled Steel Sections in Building Structures". *AISC Engineering Journal*, 1966, Vol. 3, No. 1.

[14] Johnsonbaugh, Richard and Kalin, Martin. *Applications Programming in ANSI C.* Macmillan Publishing Company, New York, 1993.

[15] Kollbrunner and Basler. *Torsion in Structures.* Springer-Verlag, New York, 1969.

[16] Ojalvo, M. "Warping and Distortion at I-Section Joints". Discussion, *Journal of Structural Division*, ASCE, Vol. 101, No. ST1, Jan. 1975.

[17] Prandtl, L. *Zur Torsion von prismatischen Staben.* Phys, Z. 4, 1903.

[18] Salmon, C.G. and Johnson, J.E. *Steel Structures: Design and Behavior 2nd Ed.*, Harper and Row, New York, 1980.

[19] Sedgewick, Robert. *Algorithms in C++.* Addison-Wesley Publishing Company, New York, 1990.

[20] Seeley, S.B. and Smith, J.O. *Advanced Mechanics of Materials.* John Wiley and Sons, New York, 1952.

[21] Timoshenko, S. "Theory of bending, Torsion and Buckling of Thin-Walled Members of Open Cross Section". *Journal of the Franklin Institute*, Philadelphia, March-April-May, 1945.

[22] Timoshenko, S. and Goodier, J. *Theory of Elasticity.* McGraw-Hill Book Co., New York, 1951.

[23] Vacharajittiphan, Porpan and Trahair, Nicholas. "Warping and Distortion at I-Section Joints". *Journal of the Structural Division*, ASCE, 100, ST3, 1974.

[24] Vlasov, V.Z. "Thin-Walled Elastic Beams". National Science Foundation, Washington, D.C., 1961.

[25] Yoo, C.H., Evick, D.R., and Heins, C.P. "Non-Prismatic Curved Girder Analysis". *Journal of Computers and Structures*, Vol. 3, 1973, Pergamon Press, London.